

EXPOLRING INVERSE CASCADE SCENARIOS
IN
ASTROPHYSICAL TURBULENCE

**Thesis submitted in partial fulfilment of the requirements
for the degree of**

DOCTOR OF PHILOSOPHY

by

R.D.PRABHU

INDAIN INSTITUTE OF SCIENCE, BANGALORE

1997

For my parents..

They have indeed waited for LONG..

For my in-laws..

who still wonder ..

whether they got the 'right guy'!

For Anna, Akka and SATYA

who have been bribing the LORDs

for my welfare..

This Thesis is...

For Deepti, Jyothi, Mamis and Sai..

who still think..

"he doesn't have petrol to come"

For my wife..

who delivered earlier than I could.

For my daughter Gitanjali...

Hoping ...She would 'understand'....

the spirit behind her DAD's DELAYS!!

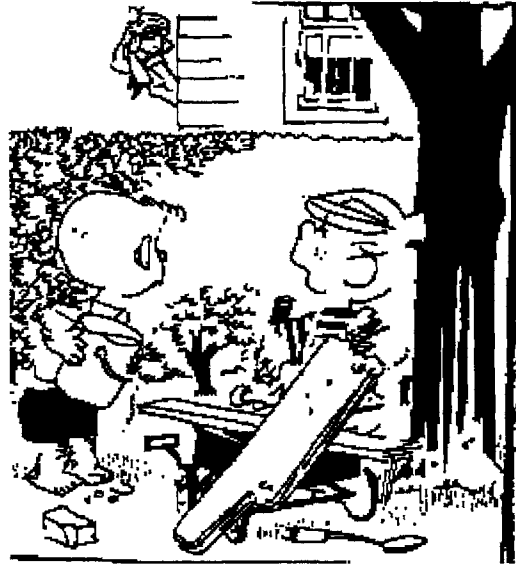
*The master in the art of living
makes little distinction between
his work and his play,
his labor and his leisure,
his mind and his body,
his education and
his recreation,
his love and
his religion.*

*He hardly knows which is which.
He simply pursues his vision of
excellence in whatever he does,
leaving others to decide whether
he is working or playing.
To him he is always doing
both.*

- Zen Buddhist text -

*The most fruitful areas for growth of the sciences are those
between established fields. Science has been increasingly
the task of specialists, in the fields which show a tendency
to grow progressively narrower. Important work is delayed
by the unavailability in one field of results that may have
already become classical in the next field. It is these
boundary regions of science that offer the richest
opportunities to the qualified investigator.*

NORBERT WIENER



"Oh Oh! I Don't like the sound of her voice. It Means I either gotta get cleaned up or I did somethin' WRONG..!"

"What happens when you stir a coffee cup ..", is what stirred this thesis! In fact that was how the apparently 'counterintuitive idea' contained in this thesis was introduced to me by my guide Prof.Vinod Krishan...simply, intuitively. And as if notwithstanding the 'novelty' of the idea ..there were the galaxies.. in waiting..to fuse into a new picture of how *it* all came to *be*. Prof.Krishan always had an open mind to both criticism as well as to new ways of looking at the problem. She encouraged a strong 'Do it yourself' culture in me. There were limits though..to my meanderings, my little quests..which she set with such deftness that you never could complain that you never got your share of freedom! And that she would do it in an unsaid "enough ..! now lets get down to business" fashion. What steered this thesis to its present state is her guidance and NOT my so called 'independent ways ' of doing things! To her I owe the successful execution of this splendid idea of 'self -organization', and I must hasten to add that there is nothing of my 'self' in the way this thesis got 'organised' from a turbulent start! Left to myself I guess it would have still remained 'turbulent' and 'disorganised'!



"We Sure Make a Good Team...You bake'em and I EAT'em !!..."

I sincerely thank the many who helped me design the 'menu' for my research.(my guide remains the super-chef though!). First and foremost Dr.Amit Basu (JNC), whose ever-willing nod gave me an opportunity to learn the basics of 'simulations' from him holding his little finger. Dr.Siddhartha Ghosh, my senior and the 'IBM SP2 superman' eased my time constraints by a crucial factor with his 'parallelizing skills' which he helped me implement on the 'paralysed parts' of our code. That in fact gave me time enough, to disturb him often to discuss many other issues of mutual interest..be it politics, research , education..whatever. His wife (and my senior again) Dr.Mausumi too has been very encouraging with a 'you CAN do it'(Tui Paarbi re!) pat. Dr.Prashant Goswami of CMMACS, (and my senior again!) made us 'salivate intellectually' when he flashed his views on the striking similarity between vortex-interactions and galaxies (!!?!?!), during one of our meetings at the Indian Institute of Astrophysics. That led to the formation of the CMMACS-IIA team with a view to develop areas of mutual interest. With the ever-jubilant Prof.Prabhakar Vaidya in the team, I am sure there are many 'dormant collaborations' in waiting!



"How 'Bout If I give'em 'til six o'clock to clear outa the house? !"

Indeed I have had a very healthy social life at IISc. Friends like potatoes came in different shapes! My house was always a ready venue for meetings and discussions, which often ranged widely between religious issues (of the "Does GOD exist..?" kind) and science and industry (of the "do we need R and D ?" kind) and films and music (of the "Wow Madhuri Dixit! " kind). Our neighbours must have had sleepless nights with our frequent night-long debates and excited exchanges!!

Whatever that meant, at the end of the day my wife and me would get engaged in another fresh debate over whether it was my garrulity (entertaining..?) or her culinary capabilities ('yummmmy! sllrrpp..') that wins us friends ! All in all I have always had lively company ..be it the CAIR gang..(Sartaj,Praveen,Vinod,Srini et al), or the Balaji-Sutapa duo or Sastry, Seshu, Srinivas Rao (the three musketeers!), or the U block cricket team (Praveen,Jaggu,Santosh,Sridhar,Vijay et al), or the IIA gang (Pandey,Arun, Sivarani,Reddy,Angom,Geetha et al), or my brother-in-law..Bhanu and family (Lakshmi, darlings Ajit and Devasena)..or Mohan (and his *nth* hand car!) or Rajguru or Sachin or Madhavi or Parker-Raju..(I guess this is data enough for a thesis in Sociology!!)...(hope my other friends forgive me after seeing this sentence end).



" But I'm not tired ! Who you gonna believe ..Me OR the CLOCK..?"

Well, since time and tide wait for none..its time for me to pack up and leave.
And as these moments trot away into a memorable past may I with due apologies to
Robert Frost state:

The Woods (IISc.) ARE ..lovely dark and deep..

But I have Promises to keep.. (Dr.R.D.Prabhu..?)

And miles to go before I sleep.. (in search of a better job)

And miles to go before I sleep. (in search of a LIFE worth LIVING!)

But before that,

Kal to is mahfile hasti se guzar jaana he lekin..

Aaaj ki raat tumhaari bajm me kuch aur sahi..

ABSTRACT

This thesis is an attempt to blend the latest observations of large scale coherent motions - coherent structures- observed in experiments with turbulent fluids, [6] with different astrophysical situations where turbulent flow is more of a rule than an exception. We highlight the need to re-invoke the once suggested [2] but long ignored role of turbulence in various astrophysical scenarios - viz.. the solar context, the galactic level, as well as on the cosmic scale- in the light of some of the latest developments in turbulence-studies. These studies have begun to emphasize the role of new invariants related to HELICITY and Helical fluctuations in the flow [73]. We feel that these new developments if incorporated in astrophysical fluid dynamics, may help in clarifying some of the long standing problems in astrophysics related to large scale structures, and large scale motions which are well known.

There is a well observed structural heirarchy in astrophysics viz. the way in which the fundamental blocks - galaxies, are clustered in groups and these groups in turn are re-grouped as superclusters over vast length scales ranging upto 100 Mpc ($1pc \sim 3 \times 10^{18}cm$). For example our Galaxy - Milky Way - belongs to the Local Group which consists of about 20 galaxies. A cluster may have upto 1000 galaxies. A typical linear extent of a cluster could be about 5 Mpc. A supercluster may be extending upto 50 Mpc. Further the 'Great Wall' is a linear structure of size 60 Mpc by 157 Mpc and is made up of several superclusters. The filamentary nature of matter distribution is well known.

Using kolmogorovic arguments and the newly identified invariants related to helicity (i.e the projection of vorticity along the velocity) and helical fluctuations viz. the helicity-helicity correlations (called the I - invariant) we can work out the inertial range stationary spectral behaviour for any turbulent medium whose net helicity is zero but the helicity variance is a constant. This spectral dependence when translated into real space reflects the average energy that resides on each length scale. Thus the real space velocity fields also could carry a signature of this behaviour.

This approach is the 3D analogue of the 2D case where apart from energy, enstrophy (i.e vorticity squared) is another invariant of the fluid flow. Upon inclusion

of dissipation each of the invariants decay at different rates. The slowly decaying invariant generally cascades towards the larger scales and the faster one cascades to the smaller scales.

Levich et al. [73], had evolved after a detailed study of the mesoscale atmospheric phenomena, a turbulent stationary spectrum which explains the energetics of the cloud complexes over a range of scales. A similar spectrum was also employed to study the solar granulation scales by Krishan [16], which again could match with the observed and predicted energetics. Later, on a cosmic - scale too Krishan [8] and, Krishan and Sivaram [17] showed that the entire hierarchy of structures ranging from a galaxy to superclusters could be visualised as the consequence of similar turbulent processes operating over the whole range and leading to self-organized coherent states at various levels.

To further verify the full spectrum in the astrophysical context we fit the real space velocity fields of various galaxies - known as 'rotation- curves'; with the predicted spectrum [9]. This exercise has yielded remarkable agreement with the spectra and galactic-velocity fields. The parameters of turbulence so extracted from the fits are comparable with similar estimates made by other methods.

Next we test our proposed velocity-laws for the galactic velocity field, with the well known Tully-Fisher relation which highlights a tight correlation between the rotation velocity and the luminosity of a galaxy in various bands [87]. This is a statistical study wherein our interest is focussed on the correlations between the galactic luminosity with the 'turbulent' and 'gravity' components of the velocity field, which our model could resolve after the proper fits are performed to the observed velocity fields. We confirm the normal trend of correlations with the *total* velocity first. For the individual correlations between the galactic luminosity and each of the velocity components, our study reveals an interesting feature. The turbulent component correlates reasonably better than the gravity component in the shorter wavebands. Whereas the gravity component correlates better than the turbulent component in the longer wavebands. This implies that the so called 'scatter' observed in the shorter wavelength bands could be a feature of galactic-turbulence which might be playing some constructive role in generating the observed large scale velocity field.

Thus our study points out the necessity to re-consider the role of the self-organizing aspects of turbulent flows on galactic scales. Our results also convey the fact that our model is doing well in estimating the extent of gravity , and turbulence induced velocities.

In an attempt to understand the generation of such large scale flows and other features of self-organization Frisch et al had performed a multi scale analysis of the Reynolds averaged set of Navier stokes equations with a well-defined forcing introduced on the small scales. They discovered that there indeed exists a large scale instability provided there is some small scale anisotropy in the flow. This is possible if the turbulent medium lacks parity on small scales (i.e the statistical averages of the medium are NOT reflection invariant). Such a situation can be brought about by injecting helicity into the medium (on small scales), by rotation, or by compressibility effects or by using the specific forcing term used by Frisch et al. in their analysis. This mechanism has its analogue in the DYNAMO MECHANISM which is invoked for the generation of large scale magnetic fields, called the alpha effect. In fact the equation for the evolution of VORTICITY, and the evolution of the MAGNETIC FIELD.. are similar in their structure.

In order to prepare the ground for studying the mechanism in the context of an expanding universe we find a set of transformations which can help us in reducing the equations in the expanding frame to the normal Navier Stokes formulation [98] . This could then be used in the study of the formation of large scale structures in the universe which is indeed a long standing problem.

Frisch et al, and Sulem et al [27];[71] had performed extensive numerical simulation of the incompressible Navier Stokes equation with a specific forcing term which produces a parity breaking velocity field on small scales. Later Druzhinin and Khomenko [101] also studied the same set of equations with compressibility effects

We have performed a 32 x 32 x 32 numerical simulation of a compressible fluid (using spectral methods in a periodic box) on the IBM SP2 Convoy (as well as on the Power Challenge system) with parallelisation techniques implemented [102]. We have not used any empirical model to close our Reynolds averaged set of equations for the large and the small scales . Instead we perform a spatial averaging over the

entire real domain of velocity field at every time step. We choose a suitable length scale over which to average, so that we get a statistically significant number of points over the grid. This we feel is a best approximation to the idea of ensemble averaging

We confirm that an inverse cascade of energy occurs when the fluid is forced on small scales with a forcing function which violates parity. We also study the evolution of helicity, vorticity, and density spectra in the simulation. We find that the compressibility of the medium also aids in generating a velocity field which lacks parity.

Contents

1	INTRODUCTION	1
1.1	Fluid turbulence: Then and Now	1
1.2	Turbulence - the Kolmogorovic way	3
1.3	Turbulence - the Navier - Stokes way	14
1.4	Astrophysical Turbulence	20
1.5	Primordial Turbulence	21
2	FLAT ROTATION - CURVES OF GALAXIES	26
2.1	Introduction	26
2.2	The Inverse Cascade	28
2.3	The Kolmogorov approach	29
2.4	Modelling of Rotation Curves	31
2.5	Results	32
2.6	Discussion and Conclusion	67
3	TURBULENCE, GRAVITY & THE TULLY-FISHER RELATION	71
3.1	Introduction	71
3.2	The Sample And The TULLY - FISHER Relation	72
3.3	Discussions	80
4	ROLE OF HELICITY IN AN EXPANDING FLUID	86

4.1	Introduction	86
4.2	The basic equations and the transformations	87
4.3	Helicity and density evolutions	92
4.4	Interesting features of the evolution	94
4.5	Conclusion	96
5	SIMULATING 'INVERSE CASCADE'	97
5.1	Coherent Structures in turbulence	97
5.2	The basic equations	98
5.3	Simulation and results	100
A	Statistics	110
A.1	Correlation coefficient	110
A.2	Skewness and Kurtosis	111
B	Notes on the I- Invariant	112
B.1	The Proof of I- invariance	112
B.2	Proof of $I(k) \propto E(k)^2$	114
	References	116

List of Figures

1.1	The complete turbulent energy spectrum	13
2.1	Rotation Curve of UGC 12498 in the Pegasus cluster	40
2.2	Rotation Curve of NGC 7593 in Pegasus cluster.	40
2.3	Rotation curve of NGC 7631 in Pegasus cluster.	41
2.4	Rotation curve NGC 2558 in the Cancer cluster	41
2.5	Rotation curve of NGC 2595 in the Cancer cluster.	42
2.6	Rotation curve of NGC 4848 in the Coma cluster.	42
2.7	Rotation curve of NGC 4921 in the Coma cluster.	43
2.8	Rotation curve of Z 160-106 in the Coma cluster.	43
2.9	Rotation curve of Z 130-008 in the Coma cluster.	44
2.10	Rotation curve of Z 119-043 in the Cancer cluster.	44
2.11	Rotation curve of Z 119-053 in the Cancer cluster.	45
2.12	Rotation curve of UGC 4386 in the Cancer cluster.	45
2.13	Rotation curve of Z 160-058 in the Coma cluster.	46
2.14	Rotation curve of NGC 4911 in the Coma cluster.	46
2.15	Rotation curve of UGC 10085 in the Hercules cluster.	47
2.16	Rotation curve of NGC 6045 in the Hercules cluster.	47
2.17	Rotation curve of NGC 7536 in the Pegasus cluster.	48
2.18	Rotation curve of NGC 3282 in Abell 539 cluster.	48
2.19	Rotation curve of UGC 4329 in Cancer cluster	49

2.20	Rotation curve of NGC 7643 in Pegasus cluster	49
2.21	Rotation curve of UGC 3269 in Abell 539 cluster	50
2.22	Rotation curves of galaxies from Rubin's data	51
2.23	Rotation curves of galaxies from Rubin's data contd..	52
2.24	Rotation curves of galaxies from Rubin's data contd..	53
2.25	Rotation curves of galaxies from Rubin's data contd..	54
2.26	Rotation curves of galaxies from Rubin's data .contd...	55
2.27	Rotation curves of galaxies from Rubin's data , contd..	56
2.28	Rotaion curves of galaxies from Rubin's data ,contd..	57
2.29	Rotation curves of galaxies from Amram's data.	58
2.30	Rotation curves of galaxies from Amram's data contd..	59
2.31	Rotation curves of galaxies from Amrams's data contd..	60
2.32	Histogram showing the distribution of the turbulence parameter ϵ	61
2.33	Histogram showing the distribution of L_z	62
2.34	Histogram showing the distribution of masses (M) derived from our modelfits.	63
2.35	Histogram showing the distribution of ω for all the galaxies in our data set.	64
2.36	Histogram showing the distribution of the turbulence parameter τ	65
2.37	Histogram showing the distribution of turbulent velocities V_0	66
3.1	The scatter plot between different velocity components and luminosities of the galaxies in different bands viz . U , B , V, I and $I_{23.5}$	81
3.2	Histogram showing the distribution of mass to luminosity ratios in the B- band	83
3.3	Histogram showing the distribution of mass to luminosity ratios in the U- band	83

3.4	Histogram showing the distribution of mass to luminosity ratios in the V- band	84
3.5	Histogram showing the distribution of mass to luminosity ratios in the I- band	84
3.6	Histogram showing the distribution of mass to luminosity ratios in the $I_{23.5}$ - band	85
5.1	Figure showing the constancy of total mass inside the periodic box . .	104
5.2	Figure showing the density of states	104
5.3	The evolution of the energy in wave modes $k=1,2,$ and 6 with forcing (at $k=4$)	105
5.4	The evolution of the energy in wave modes $k=1,2,$ and 6 without forcing	105
5.5	The energy spectrum	106
5.6	The helicity spectrum (initial) ($H(k)$ vs. $\text{Log}(k)$)	106
5.7	The helicity spectrum (final) ($H(k)$ vs. $\text{Log}(k)$)	107
5.8	The evolution of total Helicity with time.	107
5.9	The vorticity spectrum	108
5.10	The Helicity distribution in space at two different instants	109
5.11	The initial velocity field along a z-y plane	109
5.12	The final mean velocity field along the z-y plane	109
5.13	The density evolution.	109

List of Tables

2.1	Table showing the Turbulence Parameters	34
2.2	Table showing $L_z, \omega,$ and masses	35
2.3	Table showing Turbulence parameters	36
2.4	Table showing Turbulence parameters contd..	37
2.5	Table showing Mass, $\omega,$ and L_z	38
2.6	Table showing Mass, $\omega,$ and L_z contd..	39
3.1	Photometric data	74
3.2	Table showing the Photometric data, contd..	75
3.3	Table showing the Photometric data , contd..	76
3.4	Table showing the ‘gravity’ and ‘turbulent’ velocity components	77
3.5	Table showing the ‘gravity ’ and ‘turbulent’ velocity components contd..	78
3.6	Table showing the ‘gravity’ and ‘turbulent’ velocity components, contd..	79

Perhaps the Fundamental equation that describes the swirling nebulae and the condensing , revolving, and exploding stars and galaxies is just a simple equation for the hydrodynamic behavior of nearly pure hydrogen gas

Richard.P.Feynman - Lectures on Physics, Chapter 41, "Flow of wet water"

Chapter 1

INTRODUCTION

1.1 Fluid turbulence: Then and Now

A simple definition of turbulence is the existence and interaction of many spatial and temporal scales in a fluid. Fluid turbulence has remained the last unsolved classical problem in physics for nearly 300 years [1]. Moreover it is also an all pervading phenomenon. If the flow of blood in our arteries is turbulent so is the flow of air blown out of a musicians flute, and so is the flow around automobiles and aircrafts. The atmosphere of our planet is turbulent, thus keeping our meteorologists busy and guessing all the time. Indeed, turbulence is as rich in variety as it is difficult to grasp. Jupiter's red-spot has long been thought of as a 'perennial cyclone' by researchers and artists alike. Indeed they both have proved to be right for research has led us to believe that turbulence is not just 'disordered motion' it could also be a source of 'order and structure'. Talking about structure, astronomers and astrophysicists have long been wondering at the marvellous observations of 'structure on almost all scales' which the universe presents us with. The cellular structures on our sun, the spiral structure of galaxies, the clustering of galaxies, and superclustering of clusters - there seems to be a mysterious undertone of order on all scales. Studying the origins of

this 'order' has been the preoccupation of many brilliant minds. von Weizacker [2], George Gamow, [3] Jim Peebles [4], Zeldovich [5] and many others have attempted to study the role of turbulence in producing the vast fabric of observed structural - heirarchy. Their efforts have borne out results ranging from skepticism regarding the need to invoke turbulence (Peebles) to belief that turbulence is indeed needed. This wide spectrum of conclusions is understandable since the study of 'laboratory turbulence' itself is a source of tremendous possibilities of behavior. It is only recently that experiments have revealed the presence of 'coherent structures' in such turbulent - media. The numerical simulations of turbulence have corroborated this view even when restricted to their limited domain of computational capabilities [6]. (We still do not have the resources to numerically simulate even the simplest everyday turbulent phenomena like say the smoke emanating out of a chimney!!). Yet such simulations do give us an insight into the various processes at work in the evolution of a turbulent fluid. Thus this provides 'food for thought' for theoreticians who are way behind in capturing the essence of such behavior in their equations to reproduce the zoo of animals which turbulence harbors and which the experimenters have well documented by their painstaking observations. Looking at the infancy of these new developments it is understandable that the diverse views held by scientists in other communities trying to 'apply turbulence' were just the reflections of an 'incomplete picture'. This also requires that we take a fresh look at these interdisciplinary fields time and again to update ourselves with sufficiently new tools and ideas before we consider their application to any other discipline.

This thesis comes under such an interdisciplinary effort to highlight the role of new ideas in the formation of coherent structures in a turbulent media, in structure - formation scenarios in astrophysics. Although the major emphasis is laid on the mechanism, the potential for applying it to cases of astrophysical interest have also been explored with considerable success, (eg. solar granulation [7],[16], cosmic alpha effect in clustering [8], rotation curves of galaxies [9] etc..)

1.2 Turbulence - the Kolmogorovic way

Eventhough the problem of turbulence remains intractable till date, one of the most ingenious insights into the nature of turbulence was provided by Kolmogorov in a seemingly trivial style [10]. The essence of his path breaking find was based on simple assumptions regarding the turbulence - energetics. Kolmogorov assumed that the energy was being exchanged between different spatial scales (say from the large to small scales) at a constant rate which was independent of the scale and the viscosity of the fluid. Thus there exists a quasi-stationary range of scales called the *inertial range* where the energy is exchanged among scales at a constant rate independent of the scale. The energy cascades from large scales to small scales. This process continues untill the energy reaches the smallest scales corresponding to the molecular sizes where it is finally converted into heat due to the viscosity of the fluid.

Thus, if \vec{V} is the typical velocity on a scale L , and say the energy of this scale is drained to a subsequent scale within a time say T , then $V^2/T = \epsilon$ where ϵ is the rate at which energy is exchanged between the scales and is a constant for any scale within the inertial range. Therefore for any other scale l with a velocity \vec{v} the rate of energy dissipation is also ϵ . If we assume that each scales retains it's energy for a period which is the same as the eddy - turnover time τ , then $T=\tau = L/V$ (say). So, $V^2/T = V^3/L = \epsilon$ and thus for any other scale also, $v^3/l = \epsilon = \text{constant}$. Translating the same into the fourier space, so that $\tau \equiv (kV_k)^{-1}$, (where k is the wavenumber and V_k is the velocity in the fourier space)we get :

$$(kV_k)(V_k)^2 = \epsilon \quad (1.1)$$

The energy spectrum $E(k)$ is defined as :

$$kE_k = (V_k)^2 \quad (1.2)$$

Equations (1.1) and (1.2) give:

$$k (kE(k))^{3/2} = \epsilon$$

or

$$k^{5/2} E(k)^{3/2} = \epsilon$$

from which we can see that

$$E(k) = \epsilon^{2/3} k^{-5/3} \quad (1.3)$$

Equation (1.3) is the famous 'Kolmogorov's 5/3' rd law.

This approach helps us to predict the quasi-stationary spectral behavior in the inertial range. In two-dimensional inviscid fluid turbulence, apart from energy, a quantity called enstrophy is also a conserved quantity. Enstrophy Ω , is the volume integral of vorticity ($\vec{\omega} = \nabla \times \vec{v}$) squared. i.e

$$\Omega = \int (\omega)^2 dV \quad (1.4)$$

Based on this we can work out the enstrophy spectrum as:

$$\Omega_k = k^2 v_k^2$$

or, using the equation (1.2),

$$\Omega_k = k^3 E(k)$$

using the kolmogorov 5/3 rd law for the energy spectrum $E(k)$, we get

$$\Omega_k = k^{4/3} \quad (1.5)$$

Looking at the spectral dependence it can be seen that the enstrophy Ω with its k dependence as $k^{4/3}$ will dominate at large k or small spatial scales, whereas the kolmogorov energy spectrum $E(k) \propto k^{-5/3}$ will dominate at small k . Upon inclusion of dissipation, these invariants would decay. The decay rates are not necessarily the same. Since Ω is concentrated mostly on small scales, it would dissipate faster than energy. Eventually two different inertial subranges are formed wherein we find different energy spectra depending on the type of spectral dependence of the invariant with the scales. For 2D turbulence, in the inertial range corresponding to enstrophy, we have :

$$(kV_k)(k.V_k)^2 = \epsilon' \quad (1.6)$$

Combining the above equation with equation (1.2) we have

$$k^3 (kE_k)^{3/2} = \epsilon'$$

or

$$k^{5/9} E_k^{3/2} = \epsilon'$$

leading to :

$$E(k) = \epsilon'^{2/3} k^{-3} \quad (1.7)$$

These relations are based on the fact that enstrophy exchange rate ϵ' is constant like the energy exchange rate ϵ . Thus energy is expected to cascade towards larger scales and enstrophy would cascade towards smaller ones. This is a case for *Inverse Cascade of Energy*.

The foregoing discussion pertains to the *selective dissipation hypothesis*, wherein the system is said to relax towards a state of equilibrium with one invariant almost constant and the other decaying rapidly. For example in the 2D case enstrophy suffers larger dissipation than energy [11]. This problem of optimizing the state can be treated variationally.

There is a direct numerical evidence showing that the above kolmogorovic arguments coupled with the selective dissipation hypothesis are correct. Lilly et al [12] have shown such a behavior in their extensive numerical simulations. It would be natural to ask whether such an inverse cascade could occur in a three-dimensional medium. This question was not answered in the affirmative till recently . The reason being the lack of knowledge of invariants analogous to enstrophy in the 2D case. It is only a recent realization that the helicity related invariants viz..helicity - helicity correlation , is a robust invariant.

An example of Inverse Cascade in 3 D Magnetohydrodynamics (MHD) is provided by the 'dynamo - model' for generating large scale magnetic fields from small scale seed fields (see for example, the review on Galactic Magnetism, by Beck et al, [13]). The basic magnetic induction equation is :

$$\frac{\partial \vec{B}}{\partial t} = \nabla \times (\vec{v} \times \vec{B}) + \eta \nabla^2 \vec{B} \quad (1.8)$$

Where η is the magnetic diffusivity of the medium (inversely proportional to the electrical conductivity), \vec{v} is the turbulent velocity field. We decompose \vec{B} in the form

$$\vec{B} = B_0(\vec{x}, t) + b(\vec{x}, t)$$

where \vec{B}_0 is the 'mean' field varying on a scale l of the turbulence. The mean and fluctuating parts of (1.8) are then:

$$\frac{\partial \vec{B}_0}{\partial t} = \nabla \times \vec{\epsilon} + \eta \nabla^2 \vec{B}_0 \quad (1.9)$$

$$\frac{\partial \vec{b}}{\partial t} = \nabla \times (\vec{u} \times \vec{B}_0) + \nabla \times \vec{G} + \eta \nabla^2 \vec{b} \quad (1.10)$$

where $\vec{\epsilon} = \langle \vec{u} \times \vec{B} \rangle$ and $\vec{G} = \vec{u} \times \vec{B} - \vec{\epsilon}$. Equation (1.10) establishes a linear relationship between \vec{b} and \vec{B}_0 and so between $\vec{\epsilon}$ and B_0 . This relationship in general admits expansion in the form :

$$\epsilon_i = \alpha_{ij} B_{0j} + \beta_{ijk} \frac{\partial B_{0j}}{\partial x_k} + \dots \quad (1.11)$$

where the pseudo tensor coefficients α_{ij}, β_{ijk} etc.. are determined by the statistical properties of the turbulence and the parameter η . Explicit determination of these coefficients requires solution of the fluctuation equation (1.10). The simplest situation is that in which the magnetic Reynolds number of the turbulence, $R_m = u_0 l / \eta$, is small (u_0 being the root mean square velocity). In this case the term $\nabla \times \vec{G}$ in equation (1.10) can be neglected, and the resulting linear equation may be solved by standard Fourier techniques. The result for the leading coefficient α_{ij} is :

$$\alpha_{ij} = \eta \int \frac{k_i k_j H(k, \omega)}{\omega^2 + \eta^2 k^4} dk d\omega \quad (1.12)$$

where $H(\mathbf{k}, \omega)$ is the "helicity spectrum" of the turbulence, i.e the Fourier transform of the quantity

$$\langle i\vec{u}(\mathbf{x}, t) \cdot \vec{\omega}(\mathbf{x} + \mathbf{r}, t + \tau) \rangle$$

This spectrum obviously has the property

$$H = \langle \vec{v} \cdot \vec{\omega} \rangle$$

Therefore we find a direct relationship between the helicity spectrum function and the leading order term in the important expansion (1.11). If the turbulence is isotropic (in a weak sense, to indicate invariance under rotations of the frame

of reference, but not necessarily under parity transformations) then the mean field equation (1.9) takes the form

$$\frac{\partial \vec{B}_0}{\partial t} = \alpha \nabla \times \vec{B}_0 + (\eta + \beta) \nabla^2 \vec{B}_0 \quad (1.13)$$

where we have assumed that α , and β are uniform and constant, as appropriate for turbulence that is homogeneous and statistically stationary. It is easy to see that this equation admits unstable solutions.

The above equation shows that on large scales the viscous term is relatively weaker than the 'curl' term. Thus for any large-scale perturbation there can exist modes which grow, leading to a subsequent amplification of magnetic field. The coefficient α associated with the growing term vanishes for a fully isotropic medium, thus emphasising the fact that some anisotropy is needed for the dynamo to work. The presence of helicity, $h = \vec{v} \cdot \nabla \times \vec{v}$ helps in bringing about such conditions.

A striking analogy exists between the above induction equation for magnetic fields and the vorticity equation for a fluid.

$$\frac{\partial \vec{\omega}}{\partial t} = [\nabla \times [\vec{v} \times \vec{\omega}]] + \nu \nabla^2 \vec{\omega} \quad (1.14)$$

For a fluid too the presence of helicity helps in more ways than one. First helicity is an invariant for an inviscid fluid and it is related to the knottedness of the vorticity-field. Second it has also been widely conjectured that any local concentration of helicity in a fluid stems the downward cascade of energy. The idea behind this conjecture is that the normal cascade of energy from the energy containing large scales to the energy draining small scale is attributed to the intensity of the $\vec{v} \cdot \nabla \vec{v}$ term in the Navier - Stoke equation. The convective term may be re-written as :

$$(\vec{v} \cdot \nabla) \vec{v} = \vec{v} \times \vec{\omega} + \nabla(v^2/2)$$

it follows that presence of helicity i.e an alignment of \mathbf{v} and $\boldsymbol{\omega}$ implies smallness of $\mathbf{v} \times \boldsymbol{\omega}$ and therefore the weakening of the non-linear term which would in turn imply a retardation of energy decay towards small scales. Many numerical simulations have borne evidence to this idea, thus establishing a definitive connection between helicity and the retarded energy decay process.

The basic scenario of inverse cascade is based on the pertinent observations that coherent structures are inherently helical. But it is likely that most of the natural flows have zero net helicity, though they may have a random distribution of helicities

Under such circumstances it may nevertheless happen that the higher moments of the helicity distribution are constant and exert an influence on the statistics of the flow. Suppose for example that the space is divided into cells V_i bounded by surfaces S_i (which move with the fluid) on each of which the condition $\mathbf{n} \cdot \boldsymbol{\omega} = 0$ is satisfied (for all t) and let $h^{(i)} = \int_{V_i} \mathbf{u} \cdot \boldsymbol{\omega} dV$ be the net helicity of the flow in the cell V_i . Then each $h^{(i)}$ is an inviscid invariant of the flow. Consider now a large volume V containing many such cells. We may define the moments:

$$H_n = \lim_{V \rightarrow \infty} \frac{1}{V} \sum h^{(in)}$$

and these are all inviscid invariants. H_1 is the mean helicity of the flow as previously defined. If $h^{(i)}$ are randomly distributed with equal probability of positive and negative values, then

$$\sum_i h^{(i)} \simeq V^{1/2}$$

and $H_1 = 0$. However, all even moments (and in particular H_2 are finite and non-zero; and although the mean helicity is zero, the fluctuations about the mean have constant variance. Indeed in many simulations it has been found that helical fluctuations on all scales in a turbulent medium seem to play an important role in deciding the evolution of the flow. A volume of fluid containing helicity - fluctuations seems to dissipate less! Theoretical analysis proves the invariance of the quantity called I , which is defined as follows:

$$I = \lim_{V \rightarrow \infty} \frac{1}{V} \int \langle h(\mathbf{x}) h(\mathbf{x} + \mathbf{r}) \rangle d^3 r \quad (1.15)$$

The conservation of this integral is proved in Appendix B. The invariance of I has important consequences for the classical problem of the isotropic turbulence decay in its initial period. Kolmogorov found the decay laws :

$$u^2 \propto (t - t_0)^{-10/7}; l_p \propto (t - t_0)^{2/7} \quad (1.16)$$

Here $3u^2 \equiv \langle v^2 \rangle$, t is time t_0 is the fictitious time instant ; the 'integral scale' l_p is defined as $l_p \equiv u^{-2} \int_0^\infty \langle v_p(0)v_p(\mathbf{r}) \rangle d\mathbf{r}$ where v_p is the velocity projection on the vector \mathbf{r} .

Kolmogorov assumed the conservation of the Loitsiansky integral Λ

$$\Lambda \equiv \int_0^\infty r^4 \langle v_p(0)v_p(\mathbf{r}) \rangle d\mathbf{r} = \text{const} \quad (1.17)$$

The energy spectrum E_k in the 'two - range model' is given as:

$$\begin{aligned} E_k &= Bk^4 & 0 \leq k \leq k_L \\ &= K\epsilon^{2/3}k^{-5/3} & k_L \leq k \leq k_d \\ &= 0 & k > k_d \end{aligned} \quad (1.18)$$

In this model the conservation of the Loitsiansky integral is equivalent to the time independence of B . Λ and B can only be conserved approximately . Instead if the spectrum in the range of small k can be of the form $E_k = Ck^2$ (Saffman [14]),, where C is conserved, then the two -range model yields

$$u^2 \propto (t - t_0)^{-6/5}; l_p \propto (t - t_0)^{2/5} \quad (1.19)$$

The conservation of C is connected with the momentum conservation by Navier-Stokes equations like the I - invariance , which is connected with the conservation of helicity, and the Loitsiansky invariant which is related to the angular momentum conservation. But the above model is inconsistent with the invariance of I , since it leads to unacceptable results : $u^2 = \text{const}$, $k_L = \text{const}$.

Frenkel and Levich [15] suggested a new *three range model* for freely evolving homogeneous turbulence with high Reynolds numbers, in connection with the conservation of I- the density of mean square helicity. The model is as follows:

$$\begin{aligned} E_k &= Ck^2 & 0 \leq k \leq k_s(t); \\ &= M(t)k^{-q} & k_s(t) \leq k \leq k_L(t) \end{aligned} \quad (1.20)$$

$$\begin{aligned}
& k_s(t) \leq k_L(t) \\
= & K\epsilon^{2/3}(t)k^{-5/3}, \quad k_L(t) \leq k \leq k_d(t)
\end{aligned}$$

The corresponding power law of energy decay was found to be slower than in conventional two-range models for all values of q . The slowness of the decay of energy spectrum derived from the invariance of I means that the flow at any instant of time contains large scale fluctuations such that each of them has a non-zero value of helicity. Then the transfer term $\nabla \times (\vec{v} \times \vec{\omega})$ tends to zero, thus inhibiting the energy cascade to small scales. These large fluctuations of helicity, when the energy cascade to small scales is inhibited, are reminiscent of the picture of 'large eddies' envisaged by Townsend [15].

Thus in a three-dimensional medium apart from energy, I is also an invariant. We can work out the spectral dependence using dimensional arguments as follows: following equation (1.15) , :

$$I \equiv (\vec{v} \cdot \vec{\omega})^2 \times VOLUME \equiv v_k^2 (kv_k)^2 L^3$$

where we have used volume integration for the ensemble averaging . Further using equation (1.2) we can see that

$$I \equiv k^4 E(k)^2 L^3 \equiv kE(k)^2$$

now using $I \equiv \int I(k)dk$ we have from the above equation

$$I(k) \equiv E(k)^2$$

Alternatively it has been shown that for a quasi - gaussian distribution of helicities, the $I(k)$ spectrum would look like:

$$I(k) \propto E(k)^2 \propto k^{-10/3}$$

Because of the steeper dependence on k it can be inferred that the I invariant dominates towards larger scales and the energy $E(k) \propto k^{-5/3}$ dominates at comparatively small scales. Translating the spectral law to physical space we find: (Refer to

Chapter 2 for the detailed derivation)

$$E(l) \propto \text{Log}(l/l_z)$$

where l_z is any arbitrary normalizing length scale. This implies that very little energy is carried up to large scales. But with such a cascade more and more scales get involved in a correlated motion. But such a growth is restricted in the vertical direction by gravity or buoyancy. The largest vertical dimension of a fully 3D structure is given by the ratio

$$L = \frac{I}{E^2} \equiv L_z$$

, where L_z is the characteristic vertical scale. When the correlation length of helicity fluctuations reaches the limit L_z , it can only grow in the horizontal plane. The system becomes more and more anisotropic due to this. Under these circumstances, the vertical component of velocity v_z , becomes independent of (x, y, z) and the horizontal components v_x and v_y become independent of z leading to $\omega_{x,y} = (\nabla \times \vec{v})_{x,y} = 0$. The I invariant then becomes

$$\begin{aligned} I &= \int \langle (v_z \omega_z)^2 \rangle dx dy dz \\ &= L_z \langle v_z^2 \rangle k^2 v_k^2 k^{-2} \\ &\propto v_k^2 = k E(k) \propto L^{2/3} \end{aligned} \quad (1.21)$$

From $I = \int I(k) dk$, it follows that, $I(k) \propto k^{-5/3} L$, now refers to the length scale in the horizontal plane. The $I(k)$ spectrum here coincides with the energy spectrum of 2D turbulence $E(k) \propto k^{-5/3}$, corresponding to the inverse cascade. One expects that an increasing fraction of energy is transferred to large spatial scales as the anisotropy in the system increases. The growth of large structures in a highly anisotropic turbulence can be interrupted as a result of symmetry breaking caused by Coriolis force. The length scale L_c where the non-linear term of the Navier- Stokes equation becomes comparable to the Coriolis force can be determined from

$$(\vec{v} \cdot \nabla) \vec{v} = 2(\vec{v} \times \Omega) - \Omega \times (\Omega \times r)$$

or $L_c = v/\Omega$, where Ω here is the angular velocity. Given Sufficient energy, structures of size L_c must form. At these large spatial scales, the system simulates 2D behavior and the enstrophy conservation begins to play a role. One may consider scales $L \geq L_c$ as a source of vorticity injection into the system. The enstrophy then cascades towards small scales with a power-law spectrum given by

$$E(k) \propto k^{-3} \text{ and } E(L) \propto L^2 \quad (1.22)$$

Thus there is a break in the energy spectrum, as energy must cascade to larger spatial scales as $L^{2/3}$ and to small scales as L^2 . The energy must therefore accumulate at $L \simeq L_c$ and eventually pass on to the highest possible scales of the general circulation of the structure.

Since the larger structures are formed by an inverse cascade process their energy should definitely not exceed the energy contained in the small scales . This argument leads to an upper limit to the scale on which structures can be formed. In the case of the earth's atmosphere this has lead to a conclusion that structures on the scale of 300 km can be formed starting from clouds of the size of say 3 km.

In conclusion, we learn using the dimensional arguments of Kolmogorov that the energy spectrum consists of several branches; beginning with $k^{-5/3}$ at small scales, going as k^{-1} , then again as $k^{-5/3}$ to k^{-3} at the largest scales. Evidence for such a spectrum has been seen in atmospheric turbulence. We reproduce the entire spectrum below.

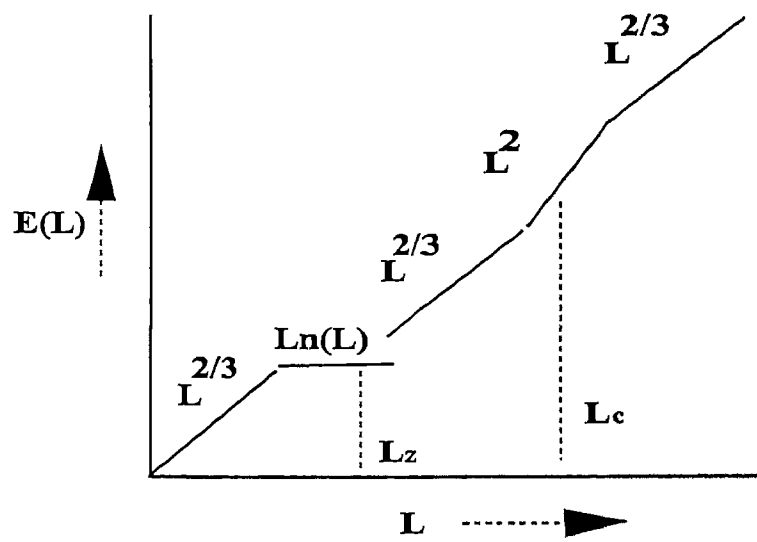


Figure 1.1: The complete turbulent energy spectrum. L_z - scale of the first break due to anisotropy; L_c - scale of the second break due to the Coriolis force.

The same spectrum has also been employed by Krishan [16], and Krishan and Sivaram [17], to explain the hierarchy of structures that have been observed on the solar atmosphere as well as for the hierarchy of structures observed in the universe. (See also [18] [19]).

Further in this thesis we shall be studying the role played by $Log(l)$ branch, in explaining the flat rotation curves of spiral galaxies.

1.3 Turbulence - the Navier - Stokes way

In the preceding section we have seen how the quasi steady-state energy spectra could be derived with the use of simple dimensional arguments. We would, in fact, wish to obtain a more rigorous proof for all that which the Kolmogorovic arguments lead us to. That is, we would expect our system of equations for a fluid ..viz.. the momentum equation - the Navier- Stokes equation, and the mass- conservation equation , continuity equation,- to yield such an energy distribution in the course of evolution of a turbulent fluid. In fact , simple as it may seem , the problem of turbulence addressed this way, leads to tremendous problems both of the analytical and conceptual kind. The Navier - Stokes equation is plagued with non-linearities generated by the advective term $(\vec{v} \cdot \nabla) \cdot \vec{v}$.

If a turbulent medium is treated in a statistical sense of considering averages only implementing the ideas of Reynolds-averaging, we encounter a *closure problem* . By this we mean that whatever we do we are always left with more unknowns in our system of equations than the number of equations ! There is no way around this problem. The only alternative is to artificially close the system of equations with empirical inputs or some other *closure hypothesis* for dealing with the averages .

Apart from this statistical approach, there are only a handful of specific situations where the Navier-Stokes equations can be solved exactly. In general, the only alternative is the Direct Numerical Simulation ! Even on the Computing front the picture is not all that bright. It calls for a huge computing infrastructure to verify what Kolmogorov predicted with his brilliant insight. Today, we are just beginning

to have a glimpse of success , for the Kolmogorov spectrum is well- observed in some of the recent numerical simulations [20].

Khomenko et al [21] have, using a statistical approach, shown that the compressible turbulence can give rise to large scale structures, through an effect analogous to the Alpha Effect for the generation of large scale magnetic field. They call it the Hydrodynamic Alpha Effect ! They treat such a phenomena as a case for the origin of structures in non-equilibrium systems, turbulence being regarded as one of the most widespread distributed non-equilibrium system in nature. Since, there generally is an external scale which feeds energy into the system , and a dissipation scale where the energy is dissipated into heat, the turbulent system is regarded as an *open system*. Their statistical analysis leads to the result that if the turbulence is considered to be helical i.e homogeneous, isotropic, but without being invariant under reflection, then the vorticity equation for the mean flow does exhibit a growing large scale instability. The evolution is accompanied by the transfer of energy from small-scale to large-scale sizes. They emphasize that *the structures so generated are not relics of the average flow as the von Karman vortices and the instability is not a modification of the instability of shear flows. What plays an important role is the fact that the turbulence is not invariant under reflection.* In such circumstances the velocity correlators are expressed in the following form :

$$\langle V_i(\mathbf{x}_1, t_1) \cdot V_k(\mathbf{x}_2, t_2) \rangle = K_{ij}(\mathbf{x}_1, \mathbf{x}_2) \phi(t_1 - t_2)$$

where $\mathbf{r} = \mathbf{x}_1 - \mathbf{x}_2$ and

$$r = |\mathbf{x}_1 - \mathbf{x}_2| = \sqrt{\sum_i (x_{1i} - x_{2i})^2} = \sqrt{(r_i)^2}$$

The spatial part of the correlator is expressed as:

$$K_{ij}(x_1, x_2) = C(r) \delta_{ij} + B(r) r_i r_j + g(r) \epsilon_{ijk} r_k$$

The last term $g(r)$ is the consequence of the fact that the turbulence is not invariant under reflection (helical), while $g(0)$ has the meaning of the average value of the product of the turbulent velocity and its curl. Let us calculate the average helicity $\langle \gamma \rangle$ as:

$$\begin{aligned}
\langle \vec{v} \cdot \vec{\omega} \rangle &= \langle \vec{v} \cdot (\nabla \times \vec{v}) \rangle \\
&= \lim_{x_1 \rightarrow x_2; t_1 \rightarrow t_2} \frac{\partial}{\partial x_{2i}} \epsilon_{ijk} \langle v_j(x_2, t_2) v_k(x_1, t_1) \rangle \\
&= \lim_{r \rightarrow 0} \epsilon_{ijk} \left[\frac{-r_i}{r} \right] \frac{\partial}{\partial r} (C(r) \delta_{jk} + B(r) r_j r_k + g(r) \epsilon_{jkl} r_l) \phi(t_1 - t_2) \\
&= \lim_{r \rightarrow 0} (-1) \epsilon_{ijk} \epsilon_{jkl} \left[\frac{g(r)'}{r} r_i r_l + g(r) \delta_{il} \right] \phi(0) \\
&= -6g(0) \phi(0)
\end{aligned} \tag{1.23}$$

Thus it can be seen that $g(0)$ relates to the average helicity. We can also obtain the equation for the evolution of the mean velocity as well as the mean vorticity, for a turbulent medium. For doing so, we need to write the instantaneous fluctuating quantities as

$$\text{instantaneous value} = \text{mean value} + \text{fluctuation}$$

Next, the Reynolds averaging approach is adopted. This allows us to separate the equations for the mean and the fluctuations. Ignoring higher order quantities in the equations we finally arrive at equations which look like [70]:

For the mean velocity :

$$\frac{\partial \langle \vec{v} \rangle}{\partial t} - \frac{1}{2} g(0) [\nabla \times \langle \vec{v} \rangle] = \nu' \nabla^2 \langle \vec{v} \rangle - f(\rho_0) \nabla \langle \rho \rangle \tag{1.24}$$

where the quantities inside the brackets ' $\langle \rangle$ ' are ensemble averages, and ρ_0 is some constant density, ν' is renormalised viscosity

$$\nu' = \nu + \frac{1}{4} C(0)$$

ν being the original molecular viscosity which is used in the Navier-Stokes equation, and $C(0)$ is the correlation coefficient as shown earlier. $f(\rho_0)$ is some function of ρ_0 , which we do not need here. taking the curl of the above equation (1.24) we can get the equation for the evolution of mean vorticity $\langle \vec{\omega} \rangle$ as follows:

$$\frac{\partial \langle \vec{\omega} \rangle}{\partial t} - \frac{1}{2} g(0) [\nabla \times \langle \vec{\omega} \rangle] = \nu' \nabla^2 \langle \vec{\omega} \rangle \tag{1.25}$$

First we note that in the above equation that *if helicity vanishes, the large scale configurations are damped out*. Let us look for solutions of the kind:

$$\langle \vec{\omega} \rangle = \langle \vec{\omega}_k \rangle e^{i(\omega t + \mathbf{k} \cdot \mathbf{x})} \quad (1.26)$$

upon substitution in the equation (1.25) we get,

$$i\omega \langle \vec{\omega}_k \rangle - \frac{1}{2}g(0) [i\vec{k} \times \langle \vec{\omega}_k \rangle] = \nu' (ik)^2 \langle \vec{\omega}_k \rangle \quad (1.27)$$

Multiply both the sides of the above equation by (-i), take the dot product with the same vector on each side and use the fact that $i\vec{k} \cdot \hat{\omega}_k = 0$ (since $\nabla \cdot \vec{\omega} = 0$, the $\hat{\omega}_k$ indicates unit vectors.), we get the following dispersion relation :

$$(\omega - i\nu' k^2)^2 = \frac{-1}{4}g(0)^2 k^2 \quad (1.28)$$

and hence for the growth rate $\gamma = i\omega$, looking for unstable solutions we get,

$$\gamma = -\nu' k^2 + \frac{1}{2}|g(0)|k \quad (1.29)$$

The maximum growth rate γ_{max} occurs for a wavenumber k_0 ,

$$k_0 = \frac{|g(0)|}{4\nu'}$$

and equals

$$\gamma_{max} = \frac{g(0)^2}{16\nu'}$$

We note that large-scale structures can develop, provided the helicity is non-zero. The size of the structure with the maximum growth rate is given by k_0 . We find that the size L of the dominant structures is proportional to the ratio of $C(0)(\alpha \langle v^2 \rangle)$ to $g(0)$, that is *to the ratio of the energy invariant to the topological (helicity) invariant*.

Moiseev et al. show that the linearized equation for the mean vorticity has the same form as the appropriate α effect equation in the mean field electrodynamics viz:

$$\partial_t \vec{\omega} + \alpha \nabla \times \vec{\omega} = \nu \nabla^2 \vec{\omega}$$

the uniform coefficients α and ν are related to the random velocity field parameters. The second term leads to the exponential growth of vorticity. The idea that the

helicity of the turbulence may influence the energy transfer from small scales to large ones has been discussed by Kraichnan [23], Brissaud et al [24], Andre and Leisur [25], and Moffat [26], but the averaged equations were not derived in these papers and so the large scale instability was not talked about.

Later people like Sagdeev, Moiseev, Tur, Gvaramadze, Khomenko, Frisch and Sulem and many others found examples of alpha effect in hydrodynamics. They had considered the incompressible case. In all cases some additional factors, such as inhomogeneous regular flow, stable or unstable stratification, gravity force or anisotropy must supplement helical turbulence to provide the instability. The α term in these cases assumes a tensorial nature α_{ij} instead of a scalar form as in the above equation.

The characteristic size of the unstable scale is found to be : $L^{-1} = \frac{\langle \mathbf{v}^t \nabla \times \mathbf{v}^t \rangle}{\langle (\mathbf{v}^t)^2 \rangle}$, which is just a ratio of the two invariants viz.. helicity and energy. Thus the characteristic scale on which structures form is determined by the 'natural' characteristics of turbulence, its invariants, and it is an internal property of turbulence itself. Also it is to be noted that the structures thus generated are helical themselves for they are characterized by a non-vanishing scalar product related to the helicity.

There are some perturbation techniques at our disposal, with which we can study the weakly nonlinear regimes of the equations to understand the stability, of the flows that ensue. We shall elaborate Frisch's multiscale approach, here to understand that there are situations wherein a large scale instability may be generated. Assuming that the basic flow $\mathbf{u}^{(0)}$ is driven by a time - dependent space and time periodic force (in the deterministic sense), or a random homogeneous and stationary force, $f(\mathbf{r},t)$, the equations in the incompressible case assume the form :

$$\partial_t u_i^0 + \partial_j (u_i^0 u_j^0) = -\partial_i p^0 + \nu \nabla^2 u_i^0 + f_i \quad (1.30)$$

Let l_0 and t_0 be the characteristic spatial and temporal scales of the basic flow, and V_0 the velocity amplitude. The $R = \frac{l_0 V_0}{\nu}$ is the small scale Reynolds number. Also assume $\langle \mathbf{f} \rangle = 0$. Now, perturb the basic flow $\mathbf{u}^0 \rightarrow \mathbf{u}$ with a large scale component such that $\mathbf{w} = \langle \mathbf{u} \rangle$, is assumed to vary on scale $L \gg l_0$ and time $T \gg t_0$. The small scale flow $\tilde{\mathbf{u}} = \mathbf{u} - \mathbf{w}$ which is advected by the mean flow satisfies the following equation:

$$\partial_t \tilde{u}_i + w_j \partial_j \tilde{u}_i + \partial_j (\tilde{u}_i \tilde{u}_j) = -\partial_i \tilde{p} + \nu \nabla^2 \tilde{u}_i + f_i \quad (1.31)$$

We may assume \mathbf{w} to be uniform and constant in the equation (1.31). The small scale Reynolds stresses $R_{ij} = \langle \tilde{u}_i \tilde{u}_j \rangle$ then become dependent on the \mathbf{w} and thus contribute to the large scale dynamics. The large scales obey the following equation:

$$\partial_t w_i + \partial_j (w_i w_j + R_{ij}) = -\partial_i p + \nu \nabla^2 w_i \quad (1.32)$$

To solve the above equation we must actually calculate the Reynolds stresses. To do so, we are required to solve for the small scales first. The equation for perturbed small scales may either be solved by using an expansion in powers of small scale Reynolds number or numerically. The equation (1.32) is referred to as the AKA equation. If the mean field is weak, the Reynolds stresses may be Taylor-expanded as follows:

$$R_{ij} = \langle u_i^0 u_j^0 \rangle + w_l \left[\frac{\partial \langle \tilde{u}_i \tilde{u}_j \rangle}{\partial w_l} \right]_{w=0} + O(w^2). \quad (1.33)$$

We may obtain the perturbed small scale flow from a linearized version of eq. (1.31) and use it to obtain the linearized AKA equation:

$$\partial_t w_i = \alpha_{ijl} \partial_j w_l - \partial_i p + \nu \nabla^2 w_i \quad (1.34)$$

with $\alpha_{ijl} = -\left[\frac{\partial \langle \tilde{u}_i \tilde{u}_j \rangle}{\partial w_l} \right]_{w=0}$. The tensor α_{ijl} may vanish in many circumstances viz.

- i). when the basic flow is parity-invariant
- ii). when the basic flow is random isotropic
- iii). when the basic flow is time independent, then the tensor calculated perturbatively in powers of the Reynolds numbers, vanishes to leading order.
- iv). when the basic flow is random and delta-correlated in time
- v). for ABC flows (i.e Beltrami flows).

Frisch. et al.,[27] consider a specific example with a particular forcing function which produces a flow lacking parity-invariance to show the growth of large scale structures from Reynolds stresses generated by small scales.

1.4 Astrophysical Turbulence

The scope of the new ideas and developments outlined in the preceding sections are by no means limited to the field of fluid dynamics only. With the range of scales ranging from a few parsecs to Megaparsecs and thus unimaginably large Reynolds number flows, the field of astrophysics could serve as a rich test bed for models which aim at understanding the complex order that has been observed over the years. Be it the identification of large scale structure of the universe or the solar granulation or the highly complex hierarchy of structures seen in the galactic environment, all such cases lack the backing of a unifying model.

The numerous N-body simulations with Hot and Cold dark matter compositions of varying proportions (Mixed or warm dark matter too !!) have failed to elicit the underlying mechanism for the formation of the hierarchy of structures around us viz.. the assumption of a homogeneous and isotropic universe has proved out to be a false one even on the largest observable scale [28],[29],[30],[31],[32]. Added to this, the origin of angular momenta of galaxies still eludes a viable solution [33], [34], [35]. The gravitational tidal torques also do not explain the spin of galaxy fully. There is factor of 2-10 discrepancy in this regard. As explained by Shu these problems demand the consideration of other 'non-gravitational' mechanisms for trying alternative ways to understand these problems. Fluid -dynamic processes offer richer and hitherto unexplored ways of generating vorticity, (and thus the spin of the galaxy) [36], [38]. The possibility of considering the galaxy as equivalent to a gaseous disk with fluid properties were already explored earlier by Hunter. This permits us to study the role of the new developments in fluid dynamics with the same model of a galaxy. This certainly opens up the possibility of understanding the dynamics of the galaxy with respect to generating structures and 'ordered flows'. Besides there is considerable amount of work done on aspects of interstellar turbulence, both from a theoretical as well as observational point of view [39]-[45]. Recent studies have also shown that the statistical properties of turbulence in molecular clouds seem to be remarkably similar to those determined from numerical simulations of ordinary compressible turbulence! [46].

1.5 Primordial Turbulence

The possibility of a turbulent beginning to the universe was long thought of by none other than von Weizsacker, Gamow, Ozernoy, Chernin and others. Gamow [3] realised that there need to be some source of seed - perturbations which could later be amplified by gravitational instability mechanism to evolve into structures of the present day. The statistical fluctuations of the thermodynamic nature, if they had arisen during the non-relativistic phase of the expansion of matter, would not have been able to grow in an expanding universe to a value at which they would have been capable of forming gravitationally bound systems. (The case for an N body system to generate sufficient seed perturbations was well exemplified by Bonnor). Bonnor's study showed that for a collection of $N=3 \times 10^{67}$ molecules of an ideal gas (typical for a nebula of hydrogen) if the initial perturbation was taken to be of the order of $N^{-1/2}$ i.e 10^{-34} in this case , then even after 1000 yrs from the singular state the amplitude would have grown to only 10^{-29} . Thus it was concluded that *small perturbations cannot grow into nebulae in the time available* [47]. This was contrary to the analysis of Jeans who showed that it was possible that the initial perturbations could amplify exponentially in a gravitationally unstable static medium. Bonnor identified the flaw in Jean's analysis due to his assumptions of a static universe, and concluded that the growth of perturbations in an *expanding universe model* was in fact much slower. From another point of analysis von Weizsacker studied the parameters for the interstellar gas and concluded that since the observed velocity difference at scales of the size of molecular clouds and HII regions could not be those generated by their thermal fluctuations, these motions had to be attributed to a compressible turbulent medium. Compression meant that the velocity fluctuations could give rise to density fluctuations, and turbulence meant irregular fluctuations of velocity. The thin filamentary structure of the Pleiades nebula on scales of 10^{15} cm (which is a reflection nebula) forced one to think that even if the mean free path of the dust particles was of the order of 10^{20} cm, it was the coupling of the dust with the gas which could by virtue of its turbulent state lent it's velocity fluctuations to the dust. This was because the observations were made in absorption spectrum which signify velocity fluctuations and thus reflect

the kinematical pattern of the medium. Considering the fact that the stellar systems of the present day could not however be treated as hydrodynamic systems von Weizsacker did emphasize that they could have originated in a turbulent environment though. He argued that in a galaxy an equipartition of energies of the single stars cannot be reached within a few billion years. But the fact that the systems actually seem to have reached equipartition, indicates that *such a state is easily reached when the matter is not yet united in stars because then the high turbulent momentum transfer is available*. Therefore the sort of degree of equipartition in a system which is not dense enough to achieve it by stellar interactions, may give a hint as to the stage of evolution of the system in which its gas was transformed into stars. He then invoked the primordial role of turbulence in producing such irregularities [2]. The issue then was when exactly could turbulence be invoked. If it was put in the post de-coupling era ..it would decay much faster even before structures form . If it was invoked in the era when matter and radiation were coupled, then it could produce a spectrum of irregularities in the Cosmic Microwave Background radiation which could be used to constrain its amplitude. The major issue involved was the production of density irregularities ..through velocity perturbations provided by turbulence. That could be only achieved if we could somehow generate longitudinal velocity fluctuations . from purely vortical ones. The vortical velocity perturbations were assumed to be either induced by thermal - instabilities (Tomita)[48] , or due to photon turbulence in the radiation- dominated era (Ozernoi [49]).

Tomita et al. studied the decay laws of primordial turbulence and derived the heating rates by its dissipation in an expanding medium . They showed that matter could not be maintained at the required temperature of $10^5 K$ which was necessary for the sustenance of turbulence and thus galaxy formation by thermal instability. They concluded that in the absence of any heating mechanism the matter temperature drops faster than the radiation temperature after the epoch of decoupling (i.e at $T_r = 4000 K$). In the matter dominant stage the excess of thermal energy is rapidly carried away by the Compton scattering process thus aiding in lowering the matter temperature further. Oort [50] pointed out another attractive feature of cosmic turbulence that a large-scale turbulent eddy might bring matter together in such a

fashion that the galaxies are formed in close association that has positive total energy. Thus we could witness the formation of structures which are close together but which are not gravitationally bound. Peebles [4] analysed the case for primeval turbulence stressing that the assumption of the velocities after matter decoupling was important in studying the after effects of mater turbulence . He found that if weak velocities were assumed (*weak turbulence*) then the model couldn't generate enough angular momentum at galactic scales (keeping the restrictions on the growth of density contrast). There was almost an order of magnitude difference between the observed and predicted values. Peebles ruled out the possibility of any accumulated computation error or the assumptions linking the perturbation-growth to the development of proto-galaxies or any inconsistency in the arguments forwarded for the statistical calculations of root mean square velocity in his analysis. On the other hand if very large velocities were assumed then the matter evolution would be a highly compressible one which can't be resisted by any source of thermal pressure . Thus turbulence would decay faster than before and thus end up forming structures (which are much denser than galactic densities) much earlier than expected. Peebles does conclude that there could be other possible (but fancier) conclusions in favour of turbulence but ends up concluding that the *the most straightforward conclusion would appear to be that there was not a primeval strong turbulence.*

Ozernoy et al.[49],[51], pointed out that there could exist a range of scales for cosmic turbulence in the radiation - dominated era which could carry over to the matter dominated era to produce shocks and thus generate density perturbations. The gravity of the plasma in the radiative phase was found to be ineffective in causing a perturbation. So, photon - induced turbulence was adopted.

They developed the view according to which the existing peculiar motions of galaxies reflected (like their internal motions) an initial vortical state of the *metagalactic substratum*. In their proposed 'photon-eddy ' hypothesis they concluded that the actual density irregularities were a result of the post-matter-radiation-decoupling effect, due to which the sound velocity of the medium drops drastically and thus generating strong density fluctuations from potential motions. On larger scales the contrast would have been considerably small and these scales participate in the hub-

ble expansion. Hydrodynamic instability is found to constitute the dominant aspect of the proposed mechanism, whereas gravitational instability would have become important only at a relatively late stage.

Ozernoi and Chibisov [52] considered the isolation of protogalaxies from the expanding medium (after virialisation of the kinetic energies) by allowing for the adiabatic cooling of the macroscopic motions due to cosmological expansion. Here the hydrodynamic damping is compensated by energy inflow from larger scales, including the largest scale of all, where the decline in energy is governed by the cosmological expansion. The basic cosmogonic parameters derived in this analysis viz. galaxy radius - mass relation, specific angular momentum - mass relation matched quite well with observations. They also conjectured that *spiral galaxies will be formed in regions of medium having primarily vortical motions, while elliptical galaxies will appear in regions with predominantly irrotational velocities*. Later Ozernoi [53] also considered the growth of clusters by gravitational instability, after the generation of these from the rotational component of the post-recombination turbulent era (by induced irrotational component due to shock-wave formations when sound velocity drops by a large magnitude). The epoch of isolation of rich clusters matched well with that inferred from observations. A comparison of the observed relation between the mean virial density of cluster systems with the size, especially with the data of Humason, Mayall, Sandage de Vaucouleurs and Holmberg (all systematized by Karachentsev) also revealed a striking resemblance to similar relations derived by the model, despite its simplicity. This work also successfully explained the observed relationship between the mean density of a cluster and its morphological type.

At this point we would like to point out that a very comprehensive review on the subject of origin of galaxies involving both the view points viz.. Gravitational Instability Picture, and the Cosmic Turbulence Theory, has been written by Jones [54]. It contains a very good introduction to both cosmology and cosmic-hydrodynamics as well. But since much has been achieved in the understanding of turbulence since the 80's we must bear in mind that the 'turbulence picture' is incomplete.

There were some pertinent difficulties with theories of *primordial cosmic turbulence* viz. 1) The amplitude of the turbulence required to explain the large-scale

structure was in conflict with the observed high degree of isotropy of the microwave background radiation. 2) Following recombination, the turbulence would have become supersonic and produced too large density contrasts on scales of galaxies and clusters of galaxies 3) A specific physical picture which would have explained the *generation of turbulence in the first place* was lacking.

So, the conflict with well established observations scuttled any hope of incorporating turbulence in the models of the universe. But the recent work of Goldman and Canuto [55] has addressed these problems in the light of inflation. Their work has revived the possibility of re-considering the role of cosmic turbulence as a viable theory for understanding cosmic structure. Goldman and Canuto have argued that inflation naturally provides mechanisms for the direct generation of turbulence on the same scales on which density perturbations are formed. They find that by the end of inflation, the amplitude of the generated turbulent velocity is suppressed by a factor of 10^{100} thus avoiding the conflict with observations of CMBR fluctuations. They have shown that the density fluctuations generated by inflation can excite longitudinal turbulence after they reenter the Hubble radius at the later cosmic epochs. The scales on which this happens are much smaller than those of galaxies. The largest scale corresponds to a present epoch size of $\leq 6.3 Kpc$ and contains a mass of $\leq 3.6 \times 10^4 M_{\odot}$. This turbulence can have an important impact on the formation of structure on scales of galaxies and clusters of galaxies mainly because any part of the turbulence that survived dissipation by the radiative viscosity will become supersonic following the decoupling time. Shock collisions will lead to large density contrasts, and such an early population of objects of the above mass can serve as a seed that could help the growth of density on the scales of galaxies and clusters of galaxies. Besides, this provides us with a novel setting for considering the inverse-cascade scenarios that may be operational at various levels.

Chapter 2

FLAT ROTATION - CURVES OF GALAXIES

The seemingly disparate phenomena of
(i) non-equilibrium motions on stellar surfaces,
(ii) the generation of large scale magnetic fields, and
(iii) the large scale structure of the Universe ..
have their origin in the inverse cascade of energy
leading to self-organisation in an otherwise
turbulent medium.

- Vinod Krishan -

2.1 Introduction

¹ In this chapter we have modelled the rotation curves of 76 galaxies observed by Amram et. al [56],[57] and Rubin et al. [58],[59] by combining the effects of rigid rotation, gravity and turbulence. The main motivation behind such modelling is to study the formation of coherent structures in turbulent media and explore its role in the formation of large scale structures of the universe. The values of the parameters

¹ *paper appeared in ApJ,428,483 (1994)*

for the galaxies such as mass, turbulent velocity and angular velocity derived from our model are in good agreement with those derived from the prevalent models.

The rotation curves of galaxies have been the subject of great speculation in the recent past. If galaxies are considered as solid bodies in rotation then their rotational velocity must increase in a linear manner i.e $V \propto r$ where r is the radial distance from the center of the galaxy. The trouble arises when the picture of a 'falling curve' as predicted by the Newtonian gravity for the outer region of a galaxy doesn't tally with what is observed. We get a flat rotation -curve on the outer scales. This has given birth to a lot of models which try to account for flat rotation curves. The suggestions include (1) a modification of the Newtonian force(e.g., [61], [62], [63] and references therein), (2) the effect of the magnetic stresses(e.g., [64], [65] and references therein), (3)the presence of a large amount of hidden mass that does the trick ! (e.g., [29], [30], and references therein) . Other recent ideas include treating the rotation curves as consequence of the hydrodynamic characteristics of galactic disks. These studies are based on the assumption that since most of the velocity measurements are derived from emission lines emitted by the galactic gas, (either neutral or ionized), it makes them inappropriate as tracers of the galactic gravitational potential [66] Soares introduces an effective potential meant to describe the hydrodynamics inside a gaseous disk, and using the Tully-Fisher relation [88]- which highlights a tight correlation between the galactic luminosity and it's rotational velocity- as an additional constraint, models the observed rotation of the galaxies. Filippov and Zhedanov [67] on the other hand study a simple model for the dust-media describing evolution of systems like spiral galaxies .Starting with an initial density fold which is quasi- one dimensional (bar-like), unlike the two dimensional disk -like distribution, they find that the disk like feature appears only during the evolution. Their model also naturally reproduces some essential features of the galaxies, in particular, it reproduces all the observed typical forms of the rotation curves for spiral galaxies, with a characteristic minimum and plateau. They interpret the plateau to be corresponding to matter escaping and not bound gravitationally. Similarly, Ambartsumyan also hypothesizes that the star clusters, galaxies, and their clusters are strongly unstable objects which arose as the results of an explosion of some protostar substance [68]. Such a hypothesis rules out

for the galaxies such as mass, turbulent velocity and angular velocity derived from our model are in good agreement with those derived from the prevalent models.

The rotation curves of galaxies have been the subject of great speculation in the recent past. If galaxies are considered as solid bodies in rotation then their rotational velocity must increase in a linear manner i.e $V \propto r$ where r is the radial distance from the center of the galaxy. The trouble arises when the picture of a 'falling curve' as predicted by the Newtonian gravity for the outer region of a galaxy doesn't tally with what is observed. We get a flat rotation -curve on the outer scales. This has given birth to a lot of models which try to account for flat rotation curves. The suggestions include (1) a modification of the Newtonian force(e.g., [61], [62], [63] and references therein), (2) the effect of the magnetic stresses(e.g., [64], [65] and references therein), (3)the presence of a large amount of hidden mass that does the trick ! (e.g., [29], [30], and references therein) . Other recent ideas include treating the rotation curves as consequence of the hydrodynamic characteristics of galactic disks. These studies are based on the assumption that since most of the velocity measurements are derived from emission lines emitted by the galactic gas, (either neutral or ionized), it makes them inappropriate as tracers of the galactic gravitational potential [66] Soares introduces an effective potential meant to describe the hydrodynamics inside a gaseous disk, and using the Tully-Fisher relation [88]- which highlights a tight correlation between the galactic luminosity and it's rotational velocity- as an additional constraint, models the observed rotation of the galaxies. Filippov and Zhedanov [67] on the other hand study a simple model for the dust-media describing evolution of systems like spiral galaxies .Starting with an initial density fold which is quasi- one dimensional (bar-like), unlike the two dimensional disk -like distribution, they find that the disk like feature appears only during the evolution. Their model also naturally reproduces some essential features of the galaxies, in particular, it reproduces all the observed typical forms of the rotation curves for spiral galaxies, with a characteristic minimum and plateau. They interpret the plateau to be corresponding to matter escaping and not bound gravitationally. Similarly, Ambartsumyan also hypothesizes that the star clusters, galaxies, and their clusters are strongly unstable objects which arose as the results of an explosion of some protostar substance [68]. Such a hypothesis rules out

the applicability of the virial theorem to such systems then. Moreover Filippov and Zhedanov also comment that the so called 'rotation curves' do not describe rotation but instead correspond to some complicated kinetic processes in the system. Some others like Mannheim [69] like to think about the possibility that the entire departure of galactic rotational velocities from their luminous Newtonian expectation is cosmological in origin. He shows that within the framework of conformal gravity every static observer sees the overall Hubble flow as a local universal linear potential which is able to account for the available data without any need for dark matter.

The issue of Dark matter has kicked considerable dust in this area, and the gravity of the dark matter appears to be a favorite candidate. This must be tested against its alternatives. Verschuur [32] has revived the old debate of the missing mass versus the missing physics. In fact 'dark matter' has also been dubbed as the *folly of the twentieth century*, similar to the concept of *ether* in the nineteenth century! The appearance of large scale structures in turbulent flows, [70], [22], [27], [71], [72], [73], [11] and references therein) which are stationary, anisotropic and parity-violating has become an exciting prospect potential enough to play a major role in the astrophysical context. The major weakness of all structure -formation models (eg. CDM, Gravitational instability models) till date is their inability to reproduce the large scale structures, observed in the universe (of the order of 100 Mpc). Krishan and Sivaram [17] showed that the clustering and superclustering of galaxies and clusters respectively could be viewed as the outcome of the 'inverse cascade' process in a turbulent medium. Here we model the flat rotation curves of the galaxies by combining the effects of rigid rotation, gravity and turbulence.

2.2 The Inverse Cascade

As reiterated by Scalo, "The properties of the interstellar medium strongly suggest that it is the turbulence in the generalized sense of nonlinear systems which exhibits unpredictable temporal behavior accompanied by self-organizing spatial fluctuations covering a wide range of size scales" [74]. A particularly interesting type of self-organizing behavior occurs in turbulent fluids in which more than one quantity is

conserved, a situation reviewed by Hasegawa [11]. In these cases one conserved quantity becomes spatially chaotic by means of a direct cascade from large scales to small scales, while the other self-organizes into large structures by undergoing an inverse cascade from small scales to large scales [74].

The concept of such an "inverse cascade" is well established for two dimensional flows in fluids as well as magnetohydrodynamic flows [75]. The three dimensional MHD case is also well established. The case for a three dimensional inverse cascade in fluids is gaining ground with the identification of a new invariant I , related to the helicity density. Numerous numerical studies are also corroborating the same viewpoint.

The problem of turbulence is addressed in two ways:

1. The Kolmogorov approach, in which we study the statistically stationary states by dimensional arguments. [73], [17]
2. The Navier Stokes way, in which we look for the solutions of the Navier-Stokes equations hoping that the stationary solutions would comply with the predictions of the former approach [8].

2.3 The Kolmogorov approach

Large helicity fluctuations present in a turbulent medium play an essential role in the inverse cascade of energy in a 3D system. The helicity density γ , a measure of the knottedness of the vorticity field $\vec{\omega}$, is defined as

$$\gamma = \vec{V} \cdot \vec{\omega}, \vec{\omega} = \nabla \times \vec{V} \quad (2.1)$$

It is found that the quantity I , defined as

$$I = \frac{1}{V} \int \langle \gamma(x) \gamma(x+r) \rangle d^3x \quad (2.2)$$

is also an invariant of an ideal 3D hydrodynamic system in addition to the total energy (see Appendix B). On the inclusion of dissipation, these invariants decay differentially.

The nature of the non-linear interaction between the fluid elements is such that the slow decaying invariant (I, here) cascades towards large spatial scales, and the fast decaying invariant (energy, here) cascades towards smaller spatial scales (see section 1.2). By assuming a quasi-normal distribution of helicities the I-invariant can be expressed as :

$$I = \text{const.} \int E^2(k) dk \quad (2.3)$$

Here $E = \int E(k) dk$ is the total energy per unit gram.

In the inertial range for the energy invariant we have, using Kolmogorov hypothesis that energy exchange rate between different scales is a constant,

$$(kV_k)V_k^2 = \epsilon = V_0^2/\tau \quad (2.4)$$

where k = wave number, V_0 is the initial rms velocity on small scales τ is the duration for which this energy is available V_k = velocity in fourier space. ϵ = average energy exchange rate between the scales (ergs/gm/sec).

This, combined with $kE(k) = V_k^2$ yields the well known Kolmogorov spectrum:

$$E(k) = \epsilon^{2/3} k^{-5/3} \quad (2.5)$$

It would be appropriate to comment on ϵ here. Kolmogorov [10] conjectured that in the quasi-steady state there should be a stationary flow of energy in the k space from the source to the sink. Thus the energy transfer rate per unit mass should be a constant and be equal to the dissipation rate at the sink. Although numerous experiments have confirmed that ϵ is a strongly fluctuating quantity, surprisingly there is no experimental evidence indicating a deviation from the Kolmogorov spectrum [76].

The value of ϵ for the Galaxy has been estimated to be of order of 8×10^{-3} ergs $g^{-1} s^{-1}$ by considering the various sources (such as supernovae, stellar winds, etc.) which contribute to the turbulence energetics. In the same vein τ is calculated to be 3×10^7 yrs [77]. From equation (2.5), we find total energy

$$E = \int E(k) dk$$

or in real space

$$E(l) = \epsilon^{2/3} l^{2/3} \quad (2.6)$$

The corresponding velocity field may be described as

$$V(l) = (l_z \epsilon)^{1/3} (l/l_z)^{1/3} \quad (2.7)$$

for some normalizing length l_z . Similarly in the inertial range for the I-invariant, we have

$$(kV_k)(kE^2(k)) = \epsilon' = I_0/\tau \quad (2.8)$$

where ϵ' = the mean square helicity density exchange rate between the scales. Combining this with

$$kE(k) = V_k^2 \quad (2.9)$$

gives

$$E(k) = (I_0/\tau)^{2/5} k^{-1} \quad (2.10)$$

Or in real space:

$$E(l) = (I_0/\tau)^{2/5} \ln(l/l_z) \quad (2.11)$$

Here, the normalizing length l_z marks the transition from one inertial law eq. (2.7) to the other eq. (2.11). The velocity field in this range may be described as

$$V(l) = (\epsilon^2 l_z \tau)^{1/5} (\sqrt{\ln(l/l_z)}) \quad (2.12)$$

where

$$I_0 = V_0^4 l_z \quad (2.13)$$

which follows from equations (2.8) and (2.9).

2.4 Modelling of Rotation Curves

The complete energy spectrum in a helically turbulent medium [16], [17] is shown in Fig.(1.2)

In this chapter we model the rotation curves of 76 galaxies observed by Amram et. al [56],[57] and Rubin et al. [59] [58] using the Kolmogorov branch ($V(l) \propto l^{1/3}$) and the flat branch ($V(l) \propto \sqrt{\ln l}$). We propose a law of velocities which is of the type

$$V(l) = Al + Bl^{1/3} \quad (2.14)$$

in the inner regions i.e., for $l \leq l_z$ and

$$V(l) = Cl^{-1/2} + D\sqrt{\ln(l/l_z)} \quad (2.15)$$

in the outer regions i.e., for $l \geq l_z$ of a galaxy, where A, B, C and D are the coefficients to be determined from the fits, with the observed velocity-fields.

The first terms on the right hand side of equations (2.14) and (2.15) correspond to rigid rotation and gravity respectively, therefore,

$$A = \omega \quad (2.16)$$

the angular velocity of a galaxy, and

$$C = \sqrt{GM} \quad (2.17)$$

(where G is the universal gravitational constant), refers to the Mass of a galaxy. The second terms on the right hand side of the Eqn. (2.14), & Eqn. (2.15) are due to the turbulent cascading so that

$$B = \epsilon^{1/3} \quad (2.18)$$

and

$$D = (\epsilon^2 l_z \tau)^{1/5} \quad (2.19)$$

By a judicious choice of l_z we can estimate: V_0 , τ , ϵ , ω and mass M of a galaxy.

2.5 Results

The values of V_0 , τ , ϵ – the parameters of turbulence – for each of the galaxies are shown in tables (2.1,2.3 & 2.4). The galaxy parameters ω , l_z & Mass M are shown in

tables (2.2,2.5 & 2.6). In order to compare the masses derived from our model with the standard masses in use, we have also included the mass(global) M_g (Table(2.1) col. [3]) calculated from the dark matter model assuming spherical symmetry [80] and the stellar mass M_S (Table(2.1) col. [4]) determined from the stellar models, using M/L ratios (mass-luminosity ratios)[80]; [60] and luminosities taken from Amram et. al [56]. This exercise has been done for the set of galaxies observed by Amram et al.[56]. The uncertainties in the M/L ratios and in the stellar models have to be taken into account before attempting any comparative study of the various types of masses. We also present the histograms (Fig(2.32)-Fig(2.37)) for each of the quantities calculated for the galaxies. Our model gives typical values of the various quantities as

$$V_0 \approx 100 \text{ km/sec}$$

$$\tau \approx 10^{14} \text{ sec}$$

$$\epsilon \approx 10^{-2} \text{ ergs/gm/sec}$$

$$\omega \approx 10^{-16} \text{ sec}^{-1}$$

$$\text{Mass} \approx 10^{10} M_{\odot}.$$

One must note that we didn't have to choose any abnormal values of l_z for obtaining the best fits and it lies in the range 2–10 kpc. This tells us that on scales smaller than l_z , the turbulence is isotropic and on the scales equal to and larger than l_z the turbulence becomes more and more anisotropic facilitating the inverse cascade of energy. We find some odd ones out in our sample of 76 galaxies, viz. UGC 3282 and NGC 2558 etc . They have exceptionally large values of the turbulent velocity V_0 and exceptionally small values of the energy injection rate parameter ϵ . It would be interesting to see if these recur in other data sets and examine if the peculiarities earn these galaxies a separate class.

We show here the fits for all the galaxies observed. Firstly we show a set of 21 galaxies wherein we have also shown the observational error bars. These error bars were useful in deciding about which points to be weighted when the fits were performed. For the remaining set error bars were not given in the published data. But a look at the first set of 21 galaxies convinces us that all the fits would fall well within the error bars .

Table 2.1: Table showing the ‘Turbulence Parameters’ for the set of galaxies observed by Amram et. al [56]

Name	V_0 (Km/s)	$\epsilon(10^{-2}$ ergs/gm/s)	$\tau(10^{13}$ s)
NGC6045	31	63.4	1.5
UGC10085	338	1.6	7100
UGC3269	85	17	42
UGC3282	8021	1.8×10^{-2}	3.5×10^8
NGC4911	62	45	8.4
Z160-058	87	9.6	78
Z130-008	0.026	12.9	5.2×10^{-6}
NGC4848	157	53	46
Z160-106	169	15.5	180
NGC4921	68	1.7	270
NGC2558	5588	6.1×10^{-3}	5.1×10^8
Z119-043	171	1.2	2.4×10^3
UGC4386	46	38	5.5
Z119-043	81	11	59
NGC2595	191	98	37
UGC4329	58	3.5	94
NGC7536	211	2.5	1700
UGC12498	42	47	3.6
NGC7593	74	11.6	47
NGC7643	26	0.3	210
NGC7631	107	21.2	53

Table 2.2: Table showing the values

Name	$(10^{10} M_{\odot}), M$	$(10^{10} M_{\odot}), M_g^a$	$(10^{10} M_{\odot}), M_s^b$	$\omega(10^{-16} s^{-1})$	$L_z(\text{kpc})$
NGC6045	23.7	4.5	1.7	0.4	12.0
UGC10085	0.2	5.8	2.3	21.9	0.9
UGC3269	1.0	12.3	5.5	3.0	3.0
UGC3282	0.9	6.0	2.3	12.4	2.6
NGC4911	6.6	16.9	7.5	5.9	4.4
Z160-058	8.9	2.9	1.1	0.3	14.0
Z130-008	3.6	1.4	0.5	1.2	6.2
NGC4848	0.8	15.8	7.9	94.0	0.6
Z160-106	2.0	5.1	2.6	0.6	4.9
NGC4921	8.6	17.5	8.7	1.4	16.2
NGC2558	3.6	8.5	4.2	20.4	3.6
Z119-043	0.1	-	-	16.6	0.9
UGC4386	14.6	6.3	2.8	0.1	11.4
Z119-043	1.2	-	-	0.07	4.2
NGC2595	0.6	6.0	2.3	151.1	0.4
UGC4329	0.7	1.8	0.7	5.6	2.7
NGC7536	0.9	5.9	2.6	2.8	4.0
UGC12498	1.0	2.9	1.3	6.4	2.9
NGC7593	0.6	1.6	0.6	3.9	2.5
NGC7643	4.7	1.7	0.6	10.0	5.7
NGC7631	0.7	4.9	2.2	4.5	2.1

^{1a} Global mass from dark matter model ^{2b} Mass in the stars (derived from assuming the global M/L ratios of each of the morphological types; Giovanelli and Haynes (1988) [80])

Table 2.3: Table showing Turbulence parameters for the set of galaxies observed by Amram, and Rubin

Name	V_0 (Km/s)	$\epsilon(10^{-2}$ ergs/gm/s)	$\tau(10^{13}$ s)
NGC668	121	39.3	5.6
NGC669	34	1.0	3×10^5
NGC688	92	4.8	3.3×10^2
UGC1347	52	1.2	2.0×10^2
NGC753	162	35.3	6.1
UGC1493	37	4.1	3.0×10^3
Z119051	50	4.2	2.1×10^2
NGC3861	18	0.1	4.8×10^6
NGC3883	2	$\simeq 10^{-5}$	3.6×10^{11}
UGC8161	51	2.2	1.2×10^2
I1179	102	2.9	2.6×10^1
NGC6050	43	2.8	4.7×10^3
NGC6054	35	1.3	4.5×10^3
NGC7591	79	25.5	4.6×10^1
J2318+0633	31	0.4	8.3×10^3
NGC4605	27	0.7	4.1×10^3
NGC1035	63	2.7	9.1×10^1
NGC4062	121	22.9	1.5×10^1
NGC2742	153	23.1	3.5
NGC701	98	4.3	0.2
NGC2608	26	1.2	1.3×10^3
NGC3495	110	5.5	8.9×10^1
NGC1087	54	3.5	2.5×10^2
UGC3691	83	2.1	1.0×10^2
NGC4682	119	18.4	2.7×10^1
NGC3672	40	0.3	1.9×10^4
NGC1421	98	15.0	3.4×10^4
NGC2715	134	11.2	2.9
NGC4321	14	0.2	2.3×10^6
I467	91	4.1	8.6×10^1

Table 2.4: Turbulence Parameters continued..

Name	V_0 (Km/s)	$\epsilon(10^{-2}$ ergs/gm/s)	$\tau(10^{13}$ s)
NGC7541	53	9.8	7.1×10^2
NGC7664	28	0.7	6.1×10^4
NGC2998	168	30.6	9.2
NGC753	69	21.6	1.5×10^2
NGC801	137	20.7	1.5×10^1
UGC2885	129	46.2	2.5×10^1
NGC4800	13	0.2	1.6×10^6
NGC2708	174	21.4	1.0
NGC3067	118	17.9	5.1
NGC4448	185	51.6	0.3
NGC1515	143	62.7	0.1
NGC1353	12	0.1	1.0×10^7
NGC1325	159	16.2	5.7
NGC7537	17	0.1	8.7×10^5
U11810	75	6.7	1.3×10^2
NGC7171	23	0.1	2.7×10^5
NGC7217	271	322.1	0.1
NGC1620	176	29.6	2.8×10^1
NGC3054	56	1.0	2.1×10^4
NGC2590	200	130.1	1.7
NGC2815	30	0.9	1.5×10^5
NGC1417	129	34.4	5.1×10^1
NGC1085	64	5.7	4.8×10^3
NGC3145	54	0.7	2.3×10^4
NGC3223	97	3.7	4.9×10^2
NGC7606	253	52.4	0.7
NGC3200	127	44.3	4.3×10^1

Table 2.5: Table showing the values of masses, ω and L_z for the set of galaxies observed by Amram and Rubin

Name	Mass ($10^{11}M_\odot$)	$\omega(10^{-16}s^{-1})$	$I_z(\text{kpc})$
NGC668	0.1	13.7	1.4
NGC669	0.16	56.3	1.2
NGC688	0.39	6.5	5.1
UGC1347	0.06	3.4	3.7
NGC753	0.28	2.8	3.9
UGC1493	0.01	51.4	0.4
Z119051	0.01	5.3	0.9
NGC3861	0.42	34.3	2.4
NGC3883	0.71	4.6	11.6
UGC8161	0.02	3.3	1.9
I1179	0.44	1.0	12.0
NGC6050	0.03	25.9	0.9
NGC6054	0.02	18.0	1.0
NGC7591	0.11	102.3	0.6
J2318+0633	0.08	16.9	2.1
NGC4605	0.01	9.9	1.0
NGC1035	0.08	4.9	2.9
NGC4062	0.07	0.1	2.5
NGC2742	0.24	0.1	4.9
NGC701	0.37	2.5	6.9
NGC2608	0.01	57.5	0.5
NGC3495	0.36	1.3	7.9
NGC1087	0.03	10.5	1.5
UGC3691	0.25	1.2	8.9
NGC4682	0.08	0.8	2.9
NGC3672	0.49	7.8	6.9
NGC1421	0.08	8.2	2.0
NGC2715	0.28	0.3	6.9
NGC4321	0.01	78.6	0.5
I467	0.17	2.2	5.9

Table 2.6: Table showing the values of masses, ω and L_z for the set of galaxies observed by Amram and Rubin contd..

Name	Mass ($10^{11} M_\odot$)	$\omega (10^{-16} s^{-1})$	I_z (kpc)
NGC7541	0.02	74.6	0.5
NGC7664	0.03	35.3	1.0
NGC2998	0.32	0.9	4.9
NGC753	0.01	45.8	0.5
NGC801	0.40	7.0	3.9
UGC2885	0.20	30.9	1.5
NGC4800	0.02	76.0	0.5
NGC2708	1.02	2.5	7.9
NGC3067	0.10	1.5	2.9
NGC4448	0.32	0.5	3.9
NGC1515	0.18	20.4	1.5
NGC1353	0.06	50.5	1.0
NGC1325	0.44	0.1	7.9
NGC7537	0.05	15.2	2.0
U11810	0.05	7.5	2.0
NGC7171	0.46	11.9	4.9
NGC7217	0.35	1.9	2.0
NGC1620	0.34	0.6	5.9
NGC3054	0.46	7.9	5.9
NGC2590	0.16	1.0	2.0
NGC2815	0.14	73.1	1.0
NGC1417	0.24	21.0	2.0
NGC1085	0.21	41.4	1.5
NGC3145	1.00	9.2	7.9
NGC3223	0.98	7.7	7.9
NGC7606	1.63	0.7	9.9
NGC3200	0.14	21.2	1.5

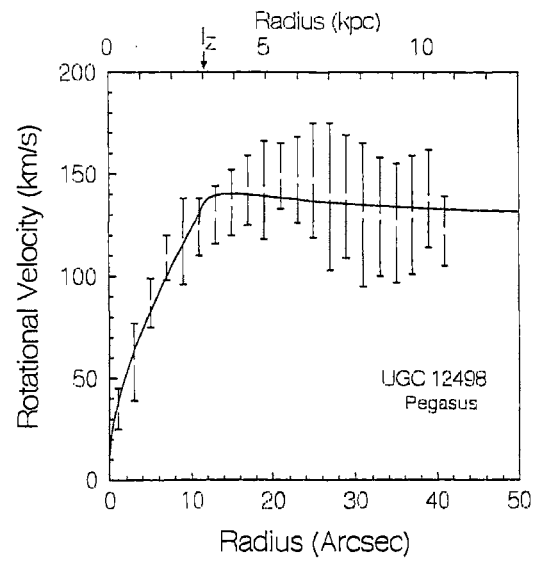


Figure 2.1: Rotation Curve of UGC 12498 in the Pegasus cluster. Observed by Amram et al. The observational error bars are also shown. The solid line is our model-fit.

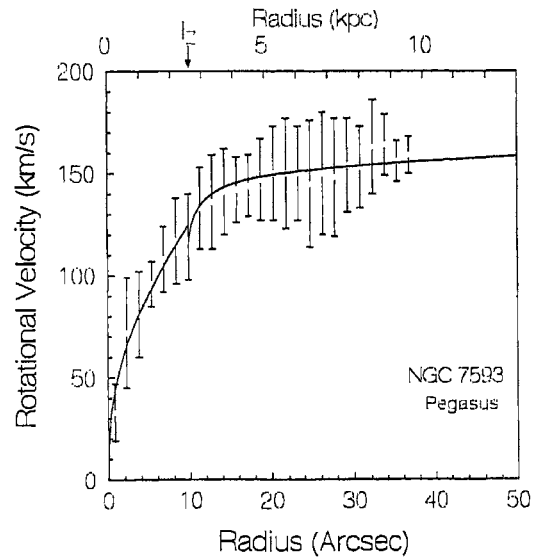


Figure 2.2: Rotation Curve of NGC 7593 in Pegasus cluster.

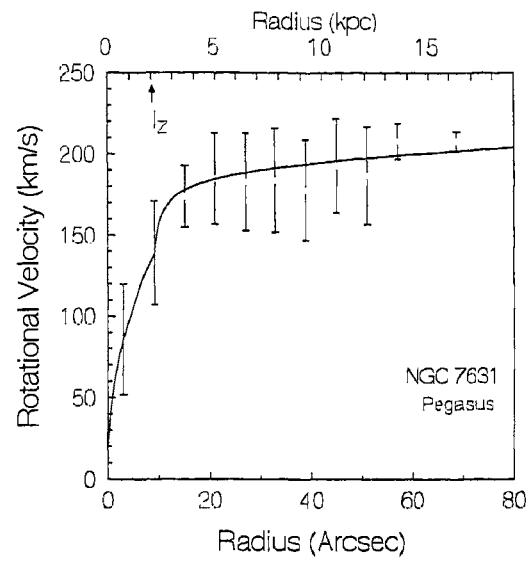


Figure 2.3: Rotation curve of NGC 7631 in Pegasus cluster.

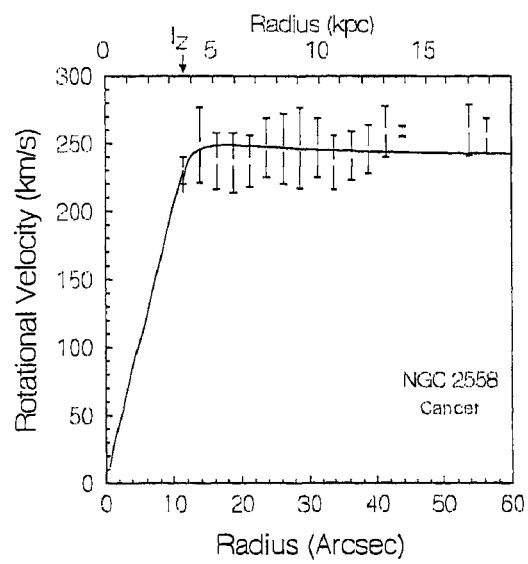


Figure 2.4: Rotation curve NGC 2558 in the Cancer cluster .

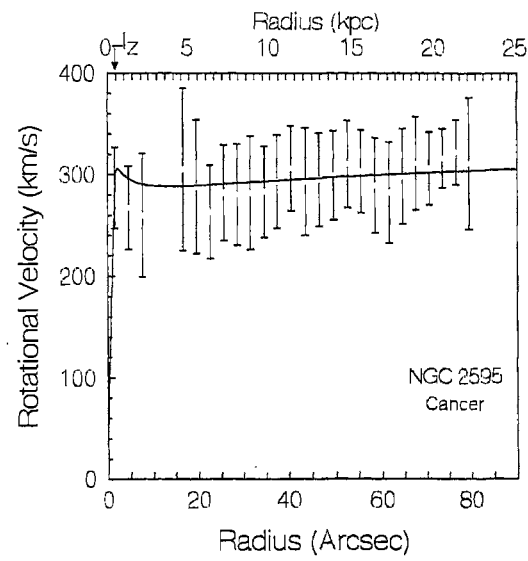


Figure 2.5: Rotation curve of NGC 2595 in the Cancer cluster.

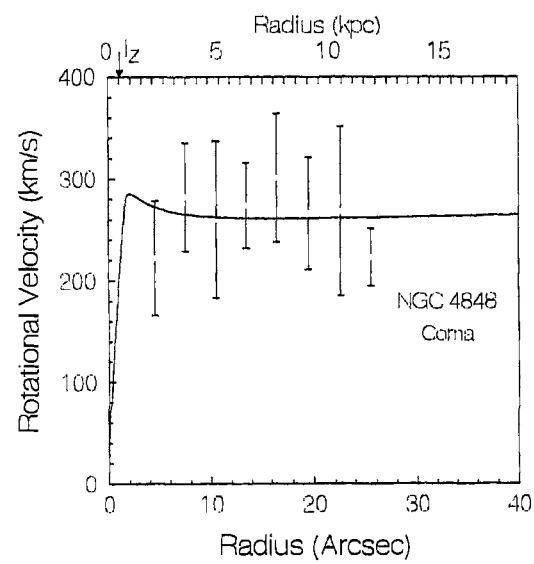


Figure 2.6: Rotation curve of NGC 4848 in the Coma cluster.

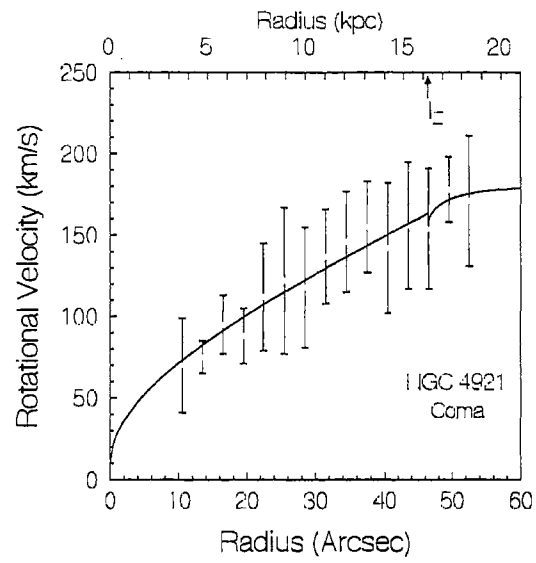


Figure 2.7: Rotation curve of NGC 4921 in the Coma cluster.

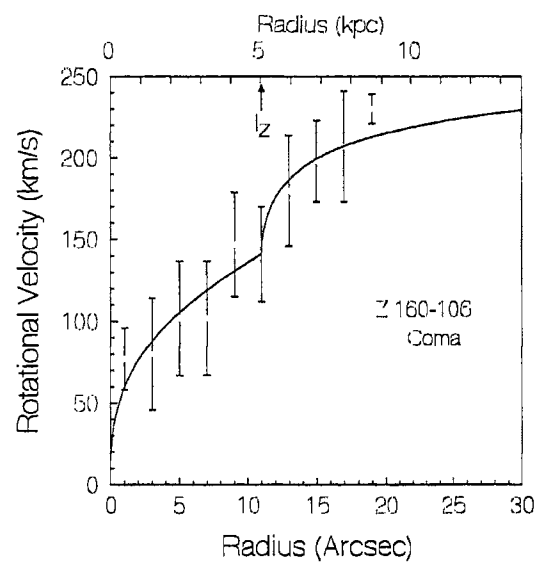


Figure 2.8: Rotation curve of Z 160-106 in the Coma cluster.

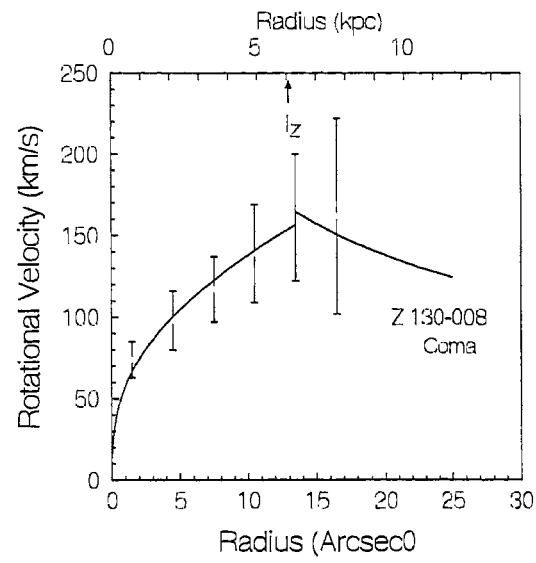


Figure 2.9: Rotation curve of Z 130-008 in the Coma cluster.

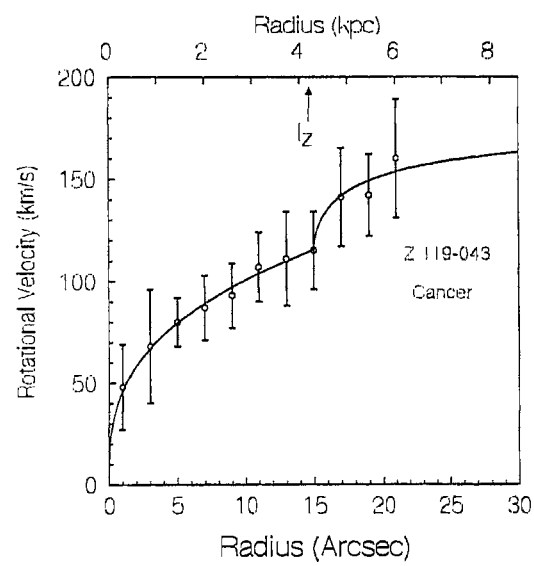


Figure 2.10: Rotation curve of Z 119-043 in the Cancer cluster.

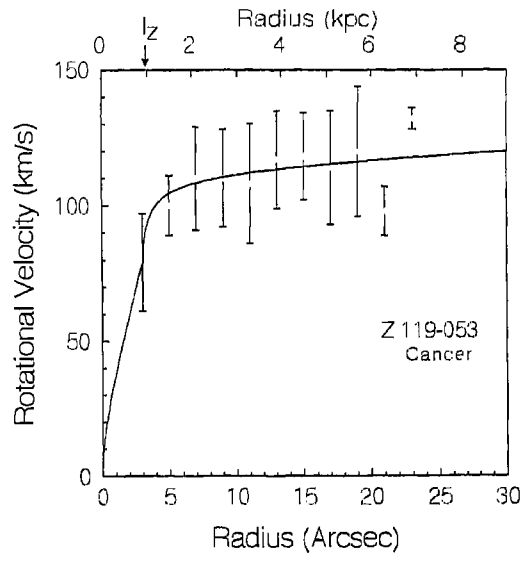


Figure 2.11: Rotation curve of Z 119-053 in the Cancer cluster.

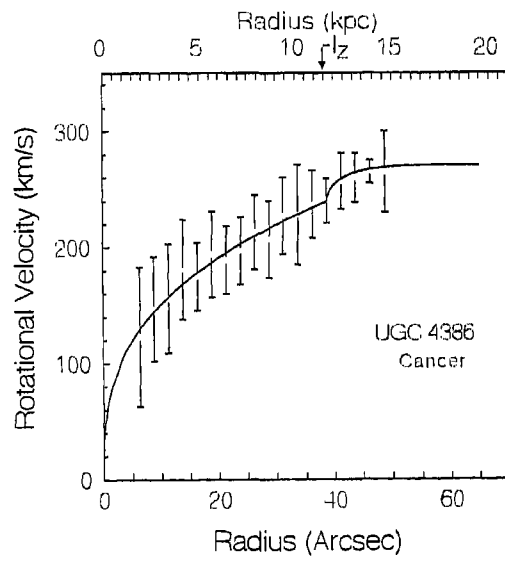


Figure 2.12: Rotation curve of UGC 4386 in the Cancer cluster.

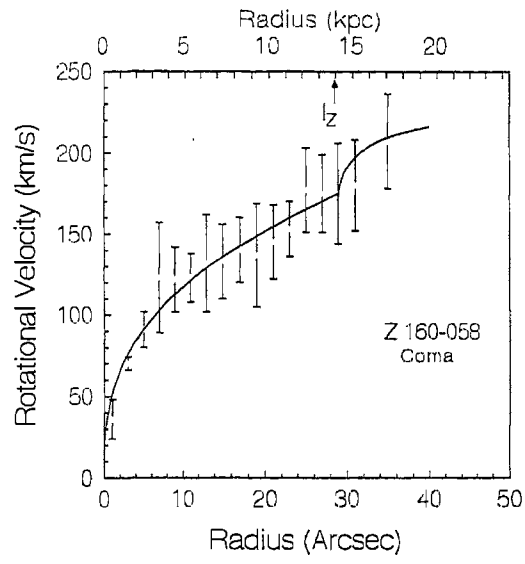


Figure 2.13: Rotation curve of Z 160-058 in the Coma cluster.

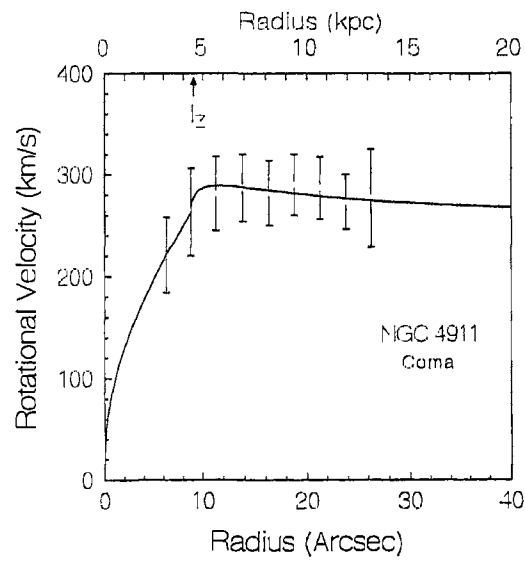


Figure 2.14: Rotation curve of NGC 4911 in the Coma cluster.

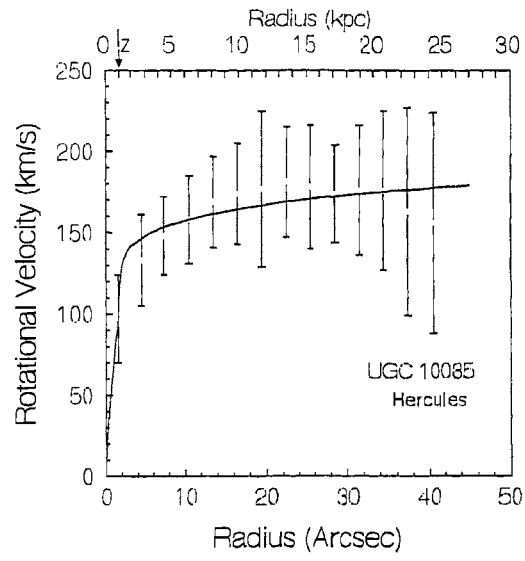


Figure 2.15: Rotation curve of UGC 10085 in the Hercules cluster.

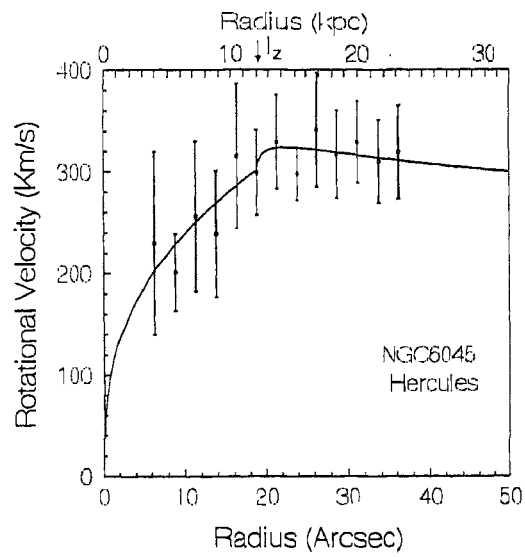


Figure 2.16: Rotation curve of NGC 6045 in the Hercules cluster.

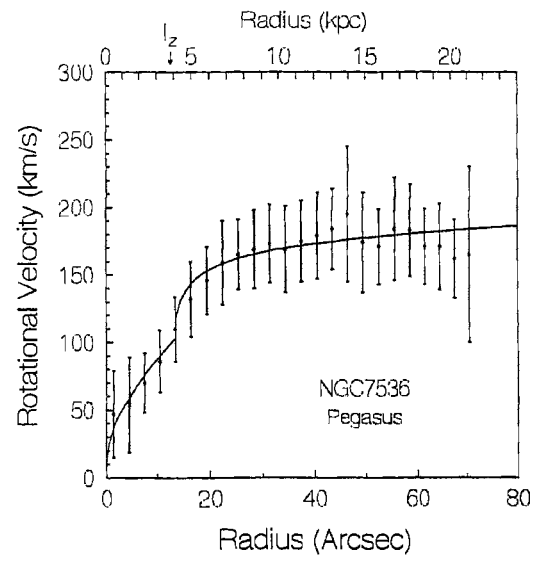


Figure 2.17: Rotation curve of NGC 7536 in the Pegasus cluster.

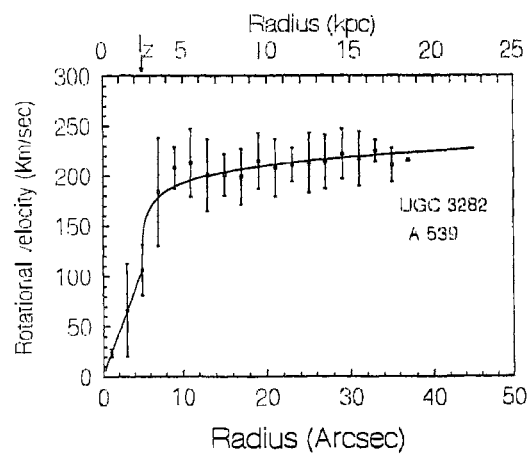


Figure 2.18: Rotation curve of NGC 3282 in Abell 539 cluster.

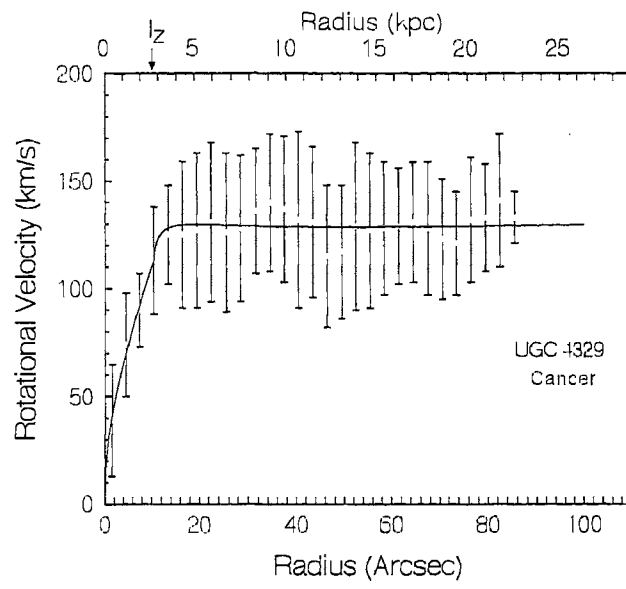


Figure 2.19: Rotation curve of UGC 4329 in Cancer cluster

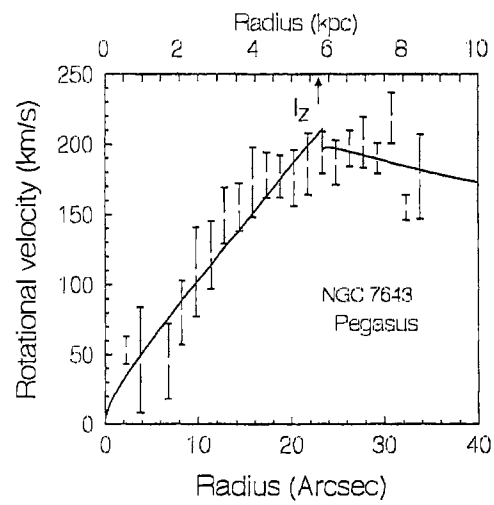


Figure 2.20: Rotation curve of NGC 7643 in Pegasus cluster

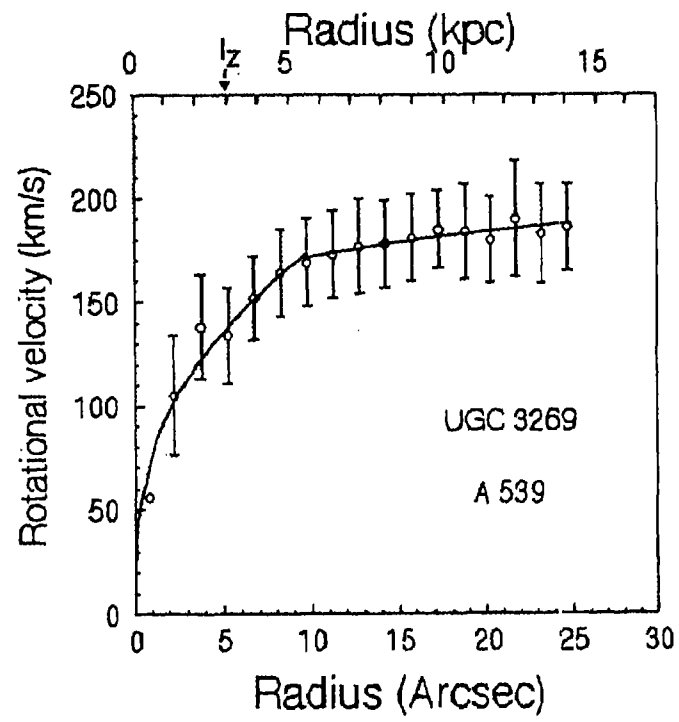


Figure 2.21: Rotation curve of UGC 3269 in Abell 539 cluster

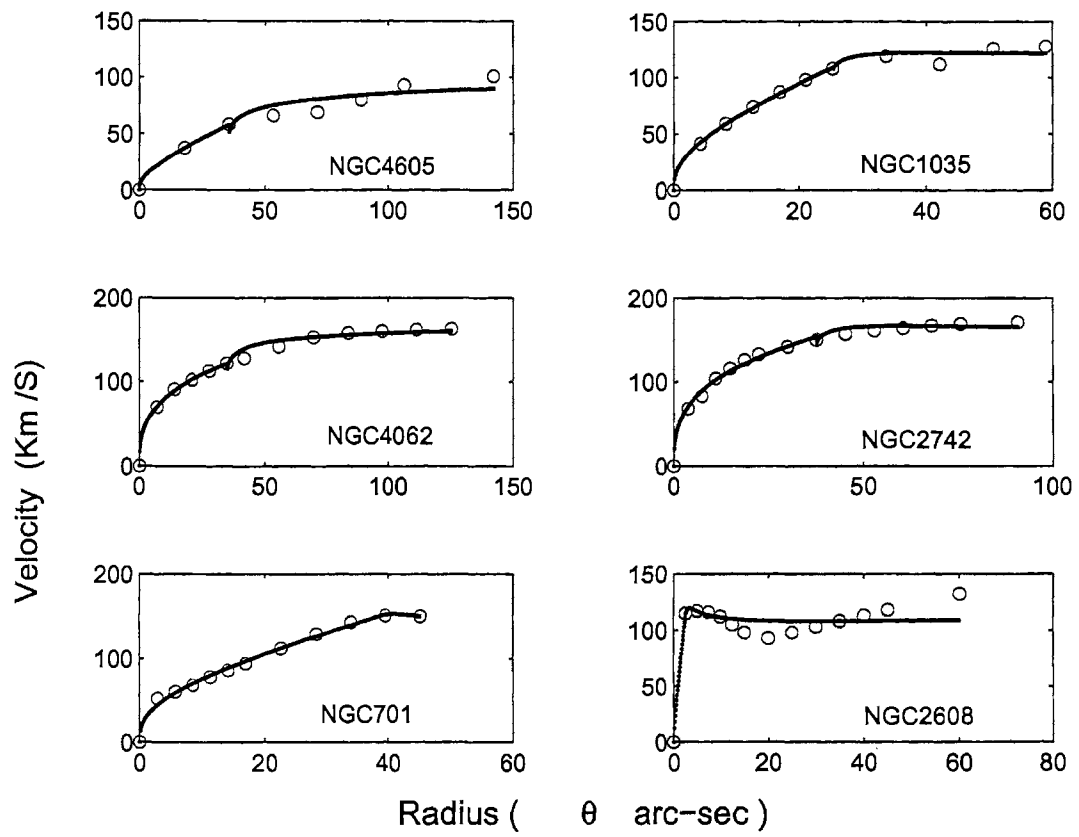


Figure 2.22: Rotation curves of galaxies from Rubin's data

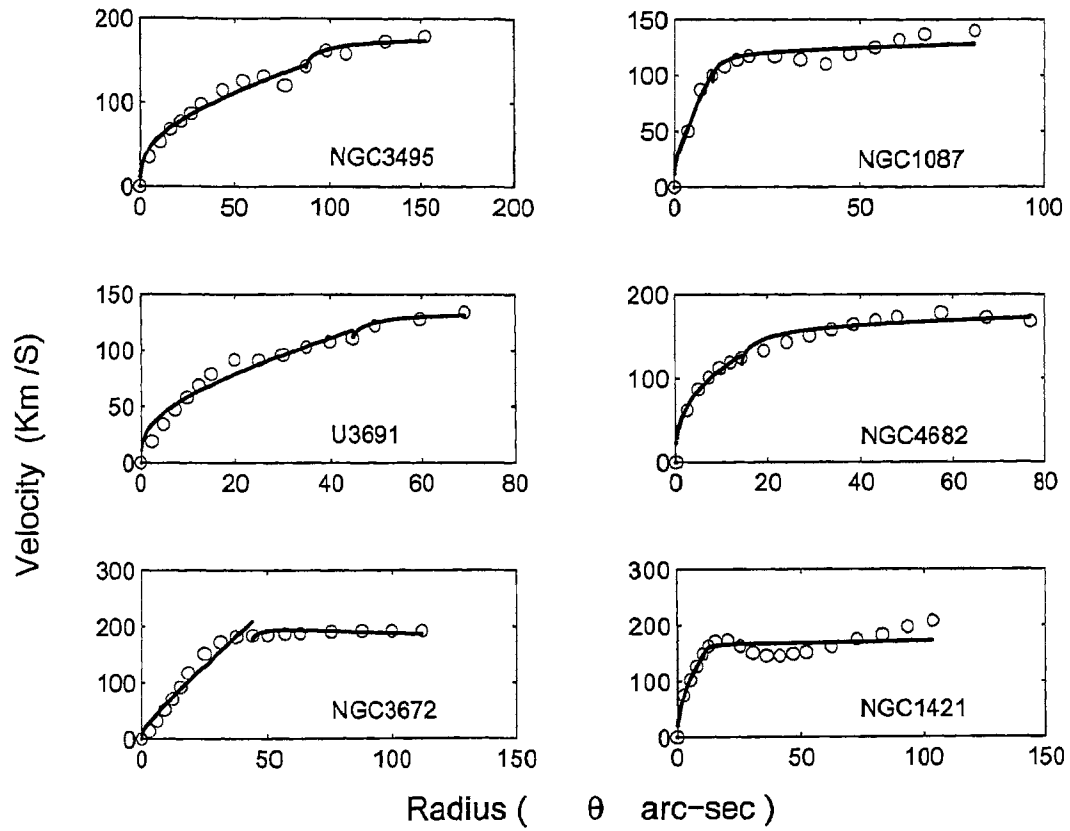


Figure 2.23: Rotation curves of galaxies from Rubin's data contd..

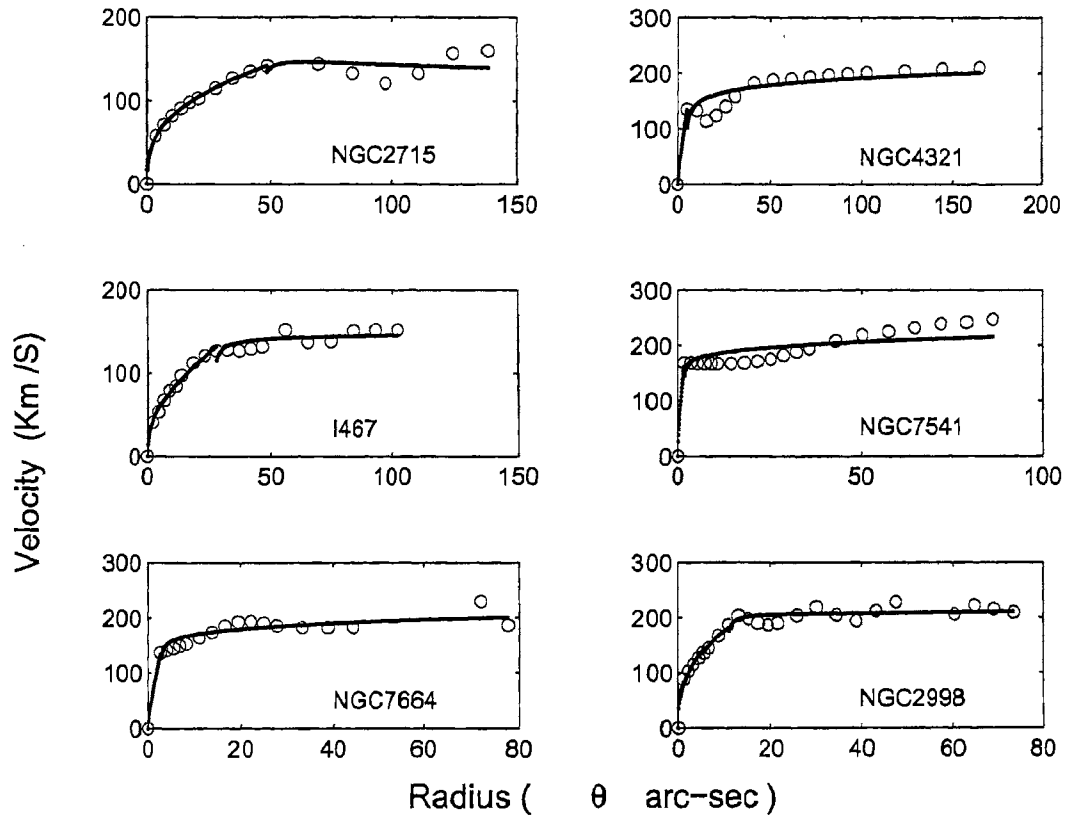


Figure 2.24: Rotation curves of galaxies from Rubin's data contd..

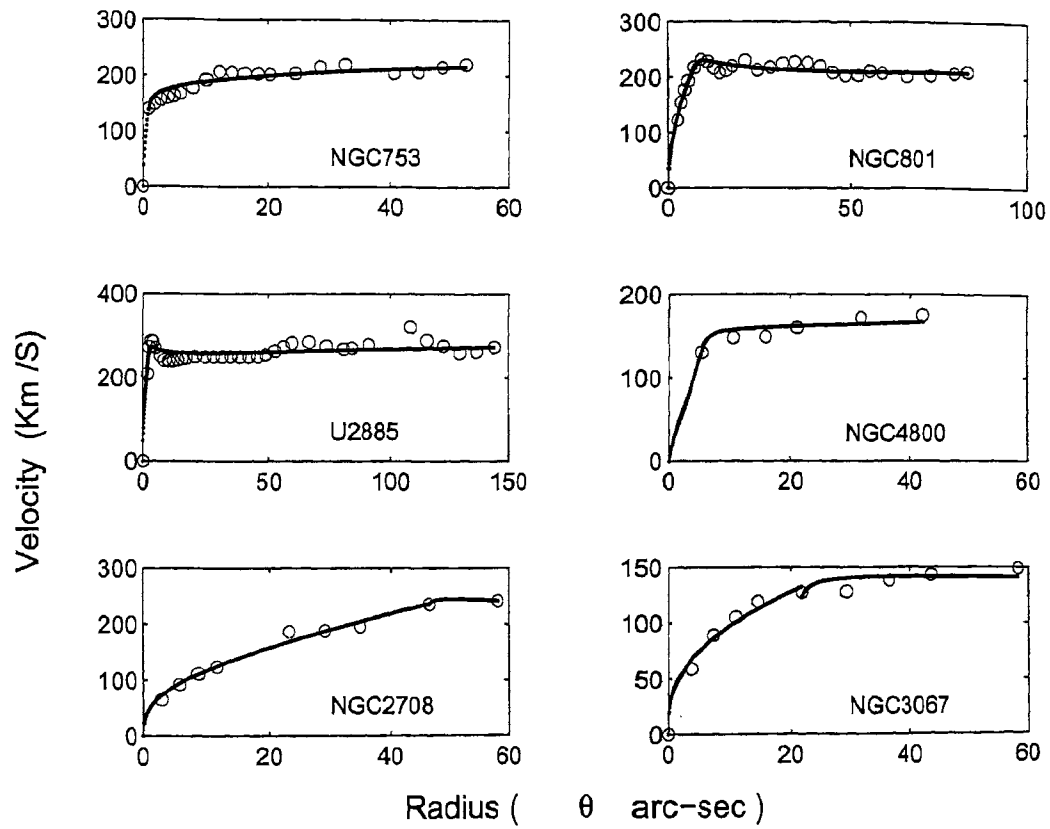


Figure 2.25: Rotation curves of galaxies from Rubin's data contd..

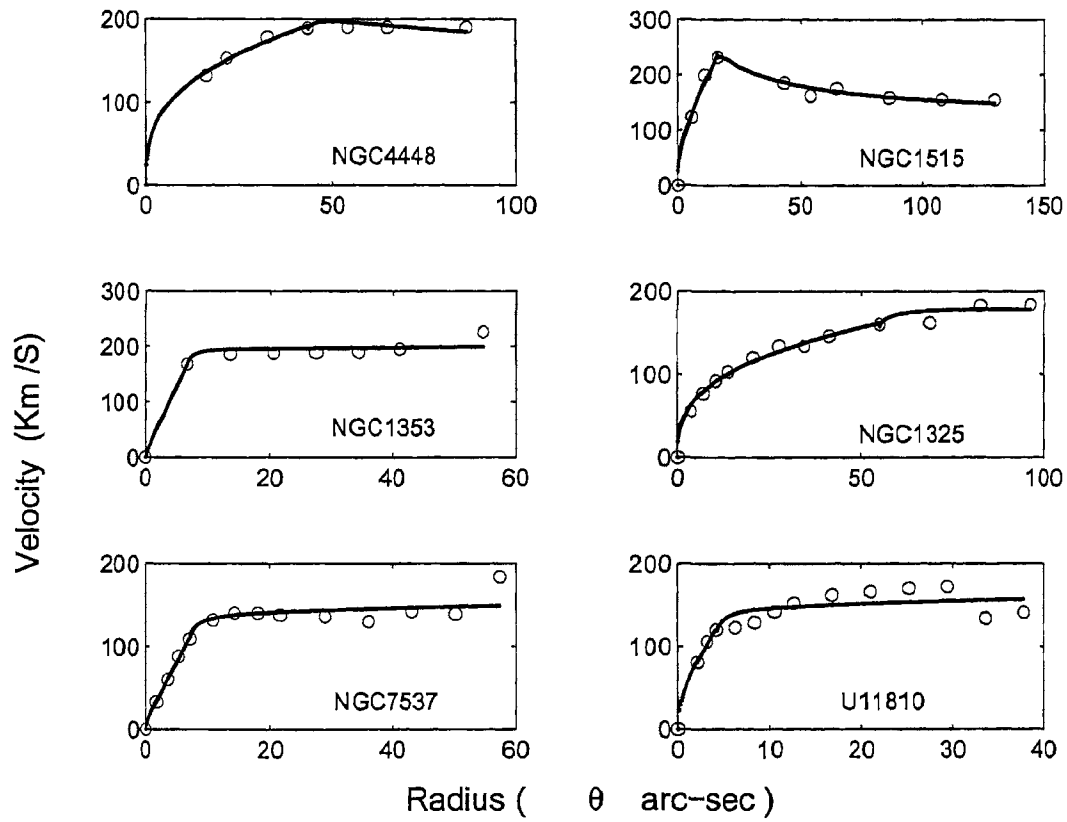


Figure 2.26: Rotation curves of galaxies from Rubin's data .contd...

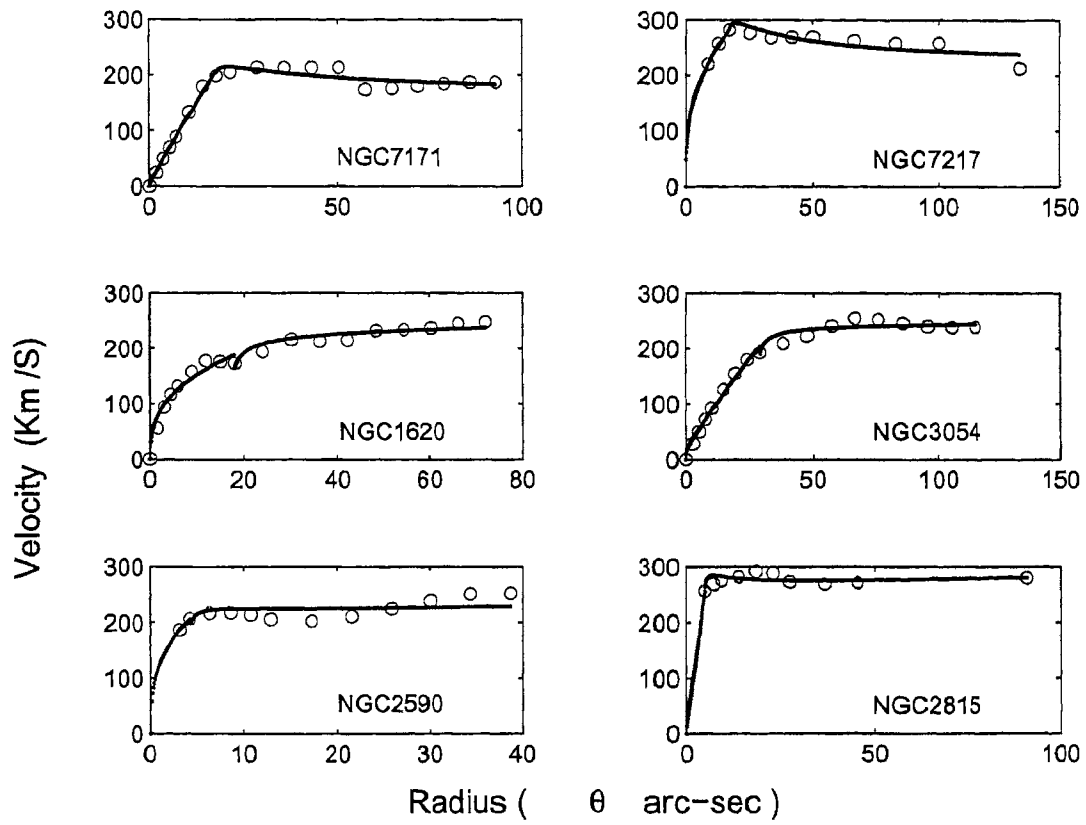


Figure 2.27: Rotation curves of galaxies from Rubin's data , contd..

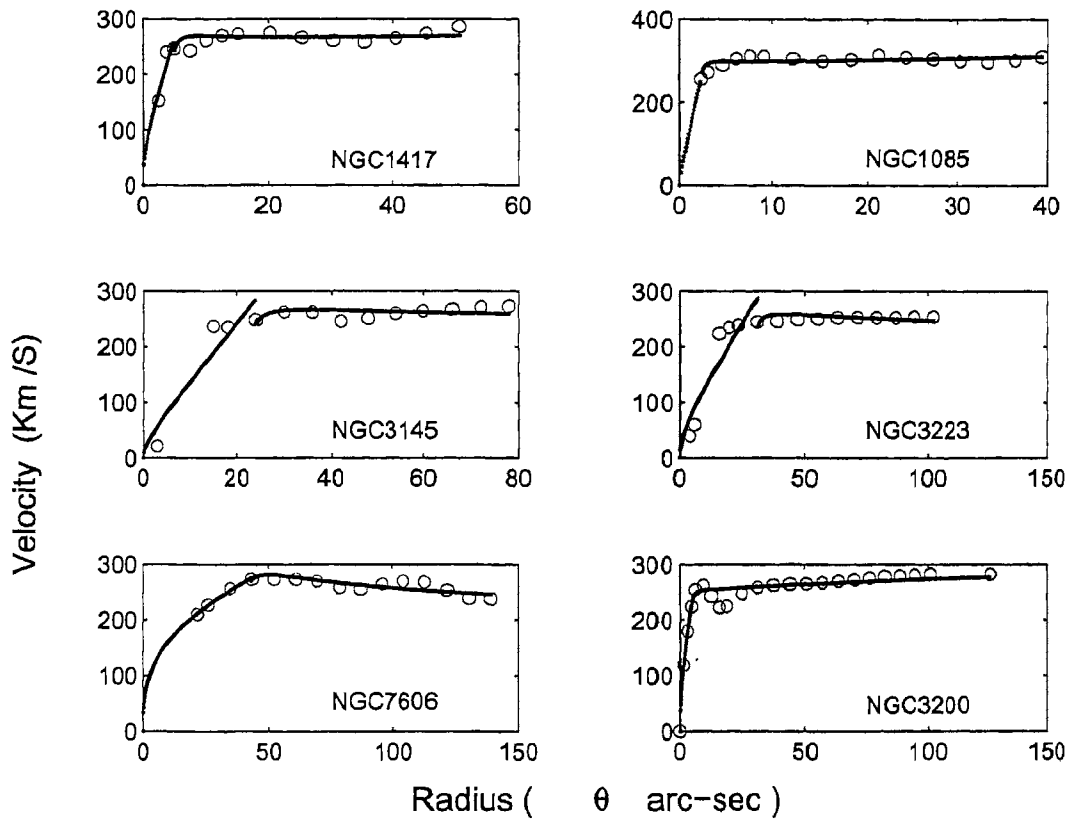


Figure 2.28: Rotation curves of galaxies from Rubin's data ,contd..

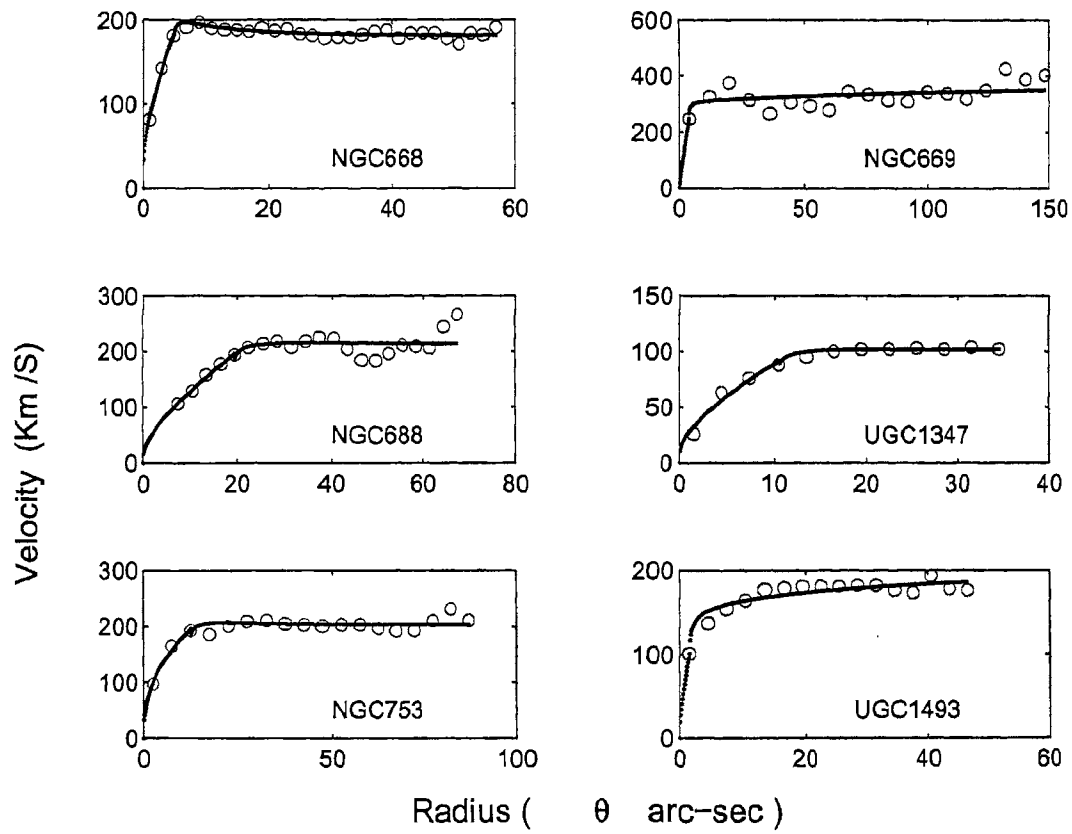


Figure 2.29: Rotation curves of galaxies from Amram's data.

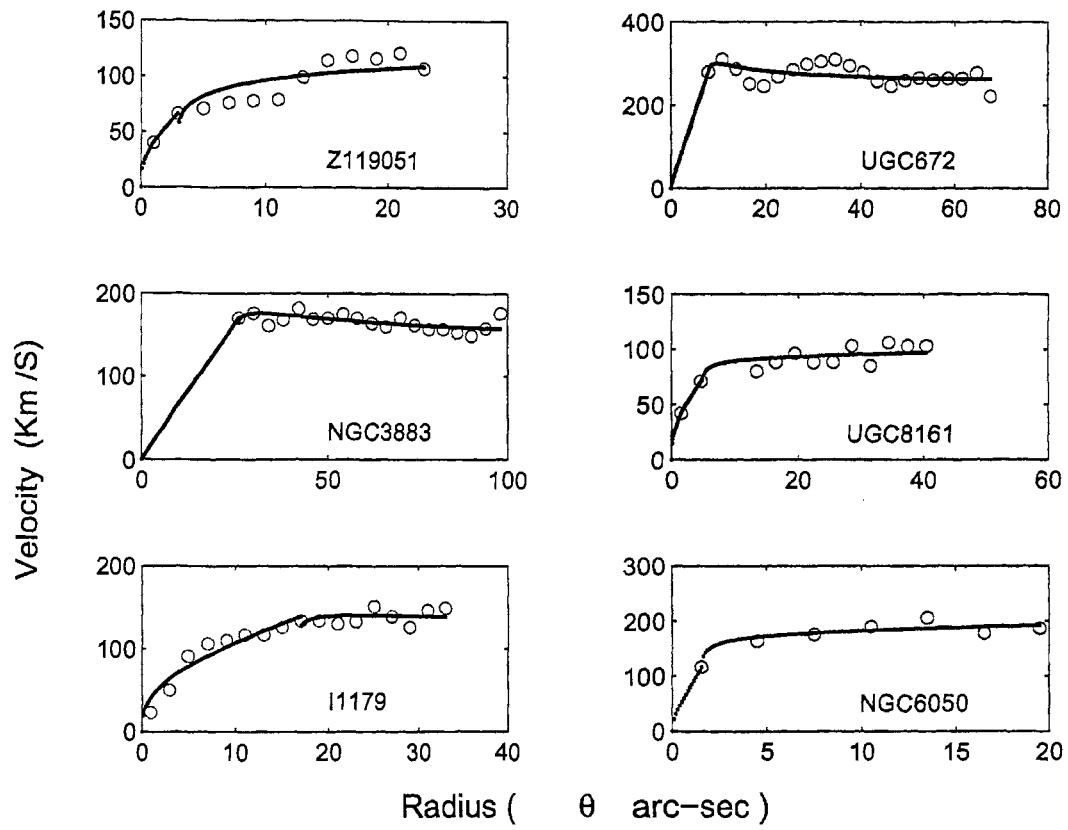


Figure 2.30: Rotation curves of galaxies from Amram's data contd..

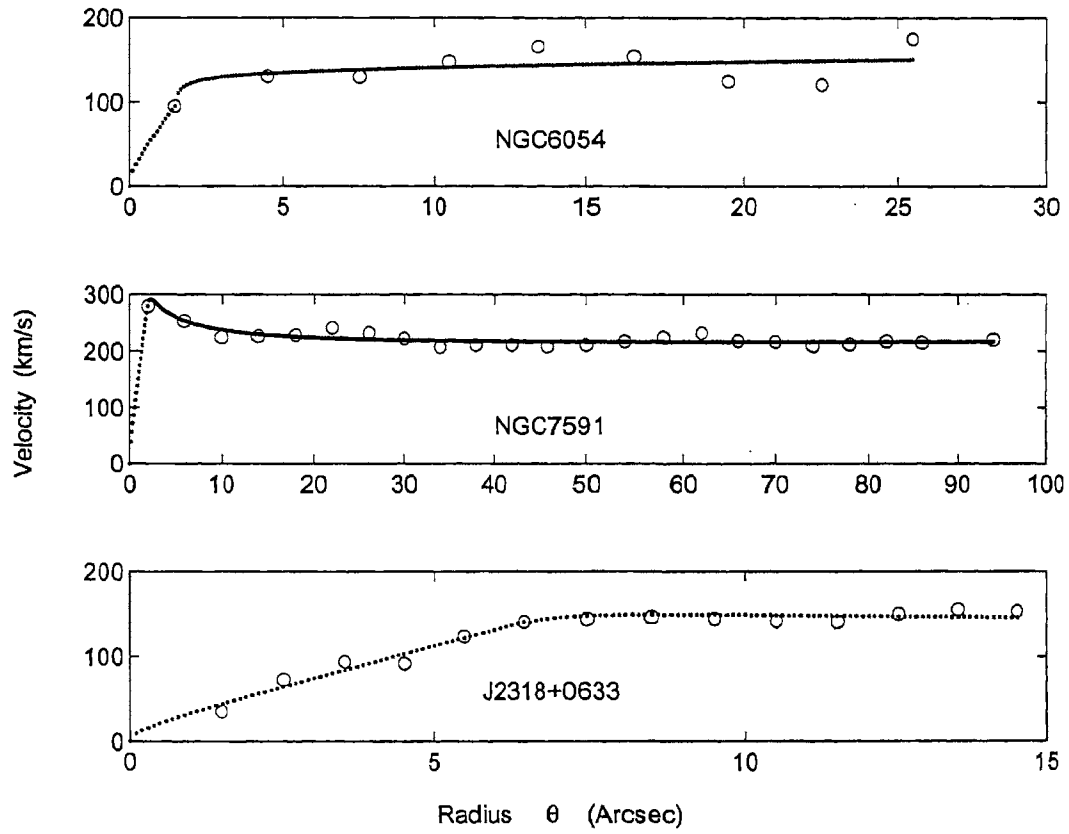


Figure 2.31: Rotation curves of galaxies from Amrams's data contd..

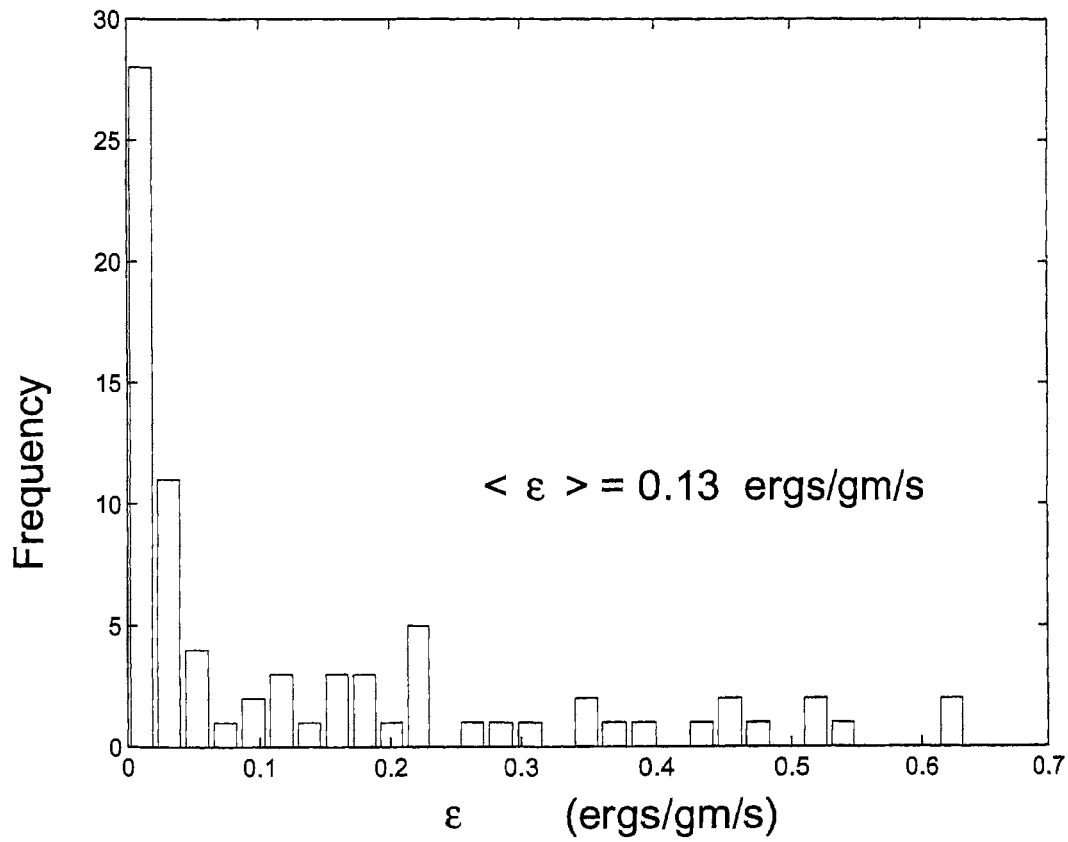
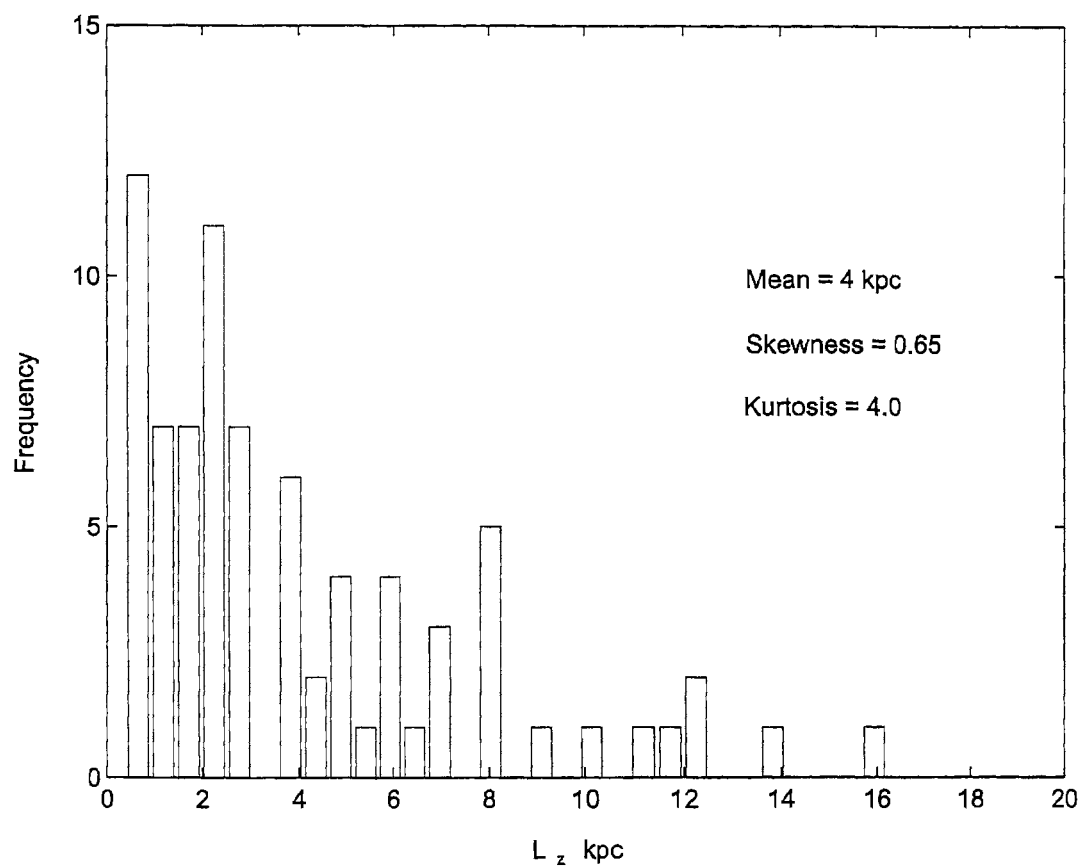


Figure 2.32: Histogram showing the distribution of the turbulence parameter ϵ

Figure 2.33: Histogram showing the distribution of L_z

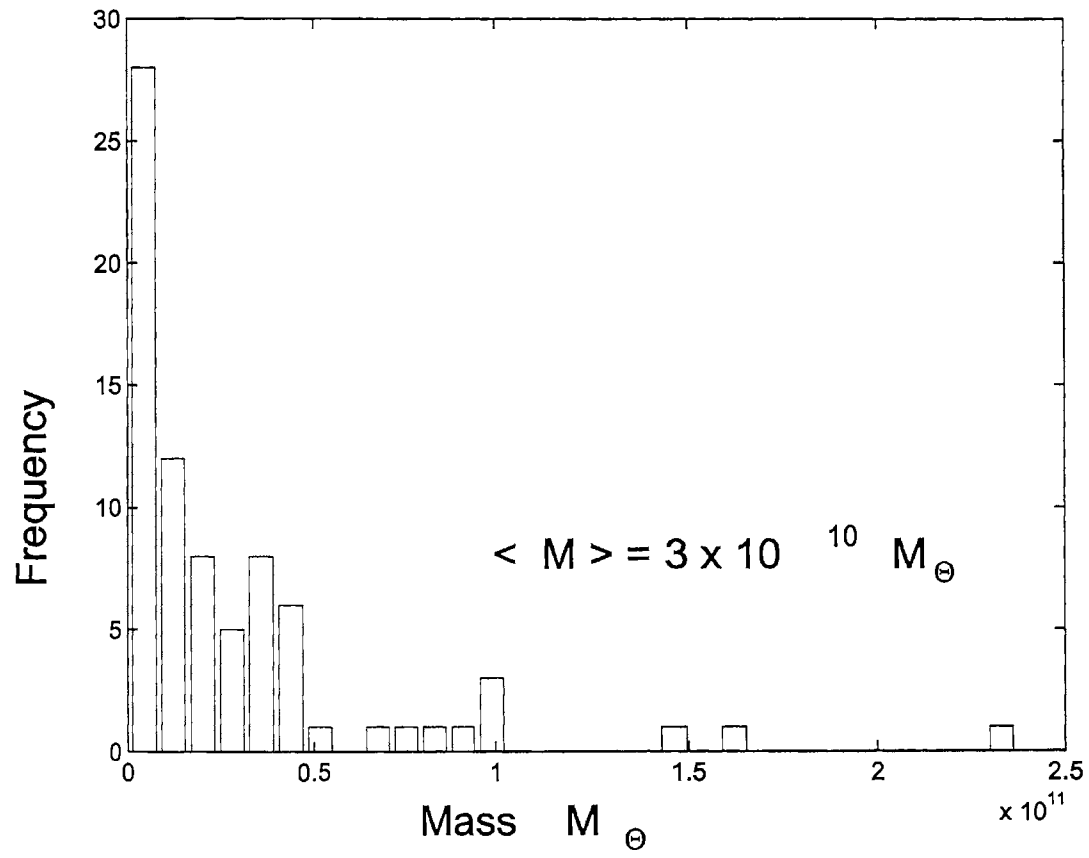


Figure 2.34: Histogram showing the distribution of masses (M) derived from our model fits.

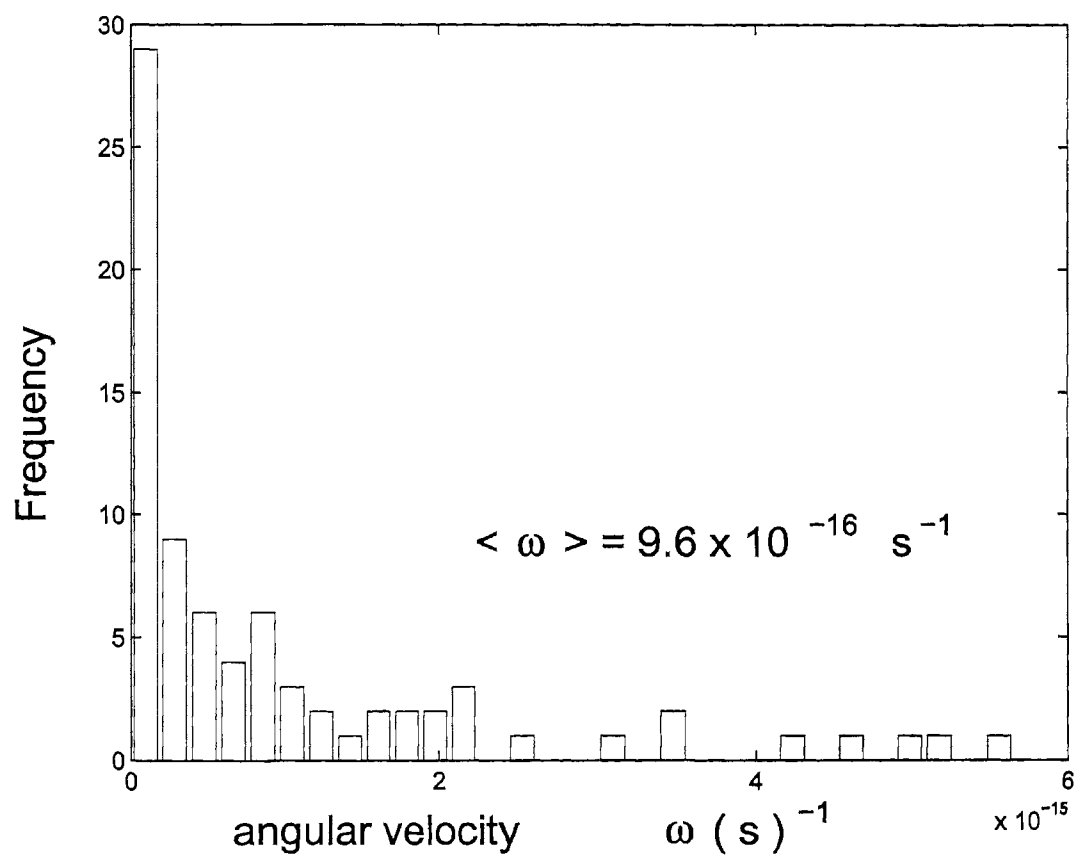


Figure 2.35: Histogram showing the distribution of ω for all the galaxies in our data set.

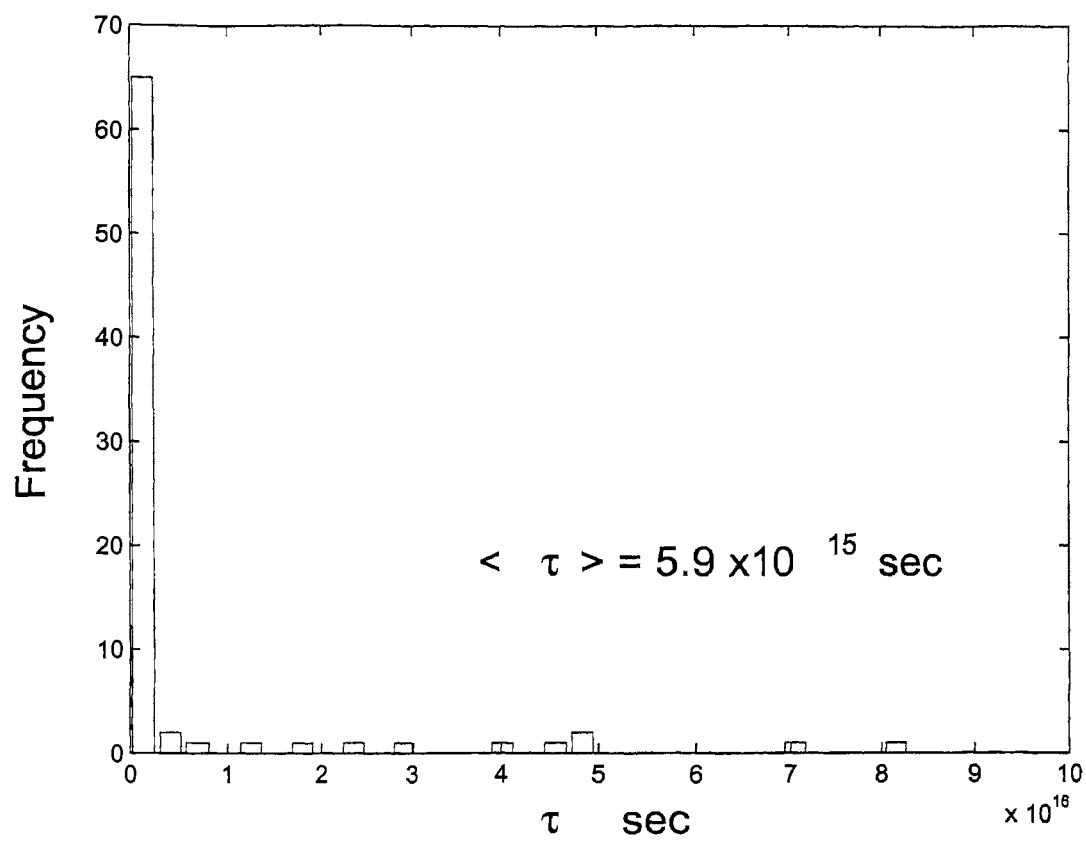


Figure 2.36: Histogram showing the distribution of the turbulence parameter τ

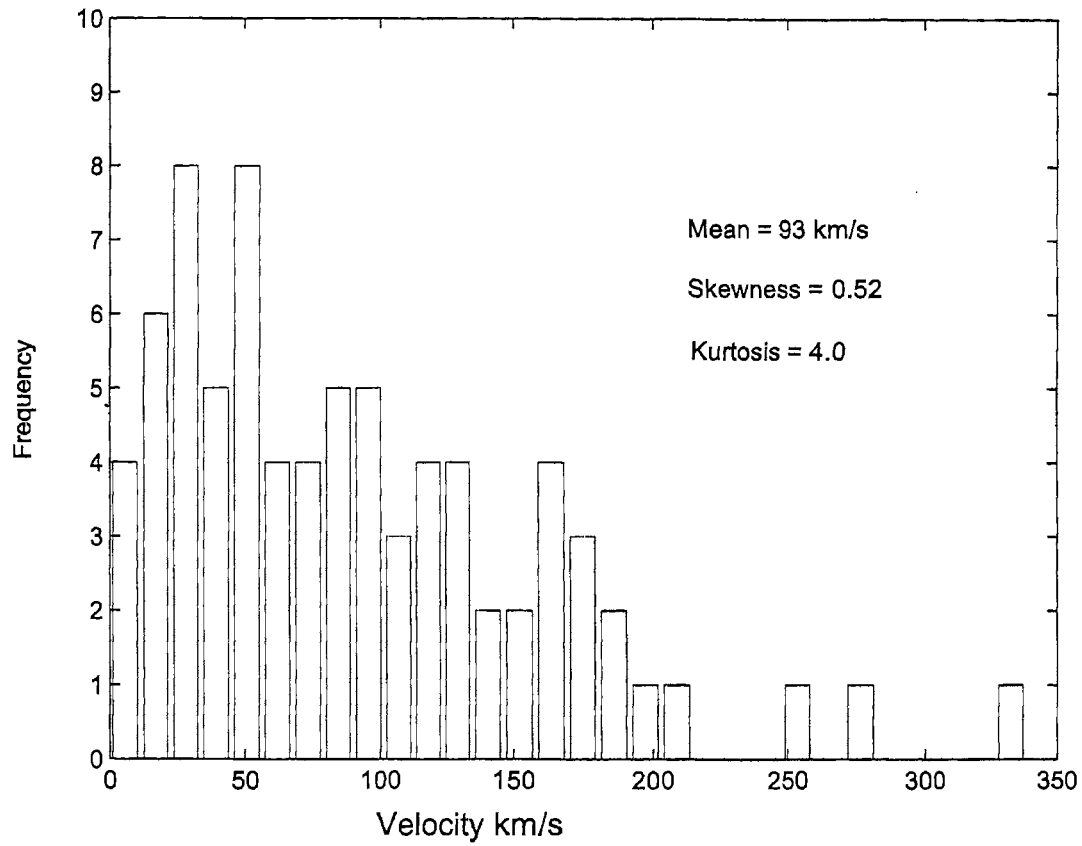


Figure 2.37: Histogram showing the distribution of turbulent velocities V_0 as derived from our model. Note the skewness, implying 'long-range' correlations in the system!

2.6 Discussion and Conclusion

The velocity-radius relation for galaxies has been derived using Kolmogorov arguments. We believe that the matter at a large radius exhibits a balance of hydrodynamic forces, i.e., dynamical pressure, and Reynolds stresses- produced by the forced small-scale flow-without the necessity of invoking a gravitational force, generated out of a mass distribution of the type $M \propto r$ (which is what is required of the dark-matter models). In other words, our system is hydrodynamically bound.

We also find that ϵ and τ values for each of the galaxies obtained by us are almost of the same order as that quoted for our Galaxy [77]. Therefore it appears possible to model the observed rotation curves of the galaxies by suitably combining the effects of rigid rotation, gravity and turbulence. The validity of the "turbulence model" can be further substantiated by confronting it with the observations of the velocity fields on the larger scales like clusters and superclusters. In a recent paper Sanchez-Salcedo [82], it was claimed that the inverse cascade hypothesis (ICH) has been critically examined as an alternative to dark matter hypothesis for explaining flat rotation curves of galaxies .Some issues related to the applicability of the ICH spectrum and the virial theorem were raised. Here, we clarify these points and provide a possible validation of the inverse cascade hypothesis.

We modelled the flat rotation curves of several galaxies without invoking the presence of any type of dark matter. Instead our model makes use of some very special properties of helically turbulent media. Sanchez-Salcedo [82] pointed out that the application of inertial range of ICH spectrum to a galaxy implies that scales larger than the galactic scales must exist. Indeed this is so. In the ICH hypothesis a galaxy has not been treated as an isolated object. It is but one element of the heirarchy of structures spanning a range of a few Kpc to hundreds of Mpc believed to exist in the universe. Further, since a galaxy is not an isolated system- it participates in the formation of larger structures through vortex-vortex nteraction- the virial theorem is not applicable at the galactic scales. As discussed below, this is true for the entire inertial range (see Fig. (1.2)) [17] since it represents interacting scales .

The new realization in astrophysics is that most of the observed structures in

astrophysical environs are helical in form and helicity is an essential ingredient of a three dimensional medium (Shore [81], Kitamura[86]) . Large scale helical vortices are expected to be generated in galactic disks (Khomenko et al)[21] . In accordance with observations (Ruzmaikin et al.)[77] , small- scale turbulent motions in galactic disks are characterized by the correlation time $\tau_{cor} \simeq 3 \times 10^{14} s$; and the correlation length $\lambda_{cor} \simeq 3 \times 10^{20} cm$. (33pc) That corresponds to a typical velocity of $10^6 cm s^{-1}$ and the non - linear term $V \cdot \nabla V \simeq V^2/L$ turns out to be $10^{-9} cm s^{-2}$. From our fits of flat - rotation curves , we find a typical velocity $V \simeq 100 km/s$ at a typical scale of $L \simeq (5 - 10) Kpc$, the non -linear term V^2/L turns out to be $3 \times 10^{-9} cm s^{-2}$, which is of the same order as found at small scales. The energy injection rate ϵ is found to be $10^{-2} erg s gm^{-1} s^{-1}$, which is close to the value obtained from our fits of the rotation curves.. The helicity is estimated to be $1/3 \times 10^{-9} cm s^{-2}$. The ratio of energy to helicity gives the typical length scale of the order of $10^{21} cm$. That is helical vortices of the scale of Kpc can exist in a time $T \simeq 10^9 yrs$ (at the same rate as large scale magnetic - fields, Khomenko et al.[21]).

Equivalently in the absence of net helicity , the second moment of the helicity the I - invariant is to be considered ; the ratio of I/E^2 (Levich and Tzvetkov [73]) gives a length scale of the order of a few Kpc. Such vorticity structures (4 Kpc in size) have been observed in the case of the galaxy Mrk1040. (Afanas'ev and Fridman [85]) . This does strengthen the case for the existence of a heirarchy of helical structures much beyond few hundred parsecs, as was conventionally thought. In fact in the survey conducted by Afanas'ev et al. they conclude that more than half of all the spiral galaxies have 'velocity- jumps' like the one seen in Mrk 1040 . Therefore all these are good candidates for supporting vortices. Our sample of fits also includes many such galaxies.

In this scheme of inverse cascade in 3D , the maximum correlation length is determined by the rate of energy - injection and the duration for which this rate is maintained. It must be appreciated that in the spectrum shown in fig. (1.2) the energy cascades to small scales near the origin, the inverse - cascade occurs in the intermediate range of scales, and stops when there is not enough energy and time to form the larger structure . Consequently the size of the system is always larger than

the size of the *coherent structures* found in it (Shore [81]).

The Reynolds stresses produced by small scale flow can act as a source for driving the large scale flow through Anisotropic-Kinetic -Alpha effect [27], the evidence for this is seen in their computer simulations [71]. *No coherent force is required* as argued by Sanchez [82]. It is reasonable to assume that a random ,anisotropic forcing with zero spatial and time averages exists in a galaxy with stellar explosions and interstellar turbulence. In fact there is ample proof to show that the interstellar medium is being driven by primarily a random force associated with kinetic energy release by supernovae and young stars. The interstellar turbulence is considerably helical. According to some conservative estimates the value of α , which is responsible for the dynamo action- is a few tenths of the turbulent velocity [78].

In conclusion ,we believe that the issue of applicability of the ICH inertial range to a galaxy , and therefore the non-applicability of the virial theorem at inertial range scales has been addressed adequately and the inverse cascade hypothesis stands vindicated . *The most favorable setting for ICH would be the early stages of galaxy-formation. We may then visualize the present day scenario as one which retains the initial signatures of velocity field.*

Some more points need to be clarified. viz..

1. First, breaks in the spectrum mark transitions from one inertial range to the next. Just as in 2D system the two invariants enstrophy and energy give rise to two inertial ranges in different spatial domains, similarly in 3D helically turbulent system there are two inertial ranges ($k^{-5/3}$ and k^{-1}) corresponding to the I-invariant and the energy invariant.
2. There is an increasing amount of evidence in favour of the k^{-1} energy spectrum for large scales, in the atmosphere. Moiseev and Onishchenko, [83] report the analysis of experiments using an active Doppler radiolocation probe. These observations were performed under conditions of tropical convective atmosphere in the western part of the Pacific ocean. A study of the property of the space-time structural function of the second order revealed interesting results. The fourier image $E(k)$ of the spatial part of the structural function of the second

order is of the order of k^{-1} . (See also [84])

3. We do not claim (neither is it needed for ICH to work), that ϵ should have a unique value for all the galaxies. ϵ is a measure of turbulent energy in a galaxy and its value depends upon the particular sources of turbulence in a given galaxy. The sources of turbulence like Supernovae explosions and stellar winds vary from galaxy to galaxy, leading to the scatter in epsilon values. Neither there is any universality or uniqueness in the observed rotation curves. This is ratified by our fits of rotation curves for nearly eighty galaxies. No single parameter can justify a mechanism but what we claim is, the fitting of rotation curves through ICH gives values of epsilon which are close to those obtained by other estimates. A galaxy may or may not show a flat rotation curve depending upon the value of epsilon and the duration for which this epsilon is maintained. Thus for small values of epsilon much larger duration would be required in order to produce large scale flow, manifested in a flat rotation curve. A typical value of epsilon 10^{-2} erg/gm/sec and a duration of 10^9 yrs seem to be the average values characteristic of a galaxy showing a flat rotation curve.
4. As we know in studies of turbulent systems for example a $k^{-5/3}$ energy spectrum is translated into a velocity spectrum going as $L^{1/3}$, where the L is identified with the real space. This implies that the average velocity on such a scale L goes as $L^{1/3}$. There is in fact no special scale or direction which is preferred. With the data for rotation curves of the galaxies being the only source of the galactic - velocity field information, we use this data set for fitting the velocity laws that we proposed. True that the galactocentric radius need not be the only scale in question but it is also a good representative of the ensemble, that we need to average over.

Chapter 3

TURBULENCE, GRAVITY & THE TULLY-FISHER RELATION

Let 'Chaos' storm

Let Cloud shapes swarm

I WAIT.....FOR FORM...

- Robert Frost -

[Pertinax]

3.1 Introduction

¹ In the preceding chapter we had proposed a model for the flat rotation curves of spiral galaxies. Therein we could resolve the galactic velocity field into a 'turbulent' and a 'gravity' component. Since the Tully-Fisher relationship ([88]) highlights a tight correlation between the galactic velocity and its luminosity we think it is worthwhile to study the individual correlation between the luminosity of a galaxy and its turbulent and gravity components of velocity. Towards this end we have modelled the velocity fields of 76 galaxies and the individual correlations were studied in the U,B,V,I and $I_{23.5}$ bands. This sample is severely limited by the fact that the overlap between

¹paper appeared in *Bull.Astron.Soc.India*, 24,787 (1996)

the set of galaxies which have been photometrically observed in all the related bands and the set consisting of galaxies whose rotation curves are available is very small. Nevertheless, the study revealed an interesting feature viz. the ‘turbulent’ component of the velocity appeared to correlate better than the ‘gravity’ component, for the U,B and V bands. Intriguingly enough the ‘gravity’ component correlated better with the luminosity in the I bands. In view of the fact that the luminosity of a galaxy is more sensitive to the mass in the longer wavelength regime, and much dominated by scatter in the shorter wavelength regime, we conclude that this study certifies that our velocity resolution law is indeed doing well in identifying the better correlating components as ‘turbulent’ and ‘gravitational’ in the respective regimes (Prabhu and Krishan[87]).

3.2 The Sample And The TULLY - FISHER Relation

The necessary data for studying the Tully - Fisher relation consists of apparent magnitudes, (usually corrected for Galactic and internal extinction,) and some measure of rotation velocities, corrected for projection effects due to the galaxy’s inclination in the plane of the sky. Usually rotation velocity is obtained via the doppler broadening of the HI 21cm line, although Fabry -Perot imaging and long slit rotation curves (both obtained via $H\alpha$) are useful as well.

The TF relation has been studied with samples drawn from the set of galaxies which are sufficiently close by . This was done presumably to get rid of the environment effects The relation has been studied in different bands also.

Hitherto the rotational velocity was obtained either by finding out the maximum of the rotation curve V_{max} or the rotational velocity at a suitably chosen radius (Holmbergh radius)- corresponding to a suitable aperture magnitude definition. Estimates of V_{max} using the line profile measured at 20% of the peak, have also been used. We use a different way to characterize the galactic velocity field. Since our model gives a good fit for the velocity field we use the flat portion of the curve to estimate

the average velocity in that regime. We use our proposed law to do this averaging numerically. As for the photometric properties of our sample, we obtained the data from the NASA extragalactic database, and the RC3 catalogue.

Our sample of galaxies were drawn from different clusters and field galaxies as observed by Rubin et al.[58], [59], and Amram et al.[56],[57]. Our primary interest was to get a sufficiently large set of galaxies, (irrespective of their distance, environment, mass, radius, or luminosity) for which the photometry (U,B,V,I& $I_{23.5}$) was done and velocity fields mapped. All in all our sample consisted of:

20 Sb galaxies - observed by Rubin et al. [58]

21 Sc galaxies - observed by Rubin et al. [59]

35 other galaxies -observed by Amram et al. [56],[57]

(drawn from different cluster environments viz. the Coma, Pegasus, Abel, Hercules,.. etc)

We reproduce the photometric data in the tables (3.1,3.2 & 3.3) We also list the values for the average turbulent velocity component and average gravity - component in the following tables. Note that the values are in general comparable.(Tables 3.4 - 3.6)

Table 3.1: Table showing the Photometric data obtained mainly from the NASA extragalactic database. '-' means no data available

Name	r(MPC)	U_T^0	B_T^0	V_T^0	I_T	$I_{23.5}$
NGC668	59.96	-	13.10	-	-	-
NGC669	63.20	-	13.00	-	-	-
NGC688	54.90	12.65	12.70	12.18	-	-
UGC1347	73.04	13.30	13.40	12.83	-	-
NGC753	64.73	12.26	12.30	11.81	-	-
UGC1493	55.24	-	13.20	-	-	-
Z119051	66.47	-	-	-	13.80	13.98
NGC3861	67.66	13.19	13.10	12.42	11.31	11.42
NGC3883	92.56	13.31	13.20	12.53	11.20	11.45
UGC8161	88.86	14.76	14.56	13.86	12.97	13.05
I1179	146.30	15.93	15.68	15.15	-	-
NGC6050	125.73	14.97	15.04	14.47	13.70	13.79
NGC6054	147.77	15.36	15.37	14.93	-	-
NGC7591	65.20	13.04	12.96	12.32	11.50	11.64
NGC7536	62.53	13.29	13.38	12.95	11.87	11.95
NGC7593	54.73	13.78	13.91	13.33	12.47	12.53
UGC12498	55.60	13.90	13.89	13.27	12.03	12.18
NGC7631	49.97	13.14	13.07	12.45	11.44	11.51
NGC7643	51.16	13.92	13.69	12.87	-	-
NGC4848	95.52	13.45	13.61	13.17	-	-
Z160058	100.84	14.59	14.58	14.06	-	-
NGC4911	105.49	13.52	13.38	12.68	-	-
NGC4921	72.66	13.21	12.85	12.05	-	-
Z160106	94.66	-	14.80	-	-	-
Z130008	96.60	-	15.30	-	-	-
Z119043	59.33	-	15.00	-	-	-
UGC4329	54.46	13.63	13.77	13.27	13.41	13.51
NGC2558	66.64	13.71	13.48	12.73	-	-
Z119053	64.66	-	15.10	-	-	-
UGC4386	61.73	13.39	13.28	12.57	11.18	11.22

Table 3.2: Table showing the Photometric data, contd..

Name	r(MPC)	U_T^0	B_T^0	V_T^0	I_T	$I_{23.5}$
NGC2595	57.64	12.60	12.59	12.02	10.98	11.10
UGC3269	118.76	-	14.02	-	12.83	12.90
UGC3282	109.64	-	13.99	-	12.66	12.79
UGC10085	129.64	14.47	14.44	13.95	13.04	13.17
NGC6045	133.13	13.71	13.81	13.13	-	-
NGC4605	5.80	10.11	10.27	9.82	-	-
NGC1035	24.50	-	12.19	-	-	-
NGC4062	14.80	11.26	11.28	10.62	-	-
NGC2742	27.30	11.46	11.47	11.01	-	-
NGC701	36.50	12.18	12.27	11.73	-	-
NGC2608	41.20	12.54	12.53	11.94	-	-
NGC3495	19.00	-	10.74	-	-	-
NGC1087	30.50	10.84	10.97	10.55	-	-
UGC3691	41.50	-	-	-	-	-
NGC4682	43.00	-	-	-	-	-
NGC3672	33.10	-	11.41	10.82	-	-
NGC1421	39.70	10.78	11.00	10.71	-	-
NGC2715	29.70	10.90	11.09	10.67	-	-
NGC4321	20.00	9.93	9.98	9.33	-	-
I467	44.30	12.12	12.22	11.75	-	-
NGC7541	57.50	11.49	11.57	11.09	-	-
NGC7664	74.20	12.61	12.66	12.08	-	-
NGC2998	95.60	-	12.52	12.07	-	-
NGC801	119.00	12.60	12.44	11.83	-	-
UGC2885	118.00	-	-	-	-	-
NGC4800	19.50	-	12.13	-	-	-
NGC2708	35.50	12.54	12.43	11.76	-	-
NGC3067	28.30	12.19	12.22	11.70	-	-

Table 3.3: Table showing the Photometric data , contd..

Name	r(MPC)	U_T^0	B_T^0	V_T^0	I_T	$I_{23.5}$
NGC4448	19.00	11.53	11.28	10.52	-	-
NGC1515	19.10	11.14	11.01	10.39	-	-
NGC1353	30.00	11.96	11.73	10.93	-	-
NGC1325	30.00	11.48	11.51	10.99	-	-
NGC7537	57.30	12.46	12.69	12.30	-	-
U11810	98.30	13.33	13.50	13.07	-	-
NGC7171	57.40	12.31	12.38	11.80	-	-
NGC7217	24.70	10.78	10.53	9.67	-	-
NGC1620	68.40	12.37	12.27	11.70	-	-
NGC3054	43.10	-	-	-	-	-
NGC2590	95.80	-	12.99	12.32	-	-
NGC2815	45.50	11.65	11.42	10.82	-	-
NGC1417	81.50	12.30	12.26	11.69	-	-
NGC1085	136.00	-	-	-	-	-
NGC3145	68.80	11.97	11.82	11.19	-	-
NGC3223	52.40	11.07	10.96	10.35	9.42	9.50
NGC7606	47.50	-	10.88	10.29	-	-
NGC3200	65.30	11.75	11.68	11.13	-	-

Table 3.4: Table showing the individual velocity components viz. 'gravity' and the 'turbulent' components, resolved by our model

Name	$\langle V_{total} \rangle$ (Km/s)	$\langle V_{turbulent} \rangle$ (Km/s)	$\langle V_{gravity} \rangle$ (Km/s)
NGC668	185	105	80
NGC669	333	265	68
NGC688	214	87	127
UGC1347	101	41	60
NGC753	205	108	97
UGC1493	173	144	29
Z119051	98	73	25
NGC3861	273	137	136
NGC3883	166	56	110
UGC8161	93	60	33
I1179	139	35	104
NGC6050	181	132	49
NGC6054	142	106	36
NGC7591	222	152	70
NGC7536	171	108	63
NGC7593	149	75	74
UGC12498	136	51	85
NGC7631	193	126	67
NGC7643	194	15	179
NGC4848	265	166	99
Z160058	200	38	162
NGC4911	281	96	185
NGC4921	171	20	151
Z160106	200	85	115
Z130008	151	2	149
Z119043	144	41	103
UGC4329	129	73	56
NGC2558	245	113	132
Z119053	112	72	40
UGC4386	265	52	213

Table 3.5: Table showing the 'gravity' and 'turbulent' velocity components contd..

Name	$\langle V_{total} \rangle$ (Km/s)	$\langle V_{turbulent} \rangle$ (Km/s)	$\langle V_{gravity} \rangle$ (Km/s)
NGC2595	296	231	65
UGC3269	176	98	78
UGC3282	207	140	67
UGC10085	165	135	30
NGC6045	317	72	245
NGC4605	82	50	32
NGC1035	121	39	82
NGC4062	153	76	77
NGC2742	165	53	112
NGC701	152	6	146
NGC2608	109	73	36
NGC3495	168	48	120
NGC1087	123	77	46
UGC3691	128	31	97
NGC4682	162	96	66
NGC3672	191	57	134
NGC1421	169	105	64
NGC2715	143	45	98
NGC4321	184	157	27
I467	141	66	75
NGC7541	201	170	31
NGC7664	187	152	35
NGC2998	207	115	92
NGC801	214	121	93
UGC2885	265	208	57
NGC4800	162	98	64
NGC2708	243	21	222
NGC3067	140	50	90

Table 3.6: Table showing the 'gravity' and 'turbulent' velocity components, contd..

Name	$\langle V_{total} \rangle$ (Km/s)	$\langle V_{turbulent} \rangle$ (Km/s)	$\langle V_{gravity} \rangle$ (Km/s)
NGC4448	192	38	154
NGC1515	173	54	119
NGC1353	196	114	82
NGC1325	176	43	133
NGC7537	143	89	54
U11810	151	97	54
NGC7171	195	74	121
NGC7217	256	111	145
NGC1620	225	121	104
NGC3054	237	116	121
NGC2590	226	134	92
NGC2815	278	188	90
NGC1417	268	159	109
NGC1085	303	208	95
NGC3145	263	97	166
NGC3223	253	89	164
NGC7606	262	72	190
NGC3200	266	200	66

3.3 Discussions

We observe an interesting trend in our statistical analysis. (see figure fig(3.1)- for the scatter plot; fig(3.1a)- for the table.)

Firstly the total velocity correlated in the same conventional way as it does for a standard Tully -Fisher relation. We confirmed the normal trend wherein the correlations improve as we go to the longer bands (from U to the I bands). So, we confirm the Tully-Fisher relation in the first step. While modelling the rotation curves of galaxies we have separated the contributions from gravity and turbulence velocity. We find that the turbulent component correlates better than the gravity component in the U, B, and V bands.(It is to be noted here that our model gives comparable magnitudes for both the components . Thus it is interesting to note that something else other than the gravity -induced velocity is correlating better !). This trend is reversed as we approach the I bands , viz. the gravity component correlates better. This is to be expected since the longer wavelength bands are more sensitive to the mass component (i.e the gravity - induced velocity..) ². We believe that the so called ‘turbulent’ component which our model resolves could be more than just scatter, for the correlations are statistically very significant (see Appendix A). We conjecture that it could be the ‘coherent’ velocity field which is contributing to the rotation as observed . Thus it would be erroneous to interpret the observed spectral line widths as ‘those induced by gravity alone’. This also emphasizes the need to study the self-organizing aspects of turbulent media, which could enrich the structure - formation scenarios in astrophysics.

Lastly, as a matter of convention we also present the mass to luminosity ratios (M/L) which we calculate for the set of galaxies in each of the photometric bands (fig 3.2 - fig 3.6) We find that almost all the values fall within an M/L ratio of 10. This is very much unlike the ‘dark -matter’ scenarios where this value increases steadily from the galactic - level (say 50s -100s) to the clusters (where it runs into 1000s). Thus our model can do away with the excess ‘matter’ required to explain the observations.

²we thank Dr.Matthew Colless (Mount Stromlo and Siding Spring Observatories, Australia), for bringing this to our notice

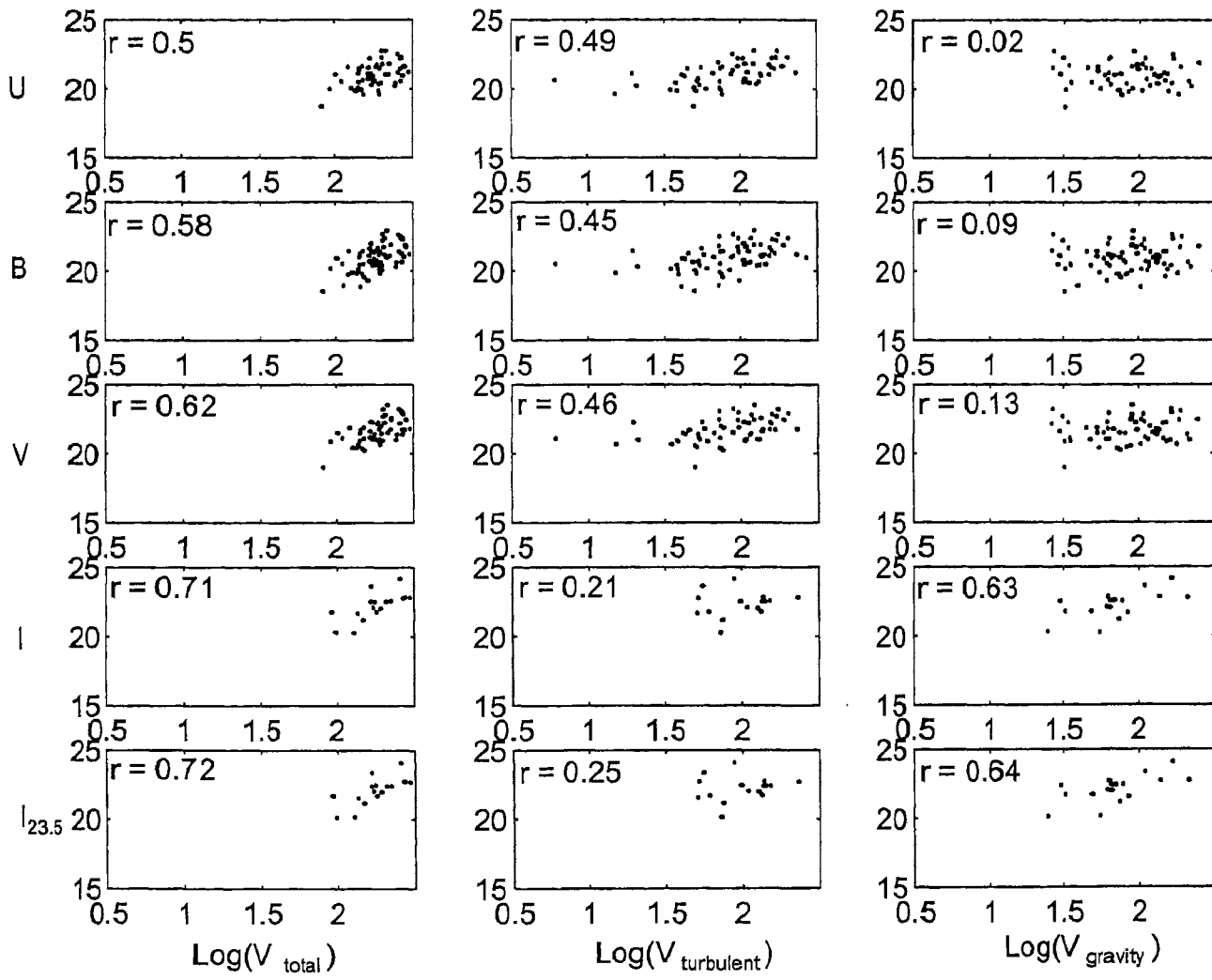


Figure 3.1: The scatter plot between different velocity components and luminosities of the galaxies in different bands viz . U , B , V, I and $I_{23.5}$.

Table summarizing the statistics of the sample.

PHOTOMETRIC BANDS

average		U	B	V	I	I _{23.5}
V _{tot}	Up	0.65	0.69	0.74	0.85	0.85
	r	0.5	0.58	0.62	0.71	0.72
	Low	0.31	0.43	0.47	0.40	0.41
	P	10 ⁻⁴ ***	10 ⁻⁸ ***	10 ⁻⁷ ***	0.001 **	0.001 **
V _{turb}	Up	0.64	0.59	0.61	0.54	0.57
	r	0.49	0.45	0.46	0.21	0.25
	Low	0.29	0.27	0.27	0.20	0.17
	P	10 ⁻⁴ ***	10 ⁻⁵ ***	10 ⁻⁴ ***	0.40 ns	0.39 ns
V _{grav}	Up	0.20	0.28	0.33	0.80	0.80
	r	-0.02	0.09	0.13	0.63	0.64
	Low	-0.24	-0.10	-0.08	0.27	0.29
	P	0.83 ns	0.44 ns	0.30 ns	0.006 **	0.005 **
df		52	68	56	15	15

r correlation coefficient
 Up upper limit on r (90% confidence interval)
 Low lower limit on r (90% confidence interval)
 P probability from t statistics
 *** => P < 0.001 (very significant correlation)
 ** => 0.001 < P < 0.01 (quite significant correlation)
 ns not significant
 df degrees of freedom

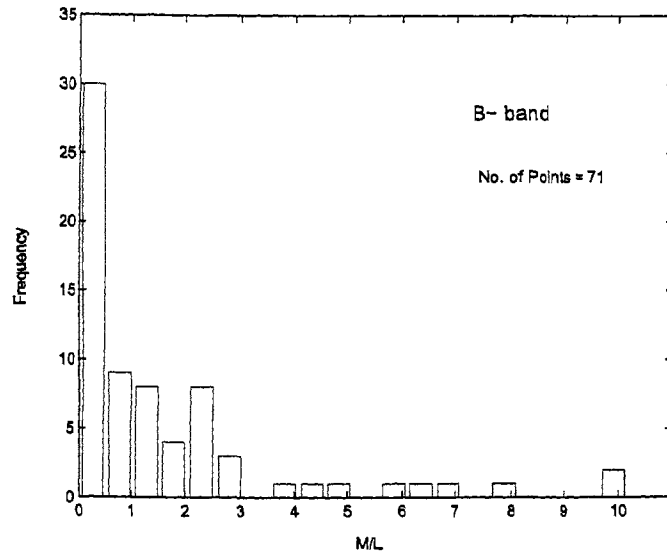


Figure 3.2: Histogram showing the distribution of mass to luminosity ratios in the B-band

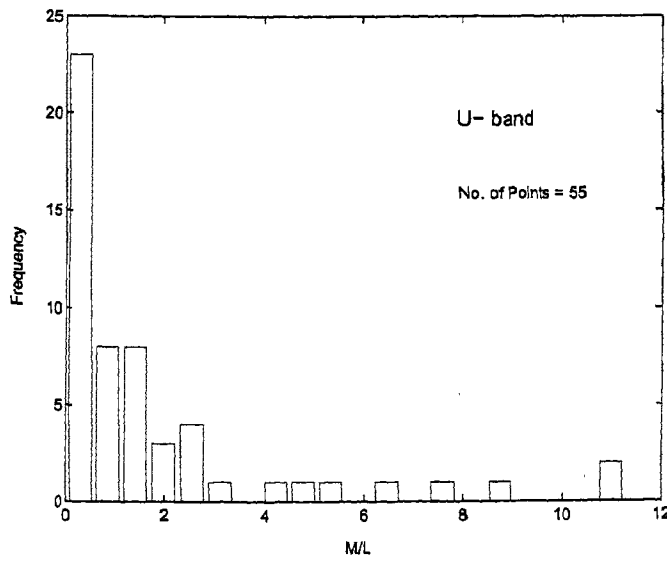


Figure 3.3: Histogram showing the distribution of mass to luminosity ratios in the U-band

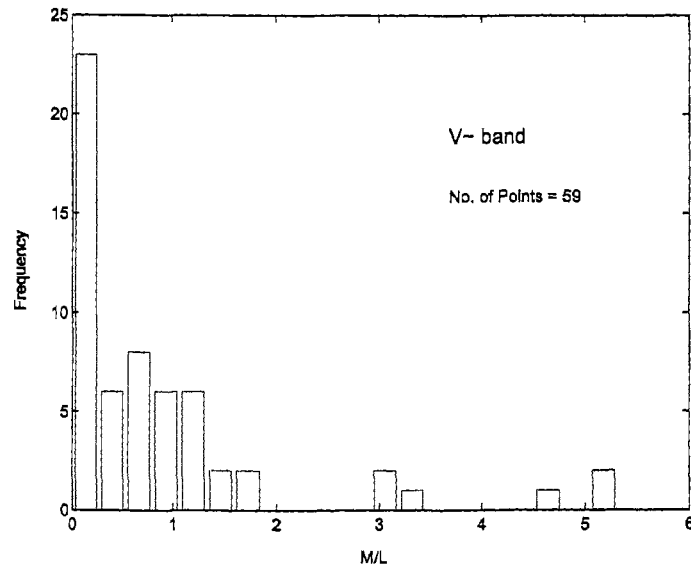


Figure 3.4: Histogram showing the distribution of mass to luminosity ratios in the V- band

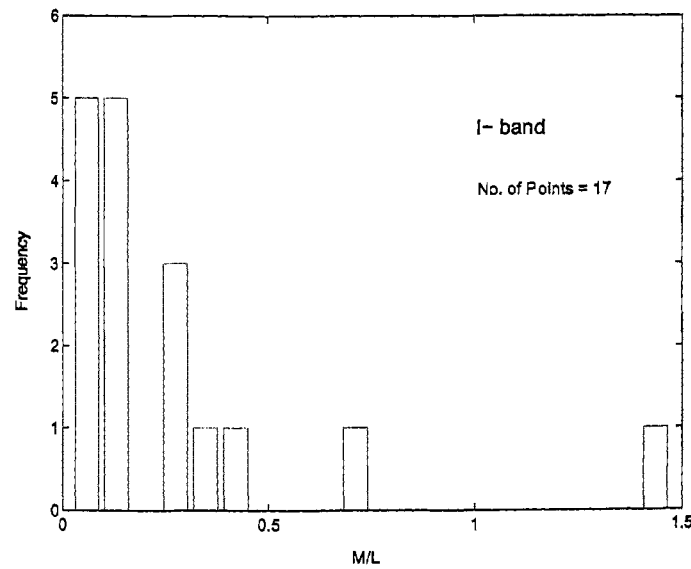


Figure 3.5: Histogram showing the distribution of mass to luminosity ratios in the I- band

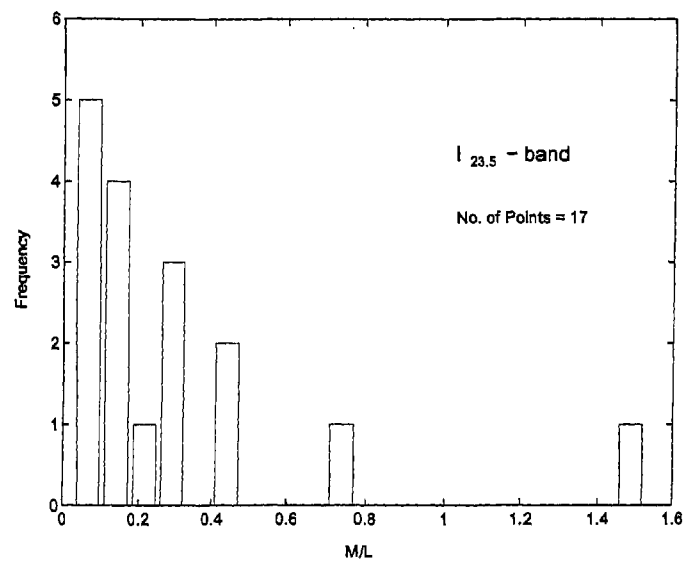


Figure 3.6: Histogram showing the distribution of mass to luminosity ratios in the $I_{23.5}$ - band

Chapter 4

ROLE OF HELICITY IN AN EXPANDING FLUID

..the topology of the atmosphere probably should be presented as a helix inside a helix, inside a helix, etc ., a vastly complicated and stable construction.

- E.Levich and E.Tzvetkov -

4.1 Introduction

We had seen in the preceeding chapters that that there is enough observational evidence, pointing out the role of turbulence as well as the helical nature of structures observed. Here in order to study the role of helicity in the context of structure formation in the universe, we consider the model of an expanding fluid. Extending Kurskov and Ozernoi's [89] work to the case of a compressible fluid we find suitable transformations using which the equations of the perturbed flow are reduced to the standard Navier - Stokes form. Subsequently it is found that there are situations when helicity evolution is coupled to the density evolution. Even though the special case which we consider may seem trivial, this is of vital consequence to the study of large scale structures in the astrophysical context. Our study underlines the need to emphasize the role of helicity in the hydrodynamic evolution of the universe [?].

The role played by helical motions is believed to be central to the problem of

understanding the dynamics of fluid turbulence and the myriad features which have been reported by the observations of fluid turbulence, [90],[72] and [91]. Amongst these it has been realised that features like intermittency and the appearance of large scale coherent structures in turbulent media can be understood by studying the nonlinear interactions in terms of helical - decomposition of the flow [92]. Such a study clearly spells out the possibility of the inverse cascade of energy to large scales starting from the small scales, thus aiding structure formation. (See also [93]- [96])

4.2 The basic equations and the transformations

The Navier - stokes equations for a fluid with density ρ and velocity components u_i (where $i=1,2,3$ are the x,y, and z components respectively) are

$$\rho \frac{\partial u_i}{\partial t} + \rho u_j \frac{\partial u_i}{\partial x_j} = \rho X_i - \frac{\partial p}{\partial x_i} + \frac{\partial}{\partial x_j} \left(\mu \left(\frac{\partial u_i}{\partial x_j} + \frac{\partial u_j}{\partial x_i} \right) - \mu \frac{2}{3} \frac{\partial u_k}{\partial x_k} \delta_{ij} \right) \quad (4.1)$$

Where X_i , is the i component of the body force acting on a fluid element; μ , is the molecular viscosity of the fluid; p, is the pressure and; δ_{ij} , is the kronecker delta function (i.e $\delta_{ij} = 1$ when $i = j$, and zero for i not equal to j)

The continuity equation expressing the conservation of mass for such a fluid is,

$$\frac{\partial \rho}{\partial t} + \frac{\partial (\rho u_i)}{\partial x_i} = 0 \quad (4.2)$$

(the Einstein summation convention is followed here .)

If the fluid is self gravitating the system has to satisfy Poisson equation also viz.

$$\nabla^2 \phi = 4\pi G \rho \quad (4.3)$$

where G is the universal gravitation constant and ϕ is the potential produced by the mass distribution specified by density function ρ . The body force in equation

(4.1) then is given as,

$$\mathbf{X} = -\nabla \phi \quad (4.4)$$

In order to model the expanding universe we must incorporate the Hubble flow into the above equations. Hubble flow may be treated as the main component over

and above which the evolution of perturbations can be studied. Therefore we resolve the velocity, pressure, density and potential into a mean and a fluctuating component in each case and write;

$$\begin{aligned} \mathbf{u} &= \mathbf{u}_0 + \mathbf{v} \\ p &= p_0 + p_1 \\ \rho &= \rho_0 + \rho_1 \\ \phi &= \phi_0 + \phi_1 \end{aligned} \quad (4.5)$$

where the subscript '0' is used for denoting the unperturbed quantity and the subscript '1' is used to represent the perturbed component. For the velocity, \mathbf{u} represents the total flow which must satisfy equation (4.1), \mathbf{u}_0 is the Hubble flow and \mathbf{v} represents the perturbed component, viz. the peculiar flow. The Hubble flow is represented as, $\mathbf{u}_0 = H\mathbf{r}$, where H is the Hubble constant. The Hubble constant is also represented as $H = \frac{\dot{a}}{a}$, where a is the scaling factor and is a function of only time. Therefore,

$$\mathbf{u}_0 = \frac{\dot{a}}{a}\mathbf{r} \quad (4.6)$$

We may note that for such an expanding fluid the viscosity terms of equation (4.1) which involve a double derivative vanish. *Therefore a uniformly expanding fluid obeying the Hubble flow doesn't experience viscosity.*

If we assume the unperturbed pressure p_0 , to be constant then in the equation for the unperturbed flow \mathbf{u}_0 only the body force term remains. Thus

$$\frac{D\mathbf{u}_0}{Dt} = -\nabla\phi_0 \quad (4.7)$$

here we have used ' $\frac{D}{Dt}$ ' to represent the material derivative, $\left(\frac{\partial}{\partial t} + \mathbf{u}_0 \cdot \nabla\right)$

Taking the divergence of equation (4.7) and using equation (4.6) and equation (4.3) we arrive at the following relation,

$$\frac{\ddot{a}}{a} = -\frac{4\pi\rho_0 G}{3} \quad (4.8)$$

implying that ρ_0 is a function of time and it satisfies the equation:

$$\frac{\partial \rho_0}{\partial t} + \nabla \cdot (\rho_0 \mathbf{u}_0) = 0$$

or

$$\frac{\partial \rho_0}{\partial t} + 3\rho_0 \frac{\dot{a}}{a} = \frac{\partial (\rho_0 a^3)}{\partial t} = 0 \quad (4.9)$$

To get the equation for the perturbed flow we simply subtract equation (4.7) from equation for \mathbf{u} . We obtain,

$$\frac{D\mathbf{v}}{Dt} + \frac{\dot{a}\mathbf{v}}{a} + (\mathbf{v} \cdot \nabla) \mathbf{v} = -\nabla \phi_1 - \frac{\nabla p_1}{(\rho_0 + \rho_1)} + \nu \nabla^2 \mathbf{v} + \frac{\nu}{3} \nabla (\nabla \cdot \mathbf{v}) \quad (4.10)$$

where we have replaced $\frac{\mu}{\rho}$ by ν the kinematic viscosity. Similarly the perturbed component of density ρ_1 , obeys the following equation,

$$\frac{D\rho_1}{Dt} + \nabla \cdot ((\rho_0 + \rho_1) \mathbf{v}) + \frac{3\dot{a}}{a} \rho_1 = 0 \quad (4.11)$$

Now going over to the comoving frame we merely have to effect the following substitutions for the temporal and spatial derivatives,

$$\begin{aligned} \left(\frac{\partial}{\partial t} + \mathbf{u}_0 \cdot \nabla \right) &\equiv \frac{D}{Dt} = \left(\frac{\partial}{\partial t} \right)_{\text{comoving}} \\ a \nabla &= \nabla_{\text{comoving}} \end{aligned} \quad (4.12)$$

Henceforth we shall drop the subscript '*comoving*' and simply use the normal notation to mean the comoving frame. Also the $\frac{D}{Dt}$ symbol shall be freely used to imply the material derivative in the *comoving* frame.

Therefore the new set of equations for the perturbed quantities (including the potential) are ,

$$\frac{\partial \mathbf{v}}{\partial t} + \frac{\dot{a}\mathbf{v}}{a} + \frac{(\mathbf{v} \cdot \nabla) \mathbf{v}}{a} = -\frac{\nabla \phi_1}{a} - \frac{\nabla p_1}{a(\rho_0 + \rho_1)} + \frac{\nu \nabla^2 \mathbf{v}}{a^2} + \frac{\nu \nabla (\nabla \cdot \mathbf{v})}{3a^2} \quad (4.13)$$

$$\frac{\partial \rho_1}{\partial t} + \frac{\nabla \cdot ((\rho_0 + \rho_1) \mathbf{v})}{a} + \frac{3\dot{a}\rho_1}{a} = 0 \quad (4.14)$$

$$\frac{\nabla^2 \phi_1}{a^2} = 4\pi G \rho_1 \quad (4.15)$$

We would like to see if it is possible to restore the standard 'Navier -Stokes' form by any set of transformations which would help us in getting rid of the extra terms in equations (4.13) and (4.14).

To begin with let us effect the following transformations,[6]

$$\begin{aligned} \mathbf{v} &= \frac{g}{2} \mathbf{v}^* \\ \frac{\partial}{\partial t} &= \frac{g}{2a} \frac{\partial}{\partial t^*} \end{aligned} \quad (4.16)$$

Inserting these into equation (4.13) and multiplying both sides by $\frac{4a}{g^2}$ gives,

$$\begin{aligned} \frac{\partial \mathbf{v}^*}{\partial t^*} + \left(\frac{\mathbf{v}^*}{g} \frac{\partial g}{\partial t^*} + \frac{2\dot{a}}{g} \mathbf{v}^* \right) + (\mathbf{v}^* \cdot \nabla) \mathbf{v}^* &= -\frac{4a}{g^2 a (\rho_0 + \rho_1)} \nabla p_1 - \frac{4a}{g^2} \frac{\nabla \phi_1}{a} + \\ &\quad \nu \frac{4a}{g^2} \frac{g}{2a^2} \nabla^2 \mathbf{v}^* + \nu \frac{4a}{g^2} \frac{g}{6a^2} \nabla (\nabla \cdot \mathbf{v}^*) \end{aligned} \quad (4.17)$$

We can see that the above equation can be made to resemble the Navier-Stokes momentum equation if the second and third terms on the left hand side (enclosed within braces) vanish. Therefore the necessary condition simplifies as,

$$\frac{1}{g} \frac{\partial g}{\partial t^*} + \frac{2\dot{a}}{g} = 0$$

or transforming from t^* to t coordinate we obtain,

$$\frac{\dot{g}}{g} = -\frac{\dot{a}}{a} \quad (4.18)$$

that implies that $g \cdot a = k$ (constant).

Now if we redefine the pressure, potential and viscosity (kinematic) in the starred frame as,

$$p_1' = \frac{4p_1}{g^2}$$

$$\begin{aligned}\phi_1^* &= \frac{4\phi_1}{g^2} \\ \nu^* &= \frac{2}{ga}\nu\end{aligned}\quad (4.19)$$

We can rewrite equation (4.17) as

$$\frac{\partial \mathbf{v}^*}{\partial t^*} + (\mathbf{v}^* \cdot \nabla) \mathbf{v}^* = -\frac{\nabla p_1'}{(\rho_0 + \rho_1)} - \nabla \phi_1^* + \nu^* \nabla^2 \mathbf{v}^* + \frac{\nu^*}{3} \nabla (\nabla \cdot \mathbf{v}^*) \quad (4.20)$$

Note that we still have to reduce the density equation to the normal form and that would effect the transformation of the pressure term above (which is why we have used the primed notation for pressure and not the starred notation which would mark the final stage of transformation).

Let us transform the density variable as

$$\rho_1 = \rho_1' a^{-3} \quad (4.21)$$

Substituting this relation in equation (4.14), multiplying both the sides by a^3 and using the velocity and time transformations along with the substitution of \mathbf{g} from equation (4.20) we get,

$$\frac{\partial \rho_1}{\partial t^*} + \nabla \cdot [(\rho_1' + \rho_0 a^3) \mathbf{v}^*] = 0 \quad (4.22)$$

Now we may use the equation (4.9) for the unperturbed density in the above equation (4.22) to get ,

$$\frac{\partial (\rho_1' + \rho_0 a^3)}{\partial t^*} + \nabla \cdot [(\rho_1' + \rho_0 a^3) \mathbf{v}^*] = 0 \quad (4.23)$$

Thus redefining our density as

$$\rho^* = \rho_1' + \rho_0 a^3 \quad (4.24)$$

we arrive at the standard form of the continuity equation for $k=1$. Equation (4.24) , implies that $(\rho_0 + \rho_1) = \rho_0 + \rho_1' a^{-3} = \rho_0 + (\rho^* a^{-3} - \rho_0) = \rho^* a^{-3}$

Substituting this in the denominator of the pressure term of equation (4.20) the new pressure is defined as:

$$p_1^* = \frac{4p_1}{g^2 a^{-3}} \quad (4.25)$$

Finally we see that equations (4.16), (4.18), (4.19) and (2.21), (4.24) and (2.25) are the set of transformations which allow us to reduce the equations of the perturbed flow in the comoving frame to the standard form .

4.3 Helicity and density evolutions

Having reduced the equations of motion to the standard form we are now in a position to talk about the conservation of helicity in the expanding frame too. In general, the governing equations for an inviscid fluid driven by an external force \vec{F} are,[2]

$$\frac{D\vec{v}}{Dt} = \frac{-1}{\rho} \nabla p + \vec{F} \quad (4.26)$$

Mass conservation would imply,

$$\frac{\partial \rho}{\partial t} + \nabla \cdot (\rho \vec{v}) = 0 \quad (4.27)$$

or

$$\frac{\partial \rho}{\partial t} + \rho(\nabla \cdot \vec{v}) + (\vec{v} \cdot \nabla) \rho = 0 \quad (4.28)$$

multiplying both sides of the above equation by $\frac{-\vec{\omega}}{\rho^2}$ and simplifying :

$$\vec{\omega} \cdot \frac{\partial}{\partial t} \frac{1}{\rho} - \frac{\vec{\omega}}{\rho} (\nabla \cdot \vec{v}) + \vec{\omega} \cdot \left(\vec{v} \cdot \nabla \frac{1}{\rho} \right) = 0 \quad (4.29)$$

Now taking the curl of the equation (4.26), multiplying both sides by $\frac{1}{\rho}$, assuming the fluid is barotropic and simplifying we get

$$\frac{1}{\rho} \frac{\partial \vec{\omega}}{\partial t} + \frac{1}{\rho} \vec{\omega} (\nabla \cdot \vec{v}) + \frac{1}{\rho} (\vec{v} \cdot \nabla) \vec{\omega} - \left(\frac{\vec{\omega}}{\rho} \cdot \nabla \right) \vec{v} = 0 \quad (4.30)$$

Adding equation (4.30) to equation (4.29) we get :

$$\frac{D}{Dt} \left(\frac{\vec{\omega}}{\rho} \right) = \left(\frac{\vec{\omega}}{\rho} \right) \cdot \nabla \vec{v} \quad (4.31)$$

where ρ is the density of the fluid, $p = p(\rho)$ the pressure (for a barotropic fluid), and $\vec{F} = -\nabla\phi$, the conservative body force. We can define helicity as the volume integral in the form given below

$$H_s = \int_V \left(\frac{h}{\rho} \right) \cdot \rho dV \quad (4.32)$$

where $h = \vec{v} \cdot \vec{\omega}$.

Then the rate of change of H_s would be given as

$$\frac{dH_s}{dt} = \int_V \frac{D}{Dt} \left[\left(\frac{h}{\rho} \right) \right] \cdot \rho dV \quad (4.33)$$

That implies that,

$$\begin{aligned} \frac{D}{Dt} \left(\frac{\vec{v} \cdot \vec{\omega}}{\rho} \right) &= \frac{\vec{\omega}}{\rho} \cdot \frac{D\vec{v}}{Dt} + \vec{v} \cdot \frac{D(\vec{\omega})}{Dt} \\ &= \frac{\vec{\omega}}{\rho} \cdot \left[\frac{-\nabla p}{\rho} + \vec{F} \right] + \vec{v} \cdot \left[\frac{\vec{\omega}}{\rho} \cdot \nabla \right] \vec{v} \\ &= \frac{\vec{\omega}}{\rho} \cdot \left[\frac{-\nabla p}{\rho} + \vec{F} \right] + \frac{\vec{\omega}}{\rho} \cdot \left[\nabla \left(\frac{v^2}{2} \right) \right] \\ &= \frac{\vec{\omega}}{\rho} \cdot \left[\nabla \left(\frac{v^2}{2} - e - \phi \right) \right] \\ &= \frac{\vec{\omega}}{\rho} \cdot [\nabla Q] \\ &= \frac{1}{\rho} \nabla \cdot (\vec{\omega} Q) \end{aligned} \quad (4.34)$$

$$\frac{D}{Dt} \left(\frac{h}{\rho} \right) = \left(\frac{\vec{\omega}}{\rho} \cdot \nabla \right) Q = \frac{1}{\rho} \nabla \cdot (\vec{\omega} Q) \quad (4.35)$$

where

$$Q = \frac{v^2}{2} - e - \phi \quad (4.36)$$

and

$$e = \int \frac{dp}{\rho} \quad (4.37)$$

is the enthalpy per unit mass.

Substituting equation (4.35) in equation (4.33) and converting the volume integral into surface integral we have for a vorticity surface on which $\vec{\omega} \cdot \hat{n} = 0$,

$$\frac{dH_s}{dt} = \int_S (\vec{\omega} \cdot \hat{n}) Q dS = 0$$

This proves the conservation of helicity.

4.4 Interesting features of the evolution

Expanding equation (4.35) we find that

$$\frac{1}{\rho} \frac{Dh}{Dt} - \frac{h}{\rho^2} \frac{D\rho}{Dt} = \left(\frac{\vec{\omega}}{\rho} \cdot \nabla \right) Q$$

This equation reveals an interesting feature for the case $\vec{\omega} \cdot \nabla Q = 0$. We find ,

$$\frac{1}{h} \frac{Dh}{Dt} = \frac{1}{\rho} \frac{D\rho}{Dt} \quad (4.38)$$

which clearly states that *the helicity and mass density of a fluid packet evolve together*

Let us recall the equation for a steady flow of a barotropic fluid i.e.,

$$(\vec{v} \cdot \nabla) \vec{v} = -\frac{\nabla p}{\rho} - \nabla \phi \quad (4.39)$$

Using the vector identity for $\nabla(\vec{A} \cdot \vec{B})$ we may substitute for the nonlinear term in the above equation and obtain

$$\nabla \left(\frac{v^2}{2} \right) + \vec{\omega} \times \vec{v} = -\frac{\nabla p}{\rho} - \nabla \phi$$

which can be rewritten as

$$\nabla \left(\frac{v^2}{2} + e + \phi \right) + \vec{\omega} \times \vec{v} = 0$$

or

$$\nabla B + \vec{\omega} \times \vec{v} = 0$$

where $B = \frac{v^2}{2} + e + \phi$ is the Bernoulli function. (Compare this with $Q = \frac{v^2}{2} - e - \phi$), e is the same as in equation (4.37), and ϕ is the potential of a conservative force \vec{F} .

If we take the dot product of the above equation with $\vec{\omega}$ we obtain

$$\vec{\omega} \cdot \nabla B = 0$$

Now the above result implies that $\vec{\omega} \cdot \nabla Q$ can also be equal to zero only when $\nabla \frac{v^2}{2}$ is zero. Therefore our assumption is valid only when v^2 is constant i.e on constant energy surfaces.

Returning now back to the equation (4.38) we discuss it's nature qualitatively. We find that since helicity can be of either positive or negative sign and density can only have a positive sign, the following cases arise.

	h	$\frac{Dh}{Dt}$	$\frac{D\rho}{Dt}$
1.	+	+	+
2.	+	-	-
3.	-	+	-
4.	-	-	+

Cases 1 and 4 imply that in regions where helicity of either sign grows (say positive becomes more positive or negative becomes more negative) density also grows. Whereas in regions where helicity decays density also shows the same trend (cases 2 and 3). These two conclusions point out the possibility of explaining the growth of 'voids' and density structures in the astrophysical context, where interestingly such features are all the more prominent (i.e the existence of large volumes of voids and large scale structures is well established.). This observation has to be viewed with seriousness in the astrophysical context, to understand more precisely how helicity influences the density evolution in various structure formation scenarios [8]. We would also like to emphasize that just as vorticity is generated through changes in the Bernoulli function in a steady flow (Crocco's theorem) [37], the changes in helicity can be produced through the variation of the function Q in a non-steady flow. At this point it may be appropriate to mention that Belyan et al. [99] studied the problem of sound propagation in a turbulent medium and found that the transformation of a sound wave (analogous to density perturbation in our case) into vortical motions is possible during its propagation through a turbulent medium, and these vortical

motions were shown to be helical in the case when the turbulence helicity is nonzero. Their work vindicates the connection between helicity and density derived here.

4.5 Conclusion

In view of the increasing realization of the role played by helical motions in the evolution of fluid turbulence we have tried to understand its role in the case of an expanding fluid. This would help us in introducing the concept of helicity and helical decomposition of flows in the context of astrophysical flows as well [92], [97]. It is found that a suitable set of transformations can be arrived at thus simplifying the equations for the perturbed flow, into the standard Navier - Stokes form. The connection between the helicity evolution and density evolution is clearly established. A particular case (i.e when $\vec{\omega} \cdot \nabla Q = 0$) is qualitatively analyzed whereby it is shown that the density growth is enhanced in regions of growing helicity of any sign whereas density is depleted in regions where helicity decays.

Chapter 5

SIMULATING 'INVERSE CASCADE'

THE PURPOSE OF SIMULATIONS IS 'INSIGHT' NOT 'NUMBERS'

5.1 Coherent Structures in turbulence

^{1 2} The study of coherent structures in turbulence has provided considerable experimental and theoretical evidence that such features are a consequence of 'self-organization' of the flow. These ideas are very much relevant to the field of astrophysics wherein we still lack a definitive theory of the formation of the observed large scale structure of the universe and the role of turbulence in producing such an organisation is still not appreciated by the community. Be it the observed hierarchy of structures (galaxies, clusters of galaxies, superclusters..etc), or the granulation scales on the sun, all such order seems to be the fallout of a self-organized system! What causes this self-organisation is believed to be related to inverse - cascade of energy in the system.

The alpha-effect, which is a large scale Magnetohydrodynamic instability, usually associated with helical flow, is well known. It is believed to play an important role in

¹ *Paper presented at the 4th International Conference on Computational Physics, Singapore, (1997)*

² *Poster accepted in the International Symposium on Supercomputing -Tokyo, (1997)*

the generation of large scale magnetic fields which are well observed in astrophysics. There is indeed a known analog for the alpha effect in compressible ordinary fluid dynamics [22]. But for statistically isotropic incompressible and helical flow no such large scale instability is obtained [100]. On the other hand anisotropic flows in 2D and 3D are known to have large scale instabilities of the *negative viscosity* type where the growth rate is proportional to the wavenumber unlike the alpha - effect.

Frisch et al. [27] asked a relevant question as to whether there exists an analog to the alpha effect for three dimensional flows which are incompressible. Their analysis led them to conclude that indeed there exists a large scale instability provided the small scale flow lacks parity. By parity - invariance we mean invariance under the simultaneous reversal of the position and velocity vectors with respect to a suitable centre, in a deterministic or statistical sense as the case may be. As reiterated by Frisch, *lack of parity invariance is a broader concept than the (essential) presence of helicity*, and could have in some instances (e.g. PRIMORDIAL TURBULENCE) have its origin in parity non-conservation of electroweak interactions. This inverse cascade could be the result of a large - scale - instability, whose existence was confirmed by Frisch et.al. ([27]; [71]) for the case of an incompressible fluid with forcing, and is since known as the Anisotropic Kinetic Alpha effect. The AKA effect is also the analogue of the well-known alpha effect for the generation of large scale magnetic fields from seed fields. A perturbative expansion of the incompressible Navier - Stokes equation using the small scale Reynolds number as a small parameter shows that the solvability condition for the set of linear PDEs obtained with multi-scale analysis, resembles the dynamo -like equation for magnetic fields. The key requirement for the AKA instability to manifest itself is the lack of reflectional symmetry in the medium (Parity non-invariance).

5.2 The basic equations

We model the flow using the Reynolds-averaged Navier Stokes equations, where the flow is separately described by the equations for mean flow and equations for small scale random flow. We force the small scales using a forcing function similar to that

of Frisch et.al. which ensures that the flow on small scales is not parity invariant. We list the respective equations below :

The main equations in the non-dimensionalized form.

$$\partial_t u_i + R_e u_j \partial_j u_i = -R_e^{-1} \mu^{-2} \partial_i \rho + \partial^2 u_i + f_i \quad (5.1)$$

$$\partial_t \rho + R_e \partial_j (u_j \rho) = 0 \quad (5.2)$$

In deriving the above equations in dimensionless form with the following transformations:

$$\begin{aligned} x &\equiv \frac{x}{L} \\ t &\equiv \frac{\nu t}{L^2} \\ u &\equiv \frac{u}{U} \\ \rho &\equiv \frac{\rho}{\rho_0} \end{aligned}$$

we have also used the polytropic relation between the pressure and density $P = \frac{1}{2} c^2 \rho^2 / \rho_0$, c being the sound speed and $\mu = \frac{M}{R_e}$ where μ is the ratio between the mach number M ($M = \frac{U}{c}$) and Reynolds number R_e .

where, f_i -is the forcing function periodic in space and time, u_i is the total velocity and ρ the total density. The assumption of Reynolds averaging implies that any randomly varying variable (velocity or density here) can be split into two parts, one consisting of the Mean and the other the fluctuating component with zero mean. (say $u_i = W_i(\text{mean}) + v_i(\text{fluctuations})$) The ensemble averages $\langle \rangle$ would imply :

$$\begin{aligned} \langle u \rangle &= W \\ \langle v \rangle &= 0 \\ \langle f_i \rangle &= 0 \\ \langle \rho \rangle &= \rho_m \\ \langle \rho^i \rangle &= 0 \end{aligned} \quad (5.3)$$

(ρ_m is the mean - density and ρ^t is the fluctuating part)

From Eq. (5.1) and eq. (5.2) we obtain the separate equations for Large and Small scales using the relations in eq. (5.3). They are :

Equations for Large Scale flow.

$$\partial_t W_i + R_e W_j \partial_j W_i + R_e \langle v_j \partial_j v_i \rangle = -R_e^{-1} \mu^{-2} \partial_i \rho_m + \partial^2 W_i. \quad (5.4)$$

$$\partial_t \rho_m + R_e \partial_k (\rho_m W_k) + R_e \partial_k \langle v_k \rho^t \rangle = 0 \quad (5.5)$$

Equations for small scale flow

$$\partial_t v_i + R_e W_j \partial_j v_i + R_e v_j \partial_j W_i + R_e v_j \partial_j v_i - R_e \langle v_j \partial_j v_i \rangle = -R_e^{-1} \mu^{-2} \partial_i \rho^t + \partial^2 v_i + f_i. \quad (5.6)$$

$$\partial_t \rho^t + R_e \partial_k (\rho_m v_k) + R_e \partial_k (\rho^t [W_k + v_k]) - R_e (\partial_k \langle \rho^t v_k \rangle) = 0 \quad (5.7)$$

where, f_i in Eq. (5.6) is given by the function

$$f_x = \sqrt{2} \cos \left(\frac{Y}{L} + \frac{\nu t}{L^2} \right); f_y = \sqrt{2} \cos \left(\frac{X}{L} - \frac{\nu t}{L^2} \right); f_z = f_x + f_y \quad (5.8)$$

5.3 Simulation and results

We have simulated the above set of equations adopting the highly accurate spectral method and using Runge-Kutta Fourth order explicit time marching using a 32 cube grid [102],[103]. The RK4 scheme used is as follows: Let \mathbf{U} be the solution function at all grid points at a given time t . We can compute the derivatives $\frac{d\mathbf{U}}{dt}$ at all grid points and then integrate the time derivatives to get the numerical solution at a later time. We denote the time level t_n with a subscript 'n'. RK4 requires three intermediate steps:

$$\mathbf{U}_1 = \mathbf{U}_n + \frac{1}{2} \Delta t \left(\frac{d\mathbf{U}}{dt} \right)_n$$

$$\mathbf{U}_2 = \mathbf{U}_n + \frac{1}{2}\Delta t \left(\frac{d\mathbf{U}}{dt} \right)_1$$

$$\mathbf{U}_3 = \mathbf{U}_n + \frac{1}{2}\Delta t \left(\frac{d\mathbf{U}}{dt} \right)_2$$

$$\mathbf{U}_{n+1} = \mathbf{U}_n + \frac{1}{6}\Delta t \left(\left(\frac{d\mathbf{U}}{dt} \right)_n + 2 \left(\frac{d\mathbf{U}}{dt} \right)_1 + 2 \left(\frac{d\mathbf{U}}{dt} \right)_2 + \left(\frac{d\mathbf{U}}{dt} \right)_3 \right)$$

The time derivatives are calculated by evaluating the spatial derivatives in the equations. The RK4 time marching is accurate to the fourth order in Δt . We used an extremely small time step $\Delta t = 0.0005$ for our simulations thus leading to errors of the order of say $\simeq 10^{-16}$. The conservation of total mass enclosed within the periodic box at any instant of time was used as a tool for consistency check of the simulation at every step (See Fig.(5.1)). This takes care of any spurious mass addition effects which are known to set in for compressible simulations, due to a change in the nature of equations in spatial regions with different mach numbers.

In our simulations the ensemble averages at each point were calculated by taking the average of sufficient number of points surrounding each grid point. This preserves the gradient-information of the averages thereby retaining the spatial structure. We feel that this is a close approximation to the concept of ensemble averages. Thus we could avoid the need to use any model to close the equations by specifying a particular form for the two-point correlations that we encounter. It is to be noted here that in the conventional practice the empirical form of the correlation tensor used would not have preserved the anisotropic nature of the flow, since none of the models really assume any small scale anisotropy. So, it was safe on our part to adopt a different strategy for the ensemble averages in question. By doing so, we are not tampering with the anisotropic nature of the flow. As the simulation proceeds we find that these averages do grow in magnitude and eventually become comparable to the remaining terms. This clearly marks the role of Reynolds stresses in the evolution of the Large scale flows. While calculating the power in each mode (for any quantity in the fourier space) the wave-vectors were so grouped into each shell that the density of states within each bin is such that it resembles the continuum distribution..viz goes

as the square of the wavenumber. Then as seen from the fig.(5.2), it is evident that the higher wavenumber modes (i.e modes for which $(\text{Log}(k))$ is greater than 1.2 , here in the case of 32 cube grid,..) do not contribute at all to the physical picture. They must be ignored. We specify random initial values over the grid for the small scale velocities (there is no Large scale component to start with) and ensure that there is maximum power in the small scales. We choose the initial conditions in such a way that most of the power resides in the small scales only. The typical parameters which we used for the simulation are:

$$\begin{aligned}
 \nu &= 0.1 \\
 Re &= 10.0 \\
 \mu &= 0.1 \\
 l_0 &= 2\pi/4 \\
 \Delta t &= 0.0005 \\
 (\text{forcing amplitude}) &= 10^{-6} \\
 \text{Forcing at } k &= 4.0
 \end{aligned}
 \tag{5.9}$$

As the simulation progresses, we notice the onset of the large scale instability , as the energy in the wave mode $k = 1$ and $k = 2$ keep increasing steadily. We also note that a steady saturation stage is reached soon which may mark the non-linear saturation by feed-back from small scales i.e as the small scales deplete their energy the contribution towards Reynolds stress terms also depletes thus reflecting itself in a saturated large scale mode!

Another feature of interest which we observe in our simulation is that of helicity evolution. With an initial helicity distribution which is mainly has lot of small scale power, our simulation clearly shows that there is a strong polarization seen in the flow in terms of well developed regions of positive and negative helicity (see Fig. (5.10)). This evolution may also be in accordance with the helicity-dynamics which some of the recent shell-model studies of turbulence are revealing [97]. (Although it is also seen that helicity as such decays.) This lends support to the idea that helicity -

helicity correlation (or the I - invariant,) may cascade towards larger spatial scales as a fluid evolves. This is precisely what was expected from our dimensional analysis of chapter 2 , also! We also note that since the flow is not inviscid, helicity conservation is not what matters. Moreover as pointed out by Levich the total helicity , no matter which predominant sign we choose to start the simulation with, eventually tends to zero!(Fig. 5.8) Thus the second order moment viz. Helicity-helicity correlation gains prominence now.

We map the large scale velocity field at one instant of time in Figs.((5.11) and (5.12)). We note that the flow is strongly driven by the density distribution viz.. regions of high and low density both aid in driving such a parity - violating flow!(see also the fig. (5.13)). Thus as explained by Moiseev, compressibility ensures that the α term (refer to Chapter 1.) doesn't vanish. This is because the Reynolds terms are no longer symmetric with respect to reflections . The evolution was studied both with and without forcing f_i and the evolution of the energy in wave - modes $k=1,2,6$ is shown in Fig. 5.3 and in Fig. 5.4. We confirm the presence of a three dimensional large scale instability leading to inverse cascade of energy as can be seen from the figure (5.5). The simulations were performed on the IBM SP2 as well as on the Power challenge platforms. The averaging routines of the code were parallelized for greater optimization of execution time per iteration. The execution time for each time-step was roughly 20 secs, and each run of the simulations was continued for almost 5000-6000 iterations.

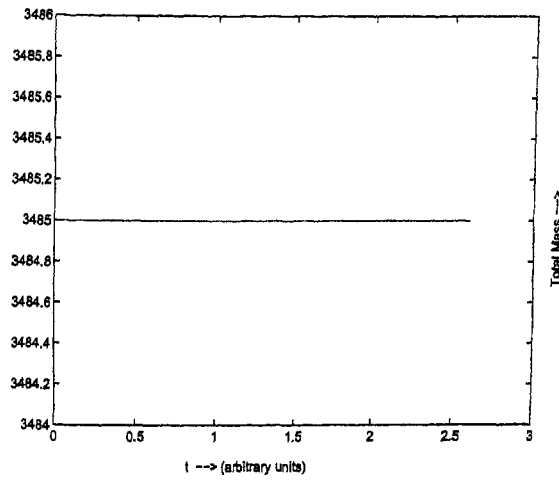


Figure 5.1: Figure showing the constancy of total mass inside the periodic box

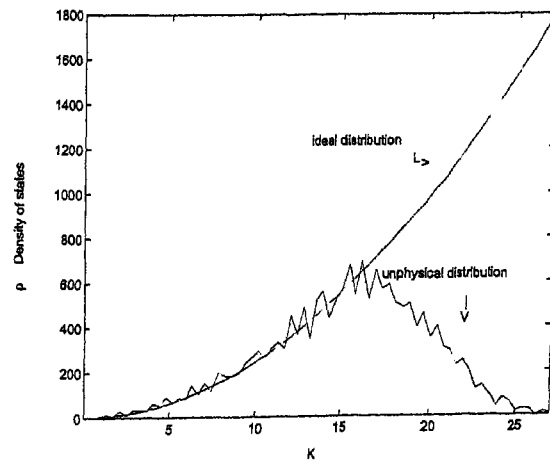


Figure 5.2: Figure showing the density of states, which is made to resemble Continuum distribution by suitably binning the modes into shells. For a 32 cube grid, the above figure shows the density of states for 70 shells.

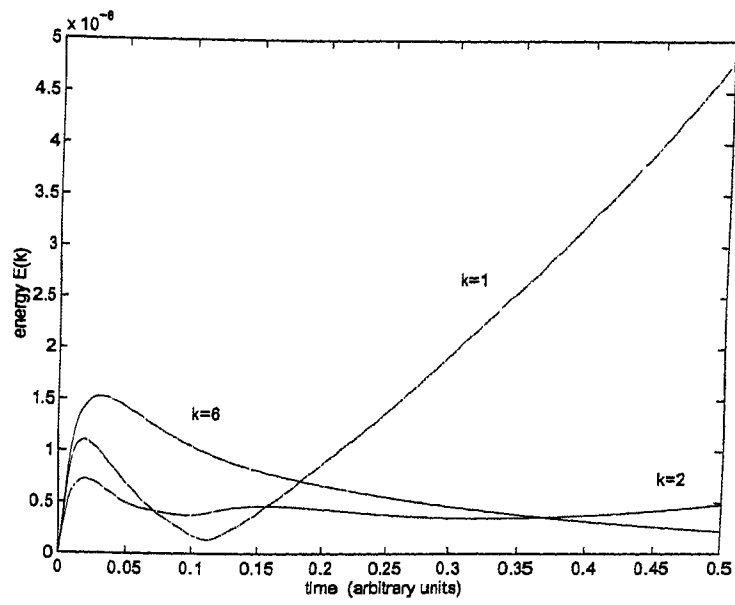


Figure 5.3: The evolution of the energy in wave modes $k=1,2,$ and 6 with forcing (at $k=4$)

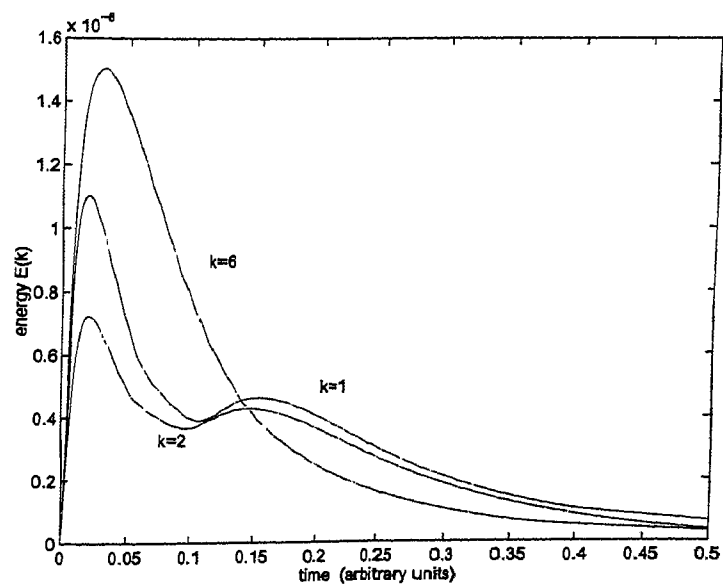


Figure 5.4: The evolution of the energy in wave modes $k=1,2,$ and 6 without forcing .

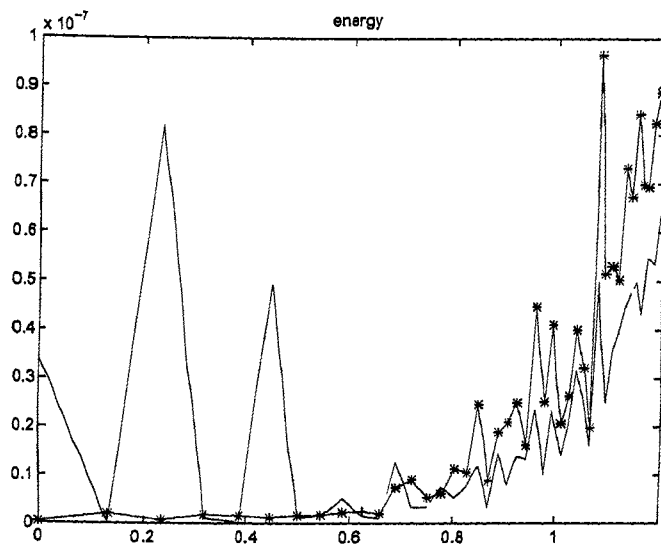


Figure 5.5: The energy Spectrum $(E(k) \text{ vs. } \text{Log}(k))$, (\dots ..dotted =initial) ($-$ continuous=final)

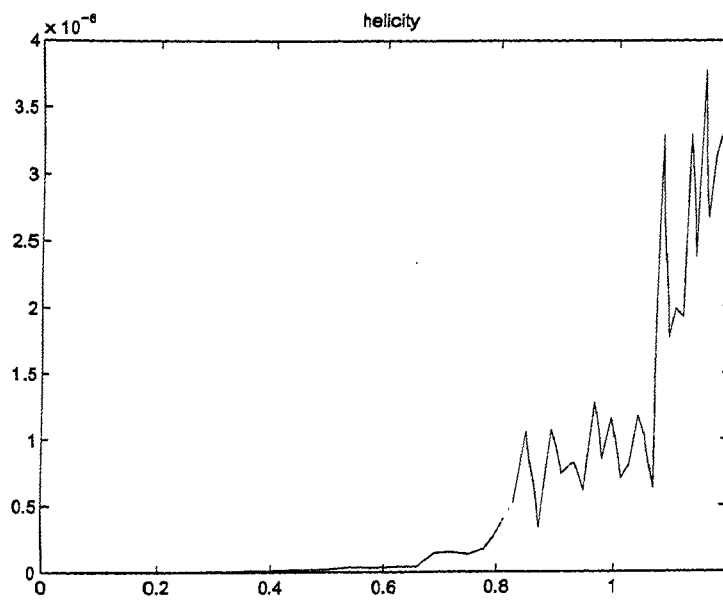


Figure 5.6: The helicity spectrum (initial) $(H(k) \text{ vs. } \text{Log}(k))$

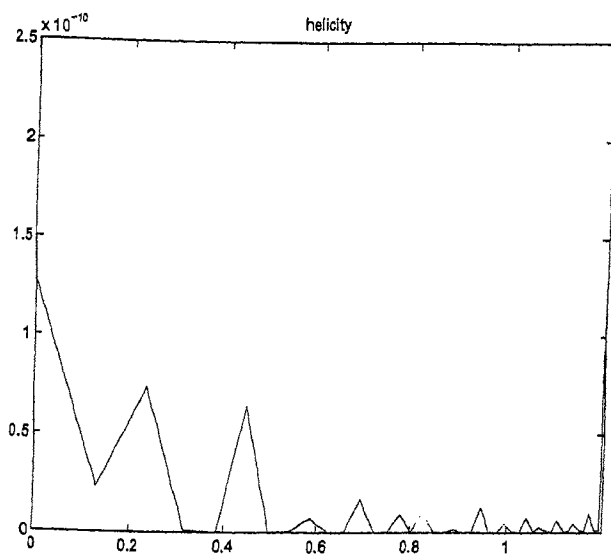


Figure 5.7: The helicity spectrum (final) ($H(k)$ vs. $\text{Log}(k)$)

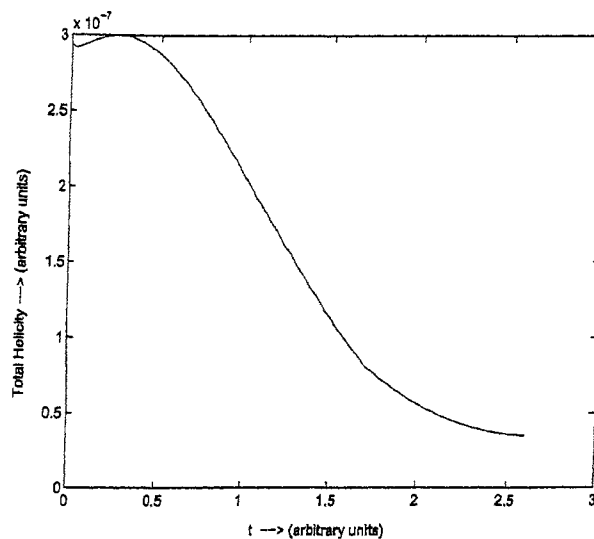


Figure 5.8: The evolution of total Helicity with time.

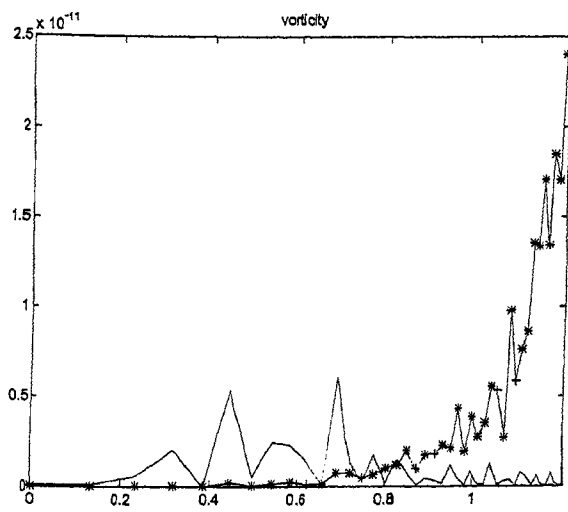


Figure 5.9: The vorticity spectrum $\omega(k)$ vs. $\text{Log}(k)$ (*- = initial) (— = final)

Figure 5.10: The spatial distribution of helicity at two different instants. Top: initial; Bottom: final. The color code is : the values range from negative (blue) and increase through green,yellow(zero), red and pink(positive).

Figure 5.11: The initial velocity field along a z-y plane. Note that there is no mean flow here, and the velocity vectors are randomly oriented. The color code is just a superposition of the density information. density increases (from a positive value) through blue,green,yellow,red and pink.

Figure 5.12: The final mean velocity field along the z-y plane. Note that a distinct large scale flow has emerged which is also driven by the density distribution as can be seen from the overlapping color code for density.

Figure 5.13: The density evolution is shown above. On the left is the density spectrum $\rho(k)$.vs. $Log(k)$, with both the intial(yellow) and final(green) spectra superposed. On the right-top is shown the initial density distribution in space.The box on the right-bottom shows the final density clumping as seen. color code: density increases (from a positive value) through blue,green,yellow,red and pink.

Appendix A

Statistics

A.1 Correlation coefficient

This appendix sums up the statistics used to arrive at the results indicating significant correlations between the variable under study.

To calculate the correlation coefficient we employed the following formula:

$$r = \frac{\Sigma y_1 y_2 - (\Sigma y_1 \Sigma y_2) / n}{\sqrt{[(\Sigma (y_1)^2 - (\Sigma y_1)^2 / n) (\Sigma (y_2)^2 - (\Sigma y_2)^2 / n)]}}$$

We can also calculate the standard error in the calculation of the correlation coefficient, and perform a t-test to determine the probability that it is equal to zero. A probability of less than 0.05 is considered evidence of a significant correlation. Note that we have based our criteria for the *significance* of the correlation on this and displayed the corresponding values in the Table.

We can also calculate the probability that N measurements of two uncorrelated variables would give a coefficient r as large as r_0 (which is our observed value from the data) i.e $P_N (|r| \geq |r_0|)$. Here too a probability of less than 5 percent (i.e $P \leq 0.05$) is considered to be indicative of a significant correlation. This value is calculated from the following integral below:

$$P_N (|r| \geq |r_0|) = \frac{2\Gamma [(N-1)/2]}{\sqrt{\pi}\Gamma [(N-2)/2]} \int_{|r_0|}^1 (1-r^2)^{(N-4)/4} dr$$

A.2 Skewness and Kurtosis

The Skewness and Kurtosis of a given distribution can be found out as follows: Let N be the total number of samples, and the mean $\langle x \rangle$:

$$\langle x \rangle = \frac{\sum f_i x_i}{N} \quad (\text{A.1})$$

and let

$$\nu_k = \frac{\sum f_i (x_i)^k}{N} \quad (\text{A.2})$$

also define

$$\mu_k = \frac{\sum f_i (x_i - \langle x \rangle)^k}{N} \quad (\text{A.3})$$

where $\mu_2 = \sigma$ is the variance.

Using the above definitions skewness is calculated as:

$$\text{Skewness} = \frac{\mu_3}{2\sigma^3}$$

and kurtosis is calculated as:

$$\text{Kurtosis} = \frac{\mu_4 / (\mu_2)^2 - 3}{2}$$

Appendix B

Notes on the I- Invariant

B.1 The Proof of I- invariance

Helicity as is an exact topological integral of motion of the Euler equation, and is also the measure of knottedness of the vorticity field ([72] $\vec{\omega} = \nabla \times \vec{v}$) lines. From the Euler equation

$$\frac{\partial \vec{v}}{\partial t} + (\vec{v} \cdot \nabla) \vec{v} = -(\nabla p) / \rho \quad (\text{B.1})$$

taking a curl of the above equation we get,

$$\frac{\partial \vec{\omega}}{\partial t} + \nabla \times [\nabla (v^2/2) - \vec{v} \times (\nabla \times \vec{v})] = 0 \quad (\text{B.2})$$

we take the dot product of (B.1) with $\vec{\omega}$, and add it with the dot product of (B.2) with \vec{v} . We get :

$$\left[\vec{\omega} \cdot \frac{\partial \vec{v}}{\partial t} + \vec{v} \cdot \frac{\partial \vec{\omega}}{\partial t} \right] + \vec{\omega} \cdot \nabla (v^2/2) + \vec{\omega} \cdot \frac{\nabla p}{\rho} - \vec{v} \cdot (\nabla \times (\vec{v} \times \vec{\omega})) = 0 \quad (\text{B.3})$$

expanding the last term in equation (B.3) as:

$$\begin{aligned} -\vec{v} \cdot (\nabla \times (\vec{v} \times \vec{\omega})) &= -\vec{v} \cdot [\vec{v} \cdot (\nabla \cdot \vec{\omega}) - \vec{\omega} (\nabla \cdot \vec{v}) + (\vec{\omega} \cdot \vec{v}) \vec{v} - (\vec{v} \cdot \nabla) \vec{\omega}] \\ &= \vec{v} \cdot [(\vec{v} \cdot \nabla) \vec{\omega} - (\vec{\omega} \cdot \nabla) \vec{v}] + \vec{v} \cdot (\nabla \cdot \vec{v}) \vec{\omega} \\ &= \vec{v} \cdot ((\vec{v} \cdot \nabla) \vec{\omega}) + \vec{v} \cdot [(\vec{\omega} \cdot \nabla) \vec{v} - 2 \cdot (\vec{\omega} \cdot \nabla) \vec{v} + (\nabla \cdot \vec{v}) \vec{\omega}] \\ &= \vec{v} \cdot ((\vec{v} \cdot \nabla) \vec{\omega}) + (\vec{\omega} \cdot \nabla) \vec{v} + \vec{v} \cdot (\nabla \cdot \vec{v}) \vec{\omega} - \vec{v} \cdot 2(\vec{\omega} \cdot \nabla) \vec{v} \end{aligned}$$

$$\begin{aligned}
&= \vec{v} \cdot \nabla H + H \nabla \cdot \vec{v} - \vec{v} \cdot 2(\vec{\omega} \cdot \nabla) \vec{v} \\
&= (\nabla \cdot H \vec{v}) - 2\vec{\omega} \cdot \nabla \left(\frac{v^2}{2} \right)
\end{aligned} \tag{B.4}$$

using the above relation in (B.3) we finally obtain:

$$\begin{aligned}
\frac{\partial H}{\partial t} + \nabla(\vec{v}H) &= \vec{\omega} \cdot \nabla \left[\frac{-p}{\rho} + \frac{v^2}{2} \right] \\
&= \nabla \cdot [\vec{\omega}(-p + v^2/2)]
\end{aligned} \tag{B.5}$$

Now that implies:

$$\frac{DH}{Dt} = \text{div} \vec{F} \tag{B.6}$$

where $\vec{F} = \vec{\omega}(-p + v^2/2)$.

By applying the above equation (B.6) at two points x , and $x + r$, averaging and using homogeneity, one obtains the following equation for the correlation $\langle H(x)H(x+r) \rangle$:

$$\frac{D}{Dt} \langle H(x)H(x+r) \rangle = \text{div}_r \left[\langle H(x+r)\vec{F}(x) \rangle + \langle H(x)\vec{F}(x+r) \rangle \right] \tag{B.7}$$

after integrating, one arrives at the conservation law :

$$I = \int \langle H(x+r)H(x) \rangle d^3r = \text{constant}$$

In deriving the I-invariant, the existence of a small viscous term on the right hand side of equation (B.6) is assumed. Otherwise the ensemble of helicities would not have been possible, since helicity itself is the exact invariant for inviscid flows. The I-invariant is such only with the accuracy of viscous terms. Below we derive it's relation with the energy spectrum for a quasi-normal distribution of helicities.

B.2 Proof of $I(k) \propto E(k)^2$

This appendix gives the derivation of the helicity - variance spectrum, that was employed in our model [104]. The Helicity spectral density $H(k)$ may be written as:

$$H(k) = \sum_{S(k)} \vec{v}(\mathbf{k}') \cdot \vec{\omega}(-\mathbf{k}')$$

where, the summation $\sum_{S(k)}$ extends over one shell in \mathbf{k} space, $k \leq |\vec{v}(\mathbf{k}')| \leq (k+1)$.

Since the velocity vectors in fourier space are complex quantities, (with a Real part $\mathbf{R}(\mathbf{k}')$ and an imaginary part $\mathbf{I}(\mathbf{k}')$) we can simplify the above spectrum as :

$$H(k) = \sum_{S(k)} 2\mathbf{k}' \cdot [\mathbf{R}(\mathbf{k}') \times \mathbf{I}(\mathbf{k}')]]$$

or

$$H(k) = \sum_{S(k)} 2kR(\mathbf{k}')I(\mathbf{k}') \sin\phi(\vec{v}')$$

We assume that ϕ is uniformly distributed over the interval $[0, 2\pi]$, then

$$\langle H(k) \rangle = \langle \sin\phi(\mathbf{k}) \rangle = 0$$

We further assume that the random variables $R(\mathbf{k}), I(\mathbf{k})$ and $\phi(\mathbf{k})$ are statistically independent and that fourth order cumulants are negligible. Also, the reality constraint on the velocity values in the real space implies that $\vec{v}(\mathbf{k}) = \vec{v}^*(-\mathbf{k})$. Then,

$$\begin{aligned} \langle \sin\phi(\mathbf{k}) \sin\phi(\mathbf{p}) \rangle &= \langle \sin^2\phi(\mathbf{k}) \rangle (\delta_{\mathbf{k},\mathbf{p}} + \delta_{\mathbf{k},-\mathbf{p}}) \\ &= \frac{1}{2} (\delta_{\mathbf{k},\mathbf{p}} + \delta_{\mathbf{k},-\mathbf{p}}) \end{aligned}$$

In this approximation the amplitudes of the velocity and the energy spectral density are related by $\langle R(\mathbf{k})^2 \rangle = \langle I(\mathbf{k})^2 \rangle = \langle E(k)/N(k) \rangle$ where $N(\mathbf{k})$ is the number of modes per shell, approximately equal to $4\pi k^2 \rho$. The density of modes in Fourier space $\rho = (V/(2\pi))^3$ is equal to one in our simulation. We obtain for the variance of helicity spectrum :

$$\begin{aligned}
\text{Var}_G(H(k)) &:= \langle H(k)^2 - \langle H(k) \rangle^2 \rangle = \langle H(k)^2 \rangle \\
&= \Sigma_{S(k)} 4k^2 \langle R(\mathbf{k}')^2 \rangle \langle I(\mathbf{k}')^2 \rangle \\
&= \Sigma_{S(k)} 4k^2 \left\langle \frac{E(k)}{N(k)} \right\rangle^2 = \frac{4k^2}{N(k)} \langle E(k) \rangle^2 \\
&= \frac{1}{\pi} \langle E(k) \rangle^2
\end{aligned}$$

Which is the relation that we employed in our model . Note here that $I = \int \langle \gamma(0)\gamma(r) \rangle dV = \int I(k)dk$ So, the above result is directly related to the I- invariant.

References

- [1] Frisch U., Orszag S.A, 1990, Physics Today, January, 24
- [2] von Weizsacker C.F., 1951,ApJ, 114, 2, 165
- [3] Gamow G., 1952, Phys. Rev., 86, 231
- [4] Peebles P.J.E., 1971, Astr.and Sp.Sc., 11, 443
- [5] Zel'dovich Ya.B., 1977, Ann.Rev.Fluid.Mech, 9, 215
- [6] Hussain F., Davinder Virk, Mogens V. Melander,1993, Surveys in Fluid Mechanics III, Ed. R.Narasimha, 193
- [7] Antia H.M, and Chitre S.M, 1993, Solar Physics, 145, 227
- [8] Krishan V., 1993, MNRAS,264,257
- [9] Prabhu R.D. and Krishan V., 1994, ApJ, 428, 483
- [10] Kolmogorov A.N., 1941, Dokl.Akad.Nauk SSSR,30,299
- [11] Hasegawa A., 1985, Adv.Phy., vol.34, 1, 1
- [12] Lilly D.K., 1969, Physics of Fluids,12,240
- [13] Beck R., Brandenburg A., Moss D., Shukurov A., Sokoloff D., 1996,Ann.Rev.Astron.Astrophys.,34,155
- [14] Saffman P.G., 1967, Phys.Fluids ,10,1349
- [15] Frenkel A.,and Levich E., 1983, Phys.Lett, 98A (1 & 2),25

-
- [16] Krishan V., 1991, MNRAS, 250, 50
- [17] Krishan V., and Sivaram C., 1991, MNRAS, 250, 157
- [18] Krishan V., and Sivaram C., 1992, *Instability, Chaos and Predictability in Celestial Mechanics and Stellar Dynamics*, Nova Science Publishers, Inc, 193
- [19] Krishan V., 1992, Indian J.Phys., 66B, (5 & 6), 569
- [20] George Em Karniadakis and Steven A. Orszag, 1993, Physics Today, March, 34
- [21] Khomenko G A., Moiseev S S., Tur A V., 1991, JFM, 225, 355
- [22] Moiseev S S., Sagdeev R Z., Tur A V., Khomenko G A., and Yanovskii V V., 1983, Sov.Phys.JETP, 58, 6, 1149
- [23] Kraichnan R H., 1973, JFM, 59, 745
- [24] Brissaud A., Frisch U., Leorat J., Lesieur M., and Mazure A., 1983, Phys.Fluids, 16, 1366
- [25] Andre' J.K., and Leiseur M., 1977, JFM, 81, 187
- [26] Moffat H.K., 1981, JFM, 106, 27
- [27] Frisch U., She Z.S., and Sulem P.L., 1987, Physica, 28D, 382-392
- [28] Longair Malcom S., 1993, Q.J.R.astr.Soc. 34, 157
- [29] Einasto J., 1990, Aust.J.Phys., 43, 123-134
- [30] Sarr E., 1990, Aust.J.Phys., 43, 159-166
- [31] Silk Joseph, 1992, Nature, 356, 741
- [32] Vershurr, 1991, Comments in Astrp., 15, 4, 189-205
- [33] Fleck Robert C. Jr., 1981, ApJ, 246, L151
- [34] Fleck Robert C. Jr., 1982, ApJ, 261, 631

- [35] Silk Joseph and Susan Ames, 1972, *ApJ*, 178, 77
- [36] Frank H.Shu, 1992, *Gas Dynamics Vol II*,University Science Books, pg 43
- [37] Frank H.Shu, 1992, *Gas Dynamics Vol II*,University Science Books, pg 72
- [38] Chernin Arthur D., 1996, *Vistas in Astronomy*, 40, 2, 257
- [39] Castaneda He'ctor O., Oriol Fuentes-Masip and Amina Helmi, 1995, *RevMexAA (Serie de Conferencias)*, 3, 259
- [40] Castaneda He'ctor O., Vilchez J.M. and Copetti M.V.F, 1995, *ibid*,3,113
- [41] Elmegreen Bruce G., 1995, *RevMexAA (Serie de Conferencias)*, 3, 55
- [42] Elmegreen Bruce G., 1995, *ibid.* , 3, 289
- [43] Larson Richard B.,1981,*MNRAS*,194,809
- [44] Va'zquez-Semadeni Enrique, 1995, *RevMexAA (Serie de Conferencias)*, 3, 61
- [45] Vishniac Ethan T., 1995, *ibid.*, 3, 69
- [46] Falgarone E.,Lis D C.,Phillips T G., Pouquet A., Porter D H., Woodward P R., 1994,*Ap.J.*,436,728
- [47] Bonnor W.B., 1957, *MNRAS*, 117, 104
- [48] TOMITA Kenji, Hidekazu NARIAI, Humitaka SATO, Takuya MATSUDA , and Hidenori TA KEDA, 1970, *Prog.Th.Ph.*, 43, 6, 1511
- [49] Ozernoi L.M, and Chernin A.D., 1968, *Sov.Phys-Astr*, 11, 6, 907
- [50] Oort J.H., 1970, *Astron. & Astrophys.* 7, 381
- [51] Ozernoi L.M., and Chernin A.D., 1969, *Sov.Phys-Astr*, 12, 6, 901
- [52] Ozernoi L.M., and Chibisov G.V., 1971, *Sov.Astron.*, 14, 4, 615
- [53] Ozernoi L.M., *Sov.Astron*, 15, 6, 923

- [54] Jones Bernard J.T., 1976, Rev.Mod.Phys., 48, 107
- [55] Goldman I. and Canuto V.M., 1993, ApJ, 409, 495
- [56] Amram P., et al., 1992, Astron.Astrophys.Suppl.Ser., 94, 175- 209
- [57] Amram P., et al., 1994, A& A Suppl. ser. 103, 5
- [58] Rubin V.C. , Ford W.K.Jr., Thonnard N., 1980, ApJ 238,471
- [59] Rubin V.C. , Ford W.K.Jr., Thonnard N., 1982, ApJ 261,439
- [60] Rubin V.C., Burstein, D., Ford, W.K., Jr., and Thonnard, N., 1985, APJ, 289
- [61] Milgrom M., 1983, ApJ, 270, 365
- [62] Milgrom M., Bekenstein, J., 1987, IAU Symp.No.117, ed.Kormendy,J., and Knapp G.R., Dark Matter in the Universe, pp 319-333
- [63] Liboff R., 1992, ApJ.Lett., 397, L71
- [64] Nelson A.H., 1988, MNRAS, 233, 115
- [65] Battaner E., et al., 1992, Nature, Vol.360, 652
- [66] Soares D.S.L, Rev.Mex.AA 01-94,(also astro-ph/9402026).
- [67] Filippov A.E. and Zhedanov A.S, preprint *Does there really exist the problem of the dark matter in Spiral galaxies ?* astro-ph/9511022
- [68] Ambartsumyan V.A., 1978,*Problems of modern cosmogony*, Nauka (in Russian)
- [69] Mannheim Philip D., astro-ph/9511045
- [70] TerHarr D., 1989, Physica Scripta, Vol.39, 731-734
- [71] Sulem P.L., She Z.S., Scholl H., Frisch U., 1989, JFM, Vol.205 , 341
- [72] Moffat H.K. and Tsinober, A. 1992, Annu.Rev.Fluid Mech, 24, 2 81-312
- [73] Levich E., Tzvetkov E., 1985, Phys. Rep., 128, 1.

- [74] Scalo John M., 1987, 349, in *Interstellar Processes*, eds. D.J. Hollenbach and H.A.Thronson, Jr., D.Reidel Publishing Company
- [75] Kraichnan R.H., and Montgomery D., 1980, Rep.Prog.Phys.,43,35.
- [76] Levich E., 1987, Phys.Rep., 151, 3-4,129
- [77] Ruzmaikin A.A., Shukurov, A.M., and Solkoff, D.D. , 1988,*Magnetic Fields of Galaxies* (Dordrecht:kluwer),150
- [78] Ruzmaikin A.A., Shukurov, A.M., and Solkoff, D.D. , 1988,*Magnetic Fields of Galaxies* (Dordrecht:kluwer),164
- [79] Ruzmaikin A.A., Shukurov, A.M., and Solkoff, D.D. , 1988,*Magnetic Fields of Galaxies* (Dordrecht:kluwer),180
- [80] Giovanelli R.,Haynes M P.,1988 in *Galactic and Extragalactic Radio Astronomy*, ed. G.L. Verschuur and K.I. Kellermann (Berlin: Springer- Verlag), 537
- [81] Shore S N.,1992, *An introduction to Astrophysical Hydrodynamics*,pp 243, Academic Press inc.
- [82] Sanchez-Salcedo F J.,1996, Ap.J., 467,L21
- [83] Moiseev S., Onishchenko O., American Institute of Aeronautics and Astronautics, series 1994, Pg 57.
- [84] Yakhot Victor, Vladimir Zakharov, 1993, Physica D, 64, 379
- [85] Afanasev V.L., and Fridman A.M, 1993, Astron.Lett 19,(5), 3 19
- [86] Kitamura Y., Sunada K., Hayashi M., and Hasegawa T., 1993, ApJ, 413, 221
- [87] Prabhu R.D. and Krishan V., 1996 BASI 24, 787
- [88] Tully R Brent. and Fisher J Richard., 1977, A&A, 54, 661
- [89] Kurskov A.A. and Ozernoi L.M., 1974, Sov.Astron., 18, 2, 157
- [90] Levich E., and Tzvetkov E., 1984, Phys.Lett., 100A, 53

- [91] Knorr G., Lynov J.P. and H.L.Pe'cseli, Z.Naturforsch.,1990,45a,1059.
- [92] Biferale L., Kerr R., 1995, *On the role of inviscid invariants in shell models of turbulence*,chao-dyn/9508007.
- [93] Fedutenko E.A., 1994, Physica Scripta 50, 514
- [94] Wallace J M, Balint J L,Ong L,1992,Phy.Fluids,4,9,2013
- [95] Yoshizawa Akira and Nobumitsu Yokoi,1991,JAPSP,60,8,2500
- [96] Yokoi Nobumitsu, Akira Yoshizawa, 1993, Phys.Fluids, 5 (2), 464
- [97] Benzi R.,Biferale L.,Trovatore E.,1995, *Helical shell models for three dimensional turbulence*,chao-dyn/9510010.
- [98] Krishan V., and Prabhu R.D., 1995, preprint
- [99] Belyan A.V., 1991, Phys.Lett. 155 (2,3), 181
- [100] Fournier J.D., Sulem P.L, and Pouquet A, 1982, J.Phys.A, 13 93
- [101] Druzhinin O.A., and Khomenko G.A., Advances in Turbulence 3, eds. A.V.Johansson and P.H.Alfredsson, pg 151.
- [102] Prabhu R.D., Basu,A.J. and Krishan V., 4th International conference on Computational Physics - Singapore (June 2-4 1997).
- [103] Prabhu R.D., Basu, A.J and Krishan V., International Symposium on Supercomputing, 1997 Tokyo.
- [104] Polifke W., and Shtilman L.,1989, Phys.Fluids. A 1 (12),2025.

